Synthesis of imidazole core based small molecules for the treatment of SMA

Sara Barranco Campos

Master Thesis in Chemistry

Universitetet i Bergen

Department of Chemistry

Laboratory for Drug Discovery in Neurodegeneration (LDDN), Brigham and Women's Hospital and Harvard Medical School, Indiana University

August 2019

Acknowledgements

I would first like to thank my supervisor Hans-René Bjørsvik for his guidance and motivation whenever I ran into trouble or had doubts, as well for believing in me enough to give me this opportunity to learn and experience chemistry in different settings.

I want to thank Francesco Angelucci, Frida Lundevall, Eirin Alme and Davide Cirillo for always being ready to help and teach me whenever it was necessary, even if it meant to change the CO_2 bottle every two weeks. Also, I would like to thank Bjarte Holmelid for helping me to use the LC-MS and to develop good separation methods.

I want to express my gratitude to Kevin Hodgetts for letting me be part of his research group and always having his door open for me. Thank you to all my fellow LDDN lab mates for all the cake breaks, the movie nights and for the great atmosphere in the lab that made going to the lab every day a pleasure.

Thank you to Maren and Robert not only for being great co-workers and making this project work but also for being my roommates and supporting me.

Finally, I would like to thank my parents and siblings, Alberto and Marta, for supporting me unconditionally regardless to where in the world I decide to go, this accomplishment would have been impossible without them. Lastly thank you to Annar who is always there to encourage me and hear me out when I need.

Thank you,

Sara Barranco Campos

Abstract

Spinal muscular atrophy (SMA) is the leading cause of infant mortality, it is the second most common autosomal recessive heritable neurodegenerative disease, after cystic fibrosis. SMA is characterized by α motor neuron loss in the anterior horn of the spinal cord and lower brainstem, progressive muscle weakness and atrophy [1-2]. SMA is caused by the absence of the gene SMN1 and the mutation of the gene SMN2. That mutation produces a change of one nucleotide in SMN2, creating an exon splicing silencer element, whose mRNA transcripts produce around 90% of a truncated and unstable form of survival motor neuron (SMN) protein that is rapidly degraded. Several small molecules and repurposed drugs were tested for an increase in the concentration of SMN in a high throughput screening using an SMN2 luciferase reporter assay resulting in the hit compound **LDN-75654** (EC_{50} = 1.8 µM, 242 %, plasma stability = 13 minutes) (Scheme 1). A structure-activity relationship (SAR) study was conducted to increase the pharmacokinetic properties, potency and plasma stability outcoming in the lead compound **LDN-27** (EC_{50} = 0.29 µM, 190 %, plasma stability = 326 minutes), whose mechanism of action is by stabilizing the SMN protein post-translationally [3].

LDN-75654
EC_{50} = 1.8 µM (242%)
Plasma stability = 13 min

LDN-27
EC_{50} = 0.29 µM, (190 %)
Plasma stability = 326 minutes
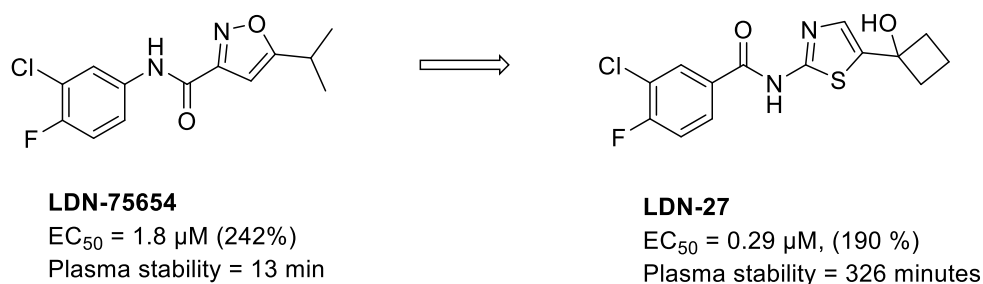
Scheme 1 Previous optimization results

New analogues of the lead compound have been developed by introducing an imidazole ring as the heterocycle core in order to further study how the effect on the SMN concentration as well as solubility and potency properties are influenced (Scheme 2).
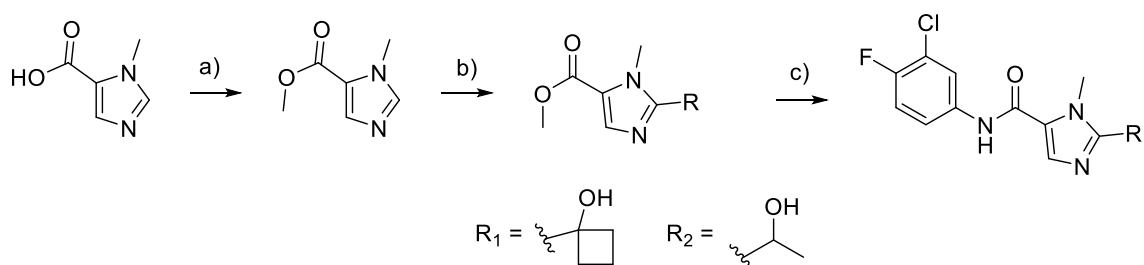
Reagents and conditions. a) MeI, K_2CO_3, Acetone, b) n-BuLi, R_1= Cyclobutanone or R_2= Acetaldehyde, THF, -78ºC (47%) c) Trimethylaluminum, 3-chloro-4-fluoroaniline, DCM, 0ºC (48%).

Scheme 2 Imidazole core analogues

Abbreviations

$AlPO_4$	Aluminium phosphate
ASO	Antisense oligonucleotides
BBr_3	Boron tribromide
C	Cytosine
cDNA	Complementary deoxyribonucleic acid
CO_2	Carbon dioxide
$CoSO_4\ 7\ H_2O$	Cobalt(II) sulphate heptahydrate
Cs_2CO_3	Caesium carbonate
DBH	1,3-Dibromo-5,5-dimethylhydantoin
DCH	1,3-Dichloro-5,5-dimethylhydantoin
DCM	Dichloromethane
DIH	1,3-Diiodo-5,5-dimethylhydantoin
DMF	N,N-Dimethylformamide
EDC	1-Ethyl-3-(3-dimethylaminopropyl)carbodiimide
EI	Electron ionization
EtOAc	Ethyl acetate
ESI	Electrospray ionization
Et_3N	Triethylamine
GC-MS	Gas chromatography mass spectroscopy
H_2	Hydrogen gas
HCl	Hydrochloric acid
HI	Hydroiodic acid
HOAt	1-Hydroxy-7-azabenzotriazole
H_2O	Water
HPLC	High performance liquid chromatography
H_2SO_4	Sulfuric acid
HTS	High-throughput screening
I_2	Iodine
K_2CO_3	Potassium carbonate

KI	Potassium iodide
KOH	Potassium hydroxide
K_2SO_3	Potassium sulphite
LC-MS	Liquid chromatography mass spectroscopy
LDDN	Laboratory for Drug Discovery in Neurodegeneration
$LiAlH_4$	Lithium aluminium hydride
Me_3Al	Trimethylaluminum
Mg	Magnesium
MeI	Methyl iodide
MeOH	Methanol
MHz	Megahertz
mRNA	Messenger ribonucleic acid
N_2	Nitrogen gas
$NaBH_4$	Sodium borohydride
NaCl	Sodium chloride
NaH	Sodium hydride
NaOH	Sodium hydroxide
$NaSO_3$	Sodium sulphite
Na_2SO_4	Sodium sulphate
n-BuLi	*n*-Butyl lithium
NH_4Cl	Ammonium chloride
NMR	Nuclear magnetic resonance
ON	Overnight
$Pd(OH)_2$/C	Palladium hydroxide on activated charcoal
PET	Positron emission tomography
ppm	Parts per million
Py	Pyridine
RT	Room temperature
SAR	Structure activity relationship
SMA	Spinal muscular atrophy

SMN	Survival motor neuron
snRNPs	Small nuclear ribonucleoproteins
$SOCl_2$	Thionyl chloride
T	Thymine
t ½	Half life
THF	Tetrahydrofuran
UV	Ultraviolet
μM	Micro molar

1 Contents

1 INTRODUCTION

1.1 Spinal Muscular Atrophy

Spinal muscular atrophy (SMA) is a serious heritable, autosomal recessive, neurodegenerative disease characterized by motor neuron loss in the anterior horn of the spinal cord and lower brainstem, muscle weakness and atrophy. It is one of the leading causes of infant mortality in the world, being the most common cause of mortality for children under the age of two, occurring in 1 in 30 154 to 1 in 36 012 live births, with a carrier frequency of 1 in 76 to 1 in 111[1].

SMA is caused by homozygous mutation of SMN1 gene that encodes for the survival motor neuron (SMN) protein. Duplication at chromosome 5q11-q13, which contains two almost identical genes, SMN1 telomeric and SMN2 centromeric (Figure 1), an exchange of C to a T nucleotide in exon 7 of SMN2 creates an exon splicing silencer element. Due to this, mutation exon 7 is excluded from the majority of SMN2 mRNA transcripts (SMNΔ7)[2-3], producing a truncated and unstable form of the SMN protein that is rapidly degraded.

SMN protein along with eight other core protein components, forms the named SMN complex, whose best described function is the assembly of small nuclear ribonucleoproteins (snRNPs) of spliceosomes, that are essential components for the splicing of RNA[4-5] in all tissues.

However, a small fraction of SMN2 transcripts include exon 7, which produces the full length SMN and provides enough SMN to avoid lethality but not enough to compensate for the loss of SMN1 and to result in motor neuron diseases, such as SMA.

Typically, healthy individuals carry two copies of SMN1 gene and one-to-two copies of SMN2 gene, which are unaffected. For SMA patients, the number of copies of the SMN2 gene and the severity of the condition have an inverse correlation; the more copies of SMN2 gene that exist, the more full-length SMN protein that is produced and the severity of the disease is reduced.

SMA has five different subtypes based on the age of onset as well as based on the number of copies of the SMN2 gene present[6-8]. Type 0, also known as prenatal SMA, typically is fatal in utero or few first months of age and is predicted to have only one copy of SMN2[9]. Type I SMA, also referred as Werdnig-Hoffman, is the most common type of SMA with two copies of SMN2; these babies show signs of the disease around 6 months after birth, when they are unable to sit unassisted. Type I patients typically do not survive past 2 years of age.

Type II SMA, also called intermediate form, has three copies of SMN2. Afflicted babies, typically are affected before 18 months of age, when they are able to sit unassisted but are unable to stand. Type III SMA, also referred as Kugelberg-Welander disease, has three or four copies of SMN2; these patients show symptoms after 2 years of age. Type IV SMA, with more than four copies of SMN2, manifests with mild proximal muscle weakness, and patients typically have normal lifespans.
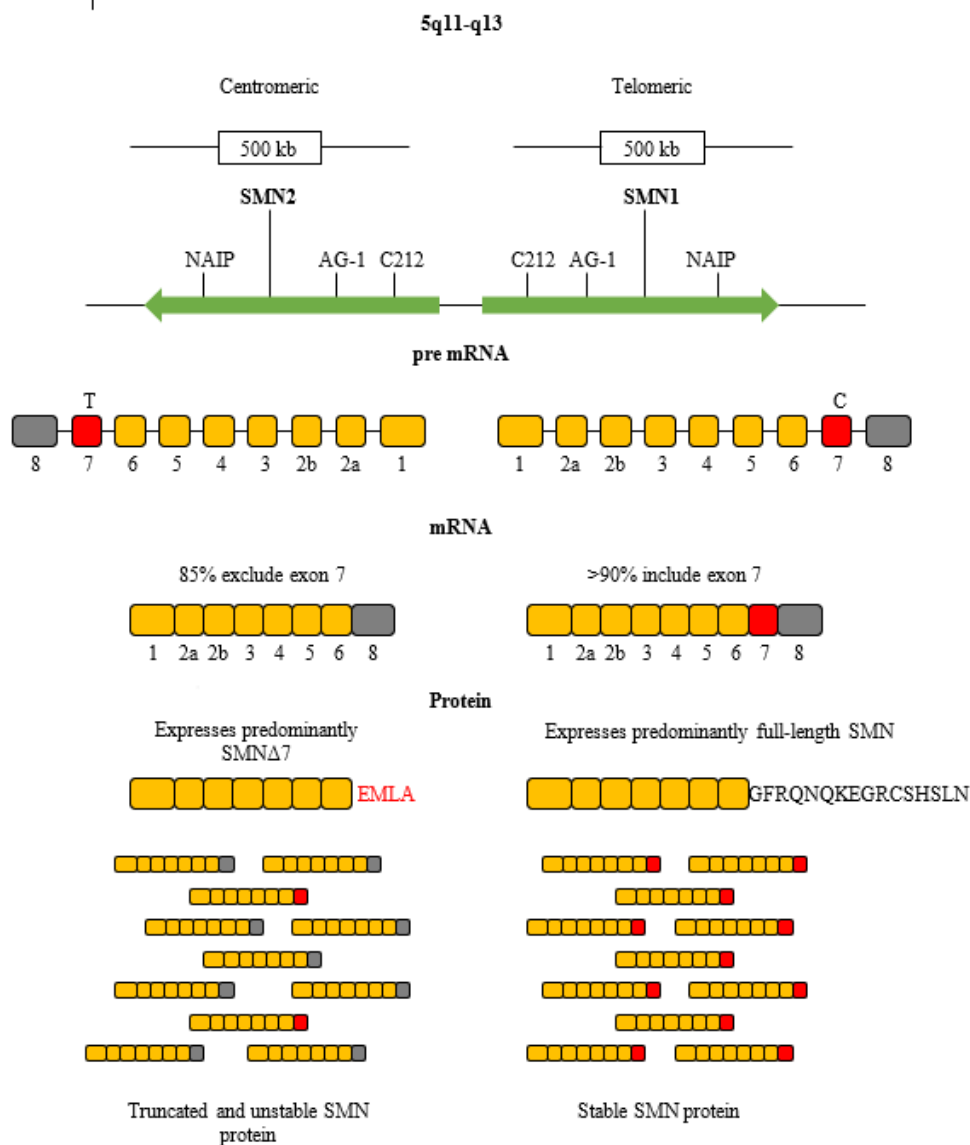
Figure 1 SMN genes

1.2 Therapeutic Strategies

Currently, several different therapeutic strategies[10] are being developed, the most interesting of which focus on SMN2, due to the inverse correlation between the number of copies of SMN2 and the severity of the disease. The possible pathways to slow the progression of the disease include increasing the transcription of SMN2, promoting the inclusion of exon 7 during the transcription, as well as stabilizing the SMN protein.

Another approach is using gene therapy to include a viral vector containing SMN1 to SMA mice. However, for gene therapy to work, the viral vector must be delivered to the correct cells after passing the blood-brain-barrier. The possibility of the immune system reacting to the introduction of the viral vector and the integration of the gene into the host genome are some

other potential problems for this strategy. For SMA, the viral vector used is self-complementary adeno associated virus 9 (scAAV9).

Another therapeutic strategy is the use of antisense oligonucleotides (ASO) designed to specifically target and inactivate the splicing silencer in order to include exon 7 and to increase the amount of protein. Spinraza, the first and only approved treatment for this illness, follows this mechanism of action.

1.3   Previous Work on Small molecules

A high-throughput screening (HTS) of small molecules, including repurposed drug[11], was tested on a cell based SMN2 reporter assay to identify the increase the SMN protein independently of the SMN2 translation. The cell-based reporter assay[12] contains luciferase that combines a SMN2 promoter, SMN exons 1-6 cDNA, followed by the splicing cassette containing intron 6, exon 7, intron 7 and exon 8. The terminal codon of exon was modified so, when spliced into exon 8, the SMN-firefly luciferase is in frame and can be detected. This was developed and used for the testing of repurposed drugs and small molecules for the increase the concentration of SMN protein.

LDN-75654 (Figure 2) is the hit compound identified by the Laboratory for Drug Discovery in Neurodegeneration (LDDN) and the Androphy Laboratory in the University of Indiana through screening in the SMN-luciferase reporter assay. **LDN-75654**, increases the stability of the SMN protein post-translationally, as proved by testing in the presence of SMN in SMA derived fibroblasts[13]. Although this compound had properties suitable for blood-brain-barrier penetration, it was established to be inactive *in vivo*, due to poor aqueous solubility and lack of metabolic stability. This small molecule, although inactive *in vivo*, presented an interesting lead for optimization.
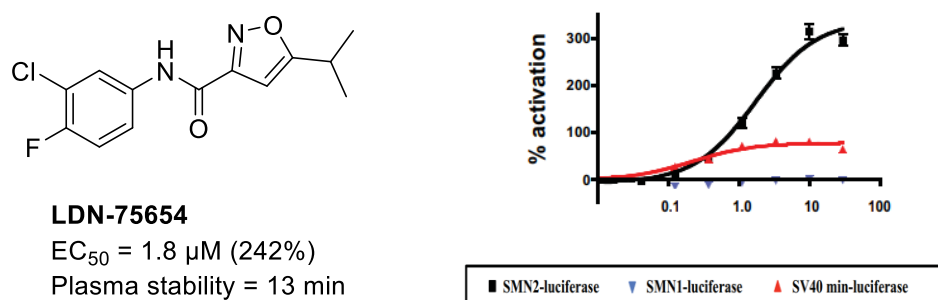

Figure 2 Structure and activity of LDN-75654 on the SMN2- luciferase

Through a structure-relationship relationship (SAR) study, several changes were introduced to the lead compound in order to increase the pharmacokinetics properties, potency and solubility (Figure 3).
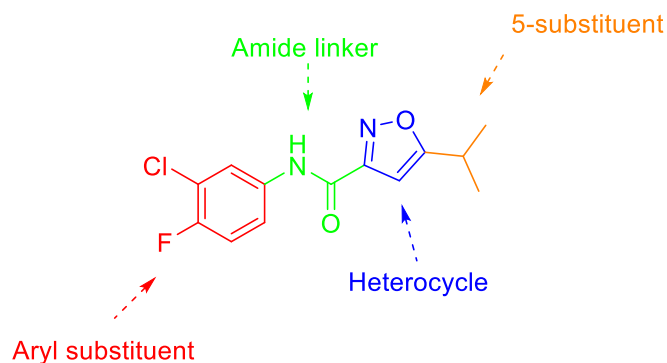
Figure 3 Hit compound and areas suitable for SAR study

To avoid the cleavage of the amide linker in the *in vivo* experiments[14], thus increasing the solubility of the compound, the amide was reversed, but the activity (**LDN-16**) (Figure 4) (EC$_{50}$ = 9.9 ± 0.8 µM, 188 ± 13) was significantly reduced. Replacing the isoxazole core with a thiazole core (**LDN-27**) increased the activity in the SMN-luciferase reporter assay.
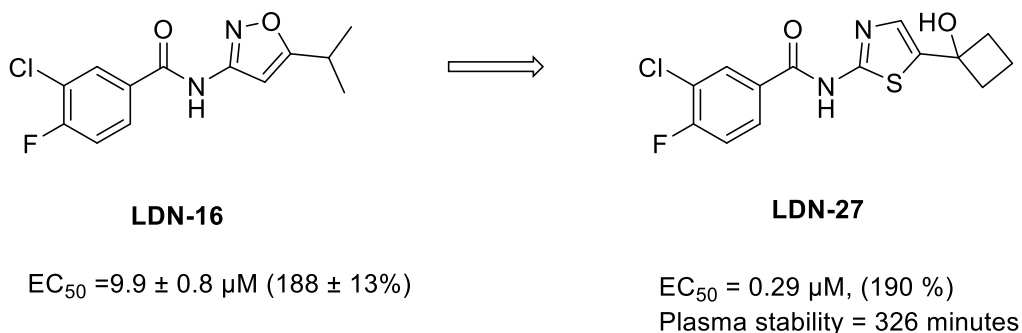

LDN-16

EC$_{50}$ =9.9 ± 0.8 µM (188 ± 13%)

LDN-27

EC$_{50}$ = 0.29 µM, (190 %)
Plasma stability = 326 minutes

Figure 4 Optimization results from SAR

A number of different heterocycles were tested as analogues with the optimization of the hit compound to improve its potency, pharmacokinetic properties, and plasma stability by a structure-activity relationship (SAR) study. This resulted in the lead compound **LDN-27** (EC$_{50}$ = 0.29 µM, 190 %, plasma stability = 326 minutes).
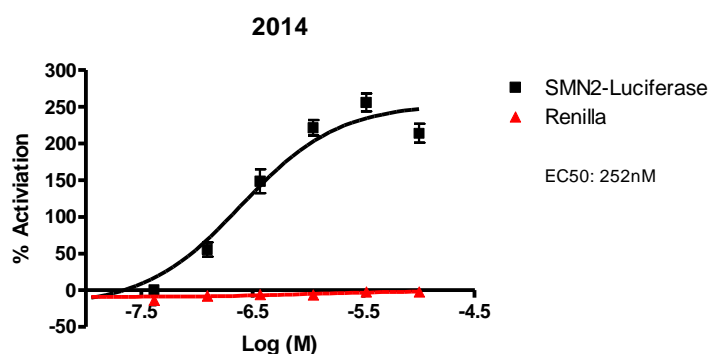
Figure 2 Activity of LDN-27 on the SMN-luciferase reporter assay

1.4 Aim of study

The aim of this project is to develop new analogues for the treatment of SMA by post translationally stabilizing the SMN protein with an imidazole core as the heterocycle, and to study its effect of the activity by means of the SMN-luciferase reporter assay as compared to the lead compound **LDN-27**.

An array of different substituents attached to the phenyl core in conjunction to various substituents to the imidazole core will be examined to observe the impact on the activity.

The imidazole ring proposed in this study is a possible heterocycle core that could improve the activity of the previous analogues. The imidazole ring is an aromatic five-member ring with two nitrogen atoms in the 1st and 3rd positions, and is present in many biologically active compounds, such as histidine and purine. Being a polar and ionisable aromatic ring, it can be used to improve the solubility and bioavailability of the previous poorly soluble lead compounds. It has amphoteric properties and the ability to form weak interactions[15].

It is widely used in the pharmaceutical industry in synthetic drugs due to the high therapeutic properties[16] it possesses, such as anticancer, anticoagulant, anti-inflammatory, anti-bacterial, antifungal, antiviral and analgesic properties, among others.

Some of the analogues synthesized for this project also will be tested as possible PET 3D scan tracers.

# 2 THEORY AND METHODS

2.1 *N*-Butyl lithium reaction

Organometallic lithium reagents are strong nucleophilic bases, with high reactivities due to the polarity of the metal-carbon bond, in presence of water subtracts a hydrogen to form the corresponding hydrocarbon and lithium hydroxide (weak acid). The disadvantages of the organometallic reagents are the necessity of using very low temperatures (0 to -78º C) to avoid the undesired competitive reactions and the use of anhydrous solvents and inert atmosphere to avoid its degradation, which can react violently with air or moisture[17].
This type of reagent is used for many different applications such as for the synthesis of tertiary alcohols by a carbon-carbon bond forming reaction from ketones[18], and its application is of interest for this project.

The *n*-BuLi reacts with the imidazole ring to form and imidazole lithium complex in the first step of the mechanism.

In the second step of the mechanism, the organometallic lithium complex acts as a nucleophile attacking the electrophilic carbon of the cyclobutanone, forming the corresponding alcohol once the reaction mixture is quenched with acid water, a saturated solution of ammonium chloride.

Nucleophilic attack of the carbanionic carbon in the organometallic reagent with the electrophilic carbon in the carbonyl to form alcohols.
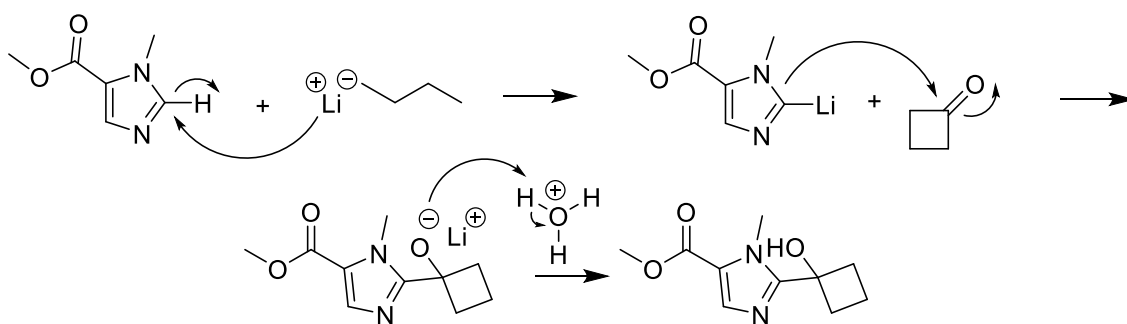
Scheme 3 n-BuLi reaction mechanism

2.2 Trimethylaluminum mediated amide coupling

The usual aminolysis starting from carboxylic esters procedure is a three-step sequence involving hydrolysis, carboxylic acid activation and treatment with an amine. Although possible, the direct conversion of amines and esters to carboxamides was limited by harsh conditions and long reaction times until the report, in 1977, by Weinreb et al, of the utilization of trimethylaluminum amides to yield the desired aminolysis under mild reaction conditions[19-

[20], making possible to avoid the three-step sequence. Trimethylaluminum (Me₃Al) is a Lewis acid that promotes the activation of electronegative atoms, such as nitrogen and the nucleophilic substitution reactions[21].

The nitrogen on the aniline acts like a Llewis base that reacts at 0° C with trimethylaluminium with evolution of methane forming a dimethylaluminum amide complex [Scheme 4], which is unstable at high temperatures and further reacts with the carboxylic ester group while gently warming up to room temperature (RT) for 2h. The aluminium complex formed is quenched with a phosphate buffer that precipitates Aluminium phosphate ($AlPO_4$) and is filtered out.

The disadvantages of this reaction are the handling of trimethylaluminum that is highly pyrophoric and the competition between functional groups like carboxylic acids or nitriles with the carboxylic ester.
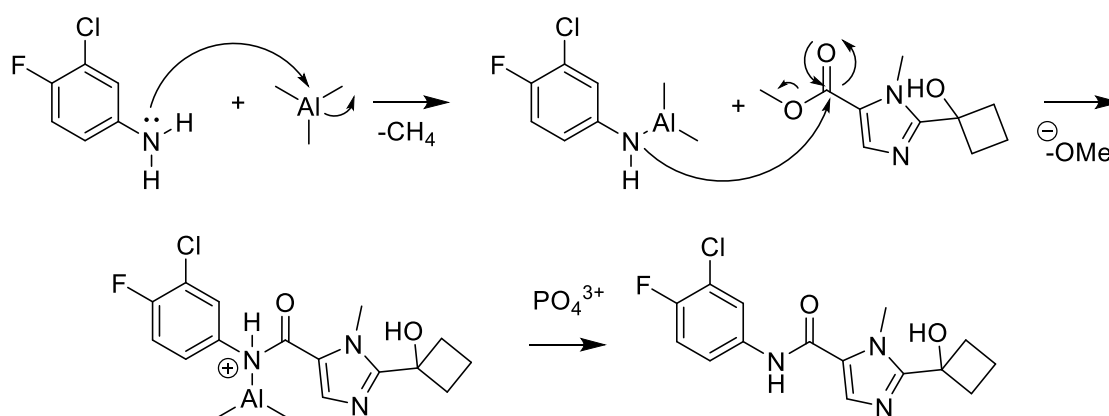
Scheme 4 Proposed mechanism for the trimethylaluminum promoted aminolysis

2.3   Nuclear Magnetic Resonance Spectroscopy

Nuclear magnetic resonance (NMR) spectroscopy is one of the most useful techniques for structure determination in organic compounds as it provides a carbon-hydrogen framework of the molecule.

This technique is based on the atoms that have isotopes with a characteristic nuclear spin (I) quantum number I = ½ such as ^{1}H and ^{13}C. In presence of an external magnetic field B_0 the spin gets orientated creating two different energy levels proportional to ±I.

In the absence of a magnetic field, the spin of the nuclei is randomly oriented, but when an external magnetic field B_0 the nuclei spins orientate into determined positions, parallel or antiparallel to the magnetic field that have different energy levels.

If the oriented nuclei are irradiated by energy with the right frequency that follows the resonance condition, the nuclei spins absorb enough energy to reverse their spin orientation. In so doing the nuclei reach a higher energy state. To have an NMR signal a difference in

population between the levels must exist and the intensity of the signal depends upon the size of the difference in population[22].
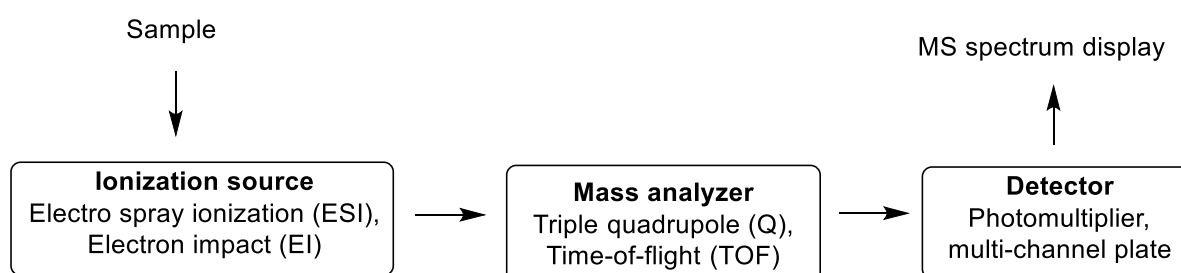
The magnet is a vital part of the NMR spectrometer, and it is directly related to the quality of the experimental measurement and the final spectrum. In modern instruments, the magnetic field B_0 is directed along the axis of the sample tube.

The probe-head of the NMR spectrometer contains the sample, its formed by the transmitter and receiver coils. The transmitter provides the various frequencies needed for the NMR experiment by means of a radiofrequency and a frequency synthesizer. It also produces the pulses required for the NMR experiment. The receiver collects the radiofrequency voltage corresponding to the energy of the NMR transition. After the signal is received, the signal must be amplified and processed by the computer.

2.4   Mass Spectrometry

Mass Spectrometry is an analytical technique used to determine the molecular weight of a molecule and to obtain structural information of the structure by measuring the molecular weight of the fragments produced when the molecule is irradiated with energy. It is a destructive technique, and it differs from other spectral analysis because the sample does not absorb radiation from the electromagnetic spectrum. Only small amounts of a sample are necessary due to the high sensitivity of the technique.

Every mass spectrometer has three basic parts, regardless of the intended use for it [Scheme 4, Figure 3]. An ionization source, in which the sample is bombarded with a stream of high-energy electrons that produces the dislodging of a valence electron form the molecule forming a radical cation [Scheme 5], that leads to the fragmentation of the molecule. A part of the fragments keeps the positive charge formed by losing an electron, the rest of the fragments keep neutral charge.

Sample

MS spectrum display

Ionization source
Electro spray ionization (ESI),
Electron impact (EI)

Mass analyzer
Triple quadrupole (Q),
Time-of-flight (TOF)

Detector
Photomultiplier,
multi-channel plate
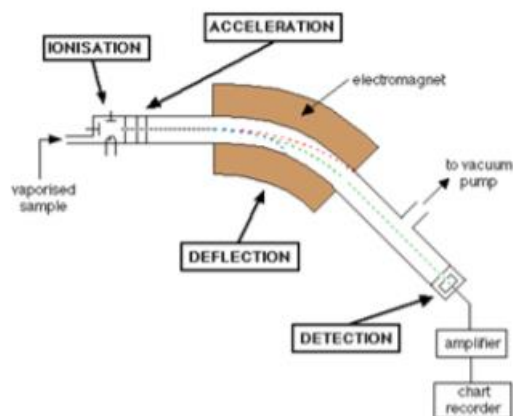
Scheme 5

Figure 3 General scheme of a mass spectrometer
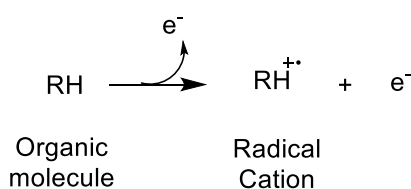
Scheme 6 Formation of the radical cation

A mass analyzer, in which the different fragment ions formed are separated by their mass to charge ratio m/z. A strong magnetic field is applied to a curved chamber in which the neutral fragments are lost on the walls and the charged fragments are deflected into different paths depending on their m/z. For this project the mass analyzer utilized for both LC-MS and GC-MS was a triple quadrupole.

The triple quadrupole analyzer consists of four parallel metal rods that transmit varying radio frequency voltages along the axis of the rods in order to scan a range of different m/z values. The quadrupole can also be set to monitor a specific m/z value. When using a triple quadrupole different operational mode can be set depending on the application, a particularly interesting configuration is obtained when a combination cell is placed in between two mass analyzers, in which two stages of mass analysis are independently applied. This combination increases the sensitivity of the analysis over single stage mass analysis.
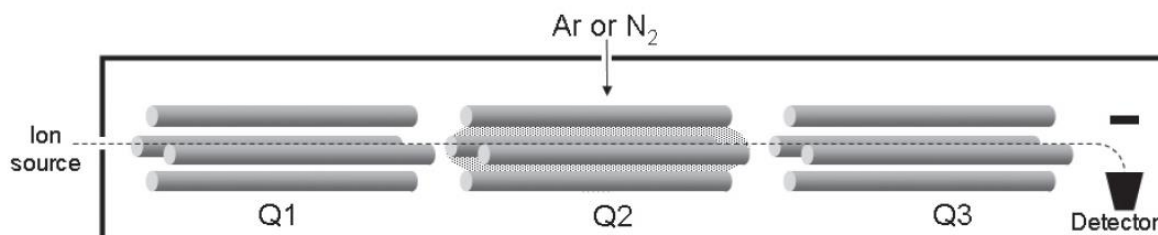
Figure 4 Triple quadrupole analyzer

And finally, a detector in which the ions are counted and recorded into peaks[23-24].

2.4.1 Liquid Chromatography Mass Spectrometry

A chromatography technique is used to separate mixtures of compounds into individual components. By coupling chromatography with mass spectrometry every component of the analyte sample can be separated and evaluated individually. The main difference about the LC-MS and GC-MS is the mobile phase used, in liquid chromatography mass spectrometry (LC-MS) the mobile phase is a solvent.

The coupling of liquid chromatography with mass spectrometry was limited by the incompatibility of ionization source with a liquid stream of the sample until the development of the electro spray ionization (ESI) source in the 1980s[25-27]. That is the same ionization source used for the analysis during this project.

ESI is a robust ionization method that operated under atmospheric pressure and is based on the nebulizer-principle as a soft ionization due to the fact that little energy is imparted to the analyte that cause little fragmentation. In the chamber there is a difference of potential between the tip of the nebulizing needle and the orifice of the dielectric capillary [Figure 5]. The difference of potential produces a pointed cone of the sample solution, known as the Taylor cone, from where a spray of charged droplets are emitted. A drying gas, normally nitrogen (N_2) evaporates the solvent until the solvated ions are expelled from the droplet and passed to the m/z analyzer. This method works well for non-volatile, thermally labile polar molecules and can be operated in order to detect both positive and negative ions.
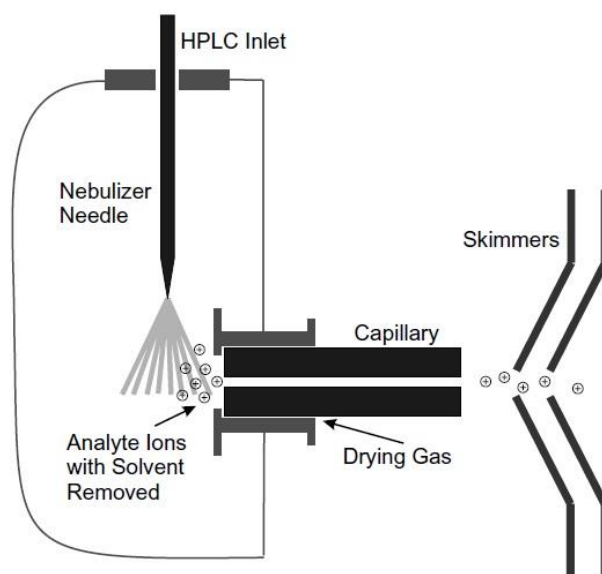
Figure 5 ESI

2.4.2 Gas Chromatography Mass Spectrometry

As mentioned previously the main difference between GC-MS and LC-MS is the mobile phase used, in this case the mobile phase is an inert gas such as nitrogen. The mobile phase carries the sample through the stationary phase in which all the components from the sample interact and elute at different rates, hence the separation of the components.

As the individual components elute from the GC column, they enter the ionization source. In this case the ionization source is electron impact (EI) [Figure 6], in which the analyte is bombarded with a high-energy electron beam producing the formation of the radical cation that further breaks into fragments [Scheme 7], some retaining charge some with neutral charge.

$$M + e^- \longrightarrow M^{+\cdot} + 2e^-$$
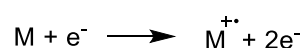
Scheme 7 Formation of the radical cation
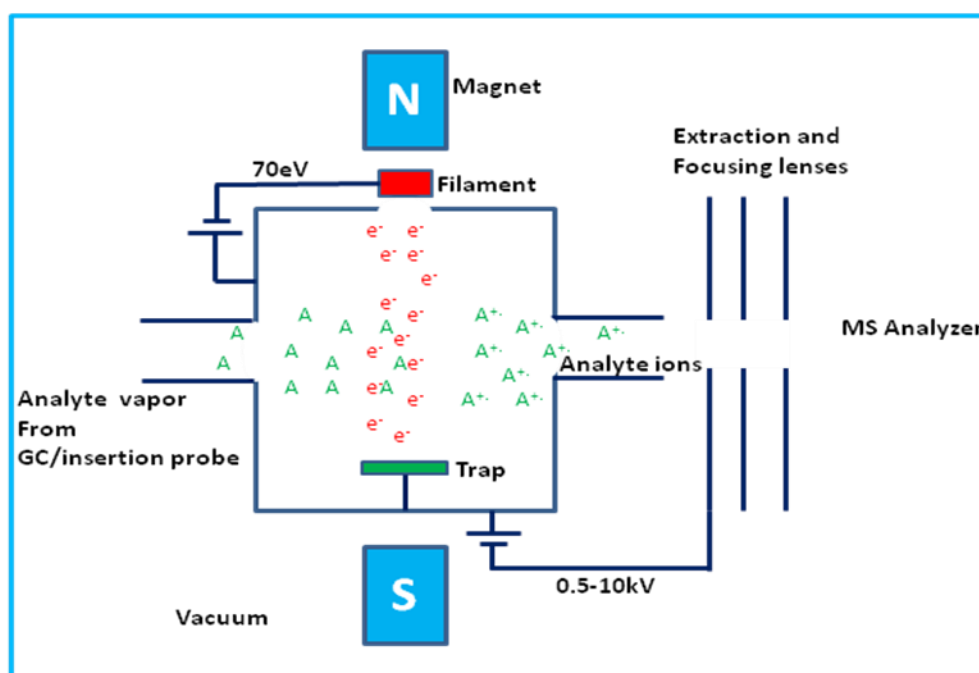
Figure 6 EI

In contrast to the little fragmentation observed by LC-MS ESI, the fragmentation observed by GC-MS EI is more extensive, and creates a spectral pattern that can be helpful for the identification of chemicals by comparing the spectral data with a mass spectra library.

This ionization method is useful to analyze non-polar insoluble samples that are volatile and thermally stable.

2.5 High Performance Liquid Chromatography

High performance liquid chromatography (HPLC) is a modern liquid chromatography technique able to separate and quantify, with high sensitivity, compounds in a mixture based on the retention time using operational pressures higher than the pressures used for ordinary liquid chromatography. More efficient separations are achieved by using a stationary phase consisting on small particles[28].

It is the method used for the separation of non-volatile, very polar and ionic compounds with high molecular mass used during this project for the most complicated separations.

2.6 SMN2 – Luciferase Reporter Assay

The testing for the increase of SMN protein was done by means of the second generation SMN-luciferase reporter assay developed by Androphy and co-workers that combines the strengths of both previous assays, a promoter-based assay and a splicing reporter. Making the assay more robust, with lower variation and more stable luciferase expression[12,13].

The activity was confirmed in the SMN-luciferase cell line and counter-screened with a control cell line expressing luciferase. Good potency, strength of activation, dose dependency and favourable chemical properties should be over >60%. For a good compound the increase in luciferase activity should be over 100% and increase the control reporter cell line by less than 40 %. The testing was done by dose response experiments, increasing concentration values from 0.04 to 30 µM. The average potency denoted as EC_{50}, concentration required in order to achieve the 50% of the maximal drug response and E_{max}, indicates the maximal % increase in luciferase activity observed with treatment.

2.7 Positron Emission Tomography 3D Scan

Nuclear functional imaging technique used to observe metabolic processes in the body. The system detects gamma rays emitted by a positron emitting radioligand.

The development of positron emission tomography (PET) during the 1930s made possible the idea of *in vivo* measurement of biological or biochemical processes by producing radionuclides of chemical elements including carbon and fluoride that decay under positron emission, also known as positive beta decay, that is radiation externally detectable. PET employs short-lived positron emitting radionucleotides such as ^{11}C ($t_{1/2}$ = 20 min), ^{13}N ($t_{1/2}$ = 10 min) and ^{18}F ($t_{1/2}$ = 110 min)[29], that can take the place of other non-radioactive atoms in an active molecule that

bind to receptors or other sites of drug action, this type of molecules are called radioactive tracers.

Due to the short half-life of the positron-emitting radioisotopes, the tracers tend to be produced in a cyclotron close to the PET facility. For this project the radiolabelling reaction was tested on an Agilent Technology 1260 Infinity with a LabLogic Radio-HPLC detector Posi-RAM model 4. The radionuclide was obtained by reducing radioactive carbon dioxide (CO_2) and reacting it with Hydroiodic acid (HI). The reaction was done at room temperature [Scheme 8].
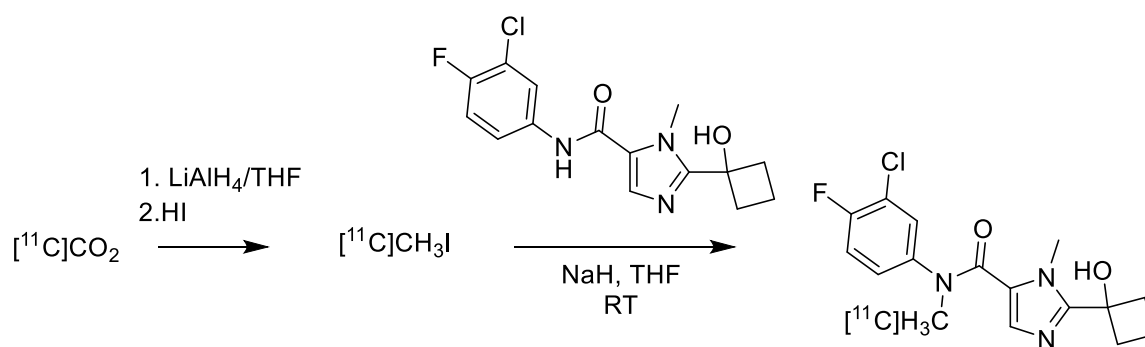
Scheme 8 Radiolabelling reaction scheme used in this project

3   RESULTS AND DISCUSSION

3.1   Synthesis of *N*-(3-chloro-4-fluorophenyl)-2-(1-hydroxycyclobutyl)-1-methyl-1*H*-imidazole-5-carboxamide (**4**) and other analogues

3.1.1   Optimization of the *N*-BuLi reaction for the synthesis of Methyl 2-(1-hydroxycyclobutyl)-1-methyl-1*H*-imidazole-5-carboxylate (**1**)

In order to attach cyclobutanone to the second position of the imidazole ring using *n*-utyl lithium (*N*-BuLi) several experiments were carried with different conditions in order to optimize the reaction and achieve the highest yield possible [Table 1]. Methyl 1-methyl-1*H*-imidazole-5-carboxylate was dissolved in anhydrous tetrahydrofuran THF and cooled down to -78º C or -40º C with a dry ice/acetone bath. *N*-BuLi was added drop-wise over a period of 15 minutes. Cyclobutanone was added either before the *N*-BuLi or after 45 minutes depending on the conditions. The reaction mixture was quenched with ammonium chloride to yield methyl 2-(1-hydroxycyclobutyl)-1-methyl-1*H*-imidazole-5-carboxylate **1** [Scheme 9].
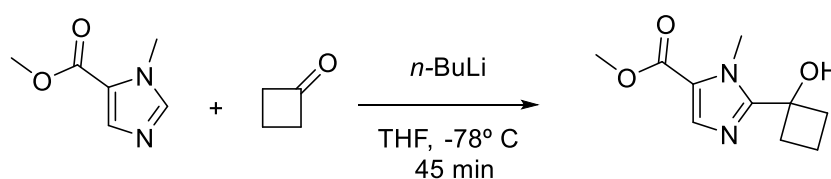
*Scheme 9 Synthesis of methyl 2-(1-hydroxycyclobutyl)-1-methyl-1H-imidazole-5-carboxylate (**1**)*

Exp	T (° C)	t	Eq	Add of cyclo	Base	Yield (%)
379-12	-78° C	30 min/ ON	1.3	2nd step	*n*-BuLi	8.33 %
379-14	-78° C	30 min/45 min	1.3	2nd step	*n*-BuLi	8.33 %
379-15	-40° C	30 min/ 45 min	1.3	2nd step	*n*-BuLi	1.32 %
379-16	-78° C	10min/ 45 min	1.3	2nd step	*n*-BuLi	8.29 %
379-17	-78° C	45 min	1.3	1st step	*n*-BuLi	35.83 %
379-19	-78° C	45 min	2	1st step	*n*-BuLi	46.96 %
379-26	-78° C	45 min	2.5	1st step	*n*-BuLi	42.08 %

*Table 1 Overview of the contions used for the optimization and symthesis of **1***

Based on the yields obtained from this series of reactions the optimal conditions for the *N*-BuLi for the synthesis of **1** were adding cyclobutanone before 2 equivalents of *n*-BuLi were added drop-wise at - 78º C for 45 minutes.

The ^{1}H NMR spectrum of the product confirms the structure of the molecule with the only aromatic proton appearing in the most downfield part of the spectrum at 7.53 ppm, the proton corresponding to the hydroxy group appearing at 5.98 ppm and the six protons corresponding to the cyclobutyl appearing in the most upfield region of the spectrum [Figure 7]. The synthesis of the compound **1** was also confirmed by LC-MS [Anexe].
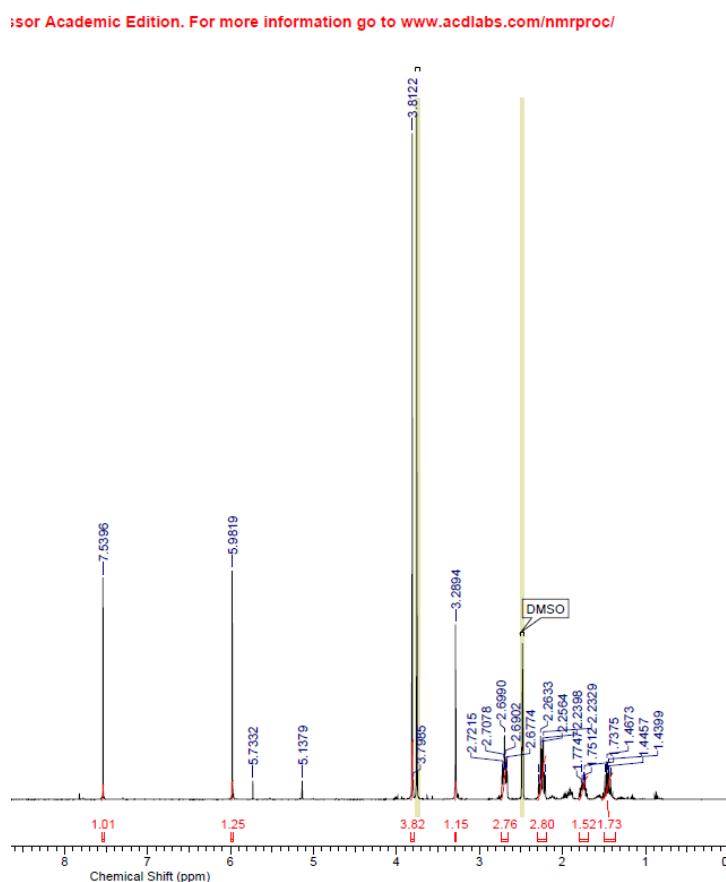
*Figure 7 ^{1}H NMR spectrum of **1***

3.1.2 Methyl 2-(1-hydroxyethyl)-1-methyl-1*H*-imidazole-5-carboxylate (**2**)

After the optimal conditions for the synthesis of methyl 2-(1-hydroxycyclobutyl)-1-methyl-1*H*-imidazole-5-carboxylate were achieved, the same reaction conditions were used for the synthesis of methyl 2-(1-hydroxyethyl)-1-methyl-1*H*-imidazole-5-carboxylate (**2**) [Scheme 10].
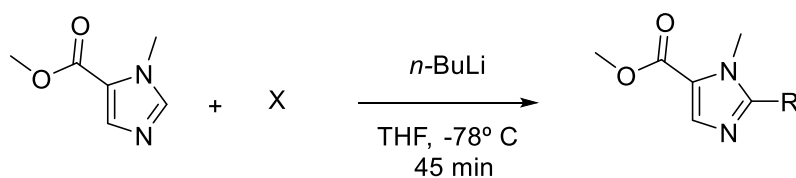
*Scheme 10 Synthesis of methyl 2-(1-hydroxyethyl)-1-methyl-1H-imidazole-5-carboxylate (**2**)*

Based on the difference on the isolated yield, the conditions for the synthesis of **2** might need to be optimized in order to obtain a similar yield as the one obtained for **1** [Table 2].

Compound #	X	R	Isolated yield
1			46.96 %
2			22.08 %

*Table 2 Comparation of yisolated yields for **1** and **2***

The structure of the compound 2 was confirmed by ^{1}H NMR spectroscopy with the sole aromatic proton of the Imidazole core appearing at 7.53 ppm in the most downfield region of the spectrum and the proton of the hydroxy substituent on the 2nd position appearing at 5.43 ppm [Figure 8].
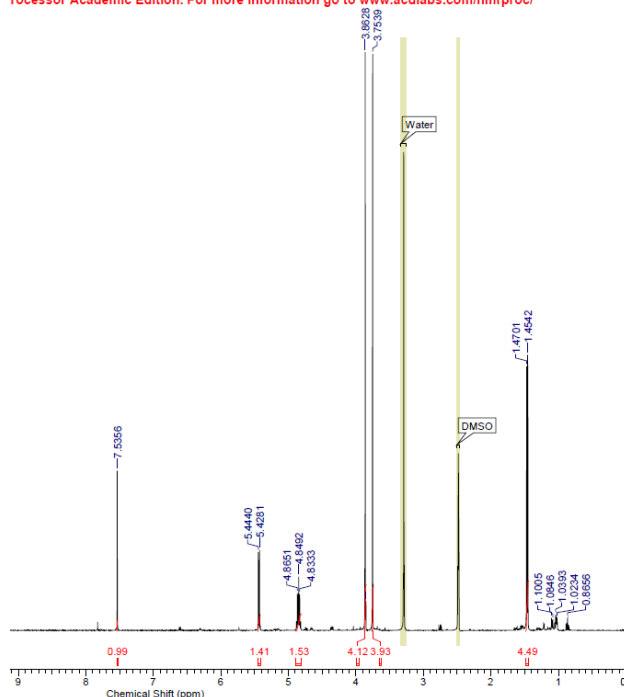
Figure 8 ¹H NMR spectrum of 2

3.1.3   Methyl 1-cyclobutyl-1*H*-imidazole-5-carboxylate (**3**)

Methyl 1*H*-imidazole-5-carboxylate and caesium carbonate were dissolved in DMF, bromocyclobutane was added dropwise and stirred overnight to yield methyl 1-cyclobutyl-1*H*-imidazole-5-carboxylate (**3**) [Scheme 11].
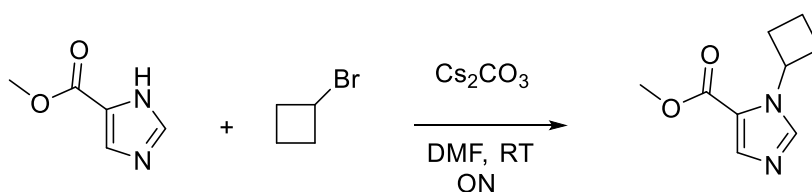
Scheme 11 Synthesis of methyl 1-cyclobutyl-1H-imidazole-5-carboxylate (3)

The main difference between the ¹H NMR spectrum for the compound 3 and the spectra for 1 and 2 is the presence of a second more deshielded aromatic proton due to the lack of a substituent in the 2nd position of the imidazole ring [Figure 9].
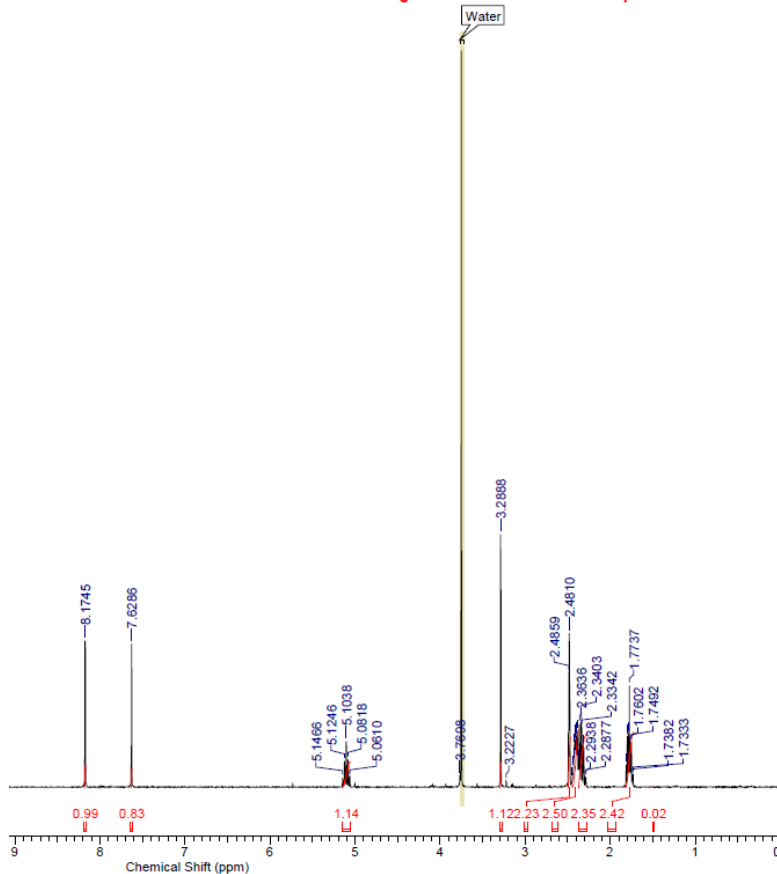
*Figure 9 ^{1}H NMR spectrum of **3***

3.1.4 *N*-(3-chloro-4-fluorophenyl)-2-(1-hydroxycyclobutyl)-1-methyl-1*H*-imidazole-5-carboxamide (**4**) and analogues

A series of different analogues were synthesised by using the aminolysis procedure [Scheme 12]. The corresponding aniline was dissolved in dry DCM and cooled down to 0º C, trimethylaluminum, under inert atmosphere to avoid a violent reaction with air and moisture, was added dropwise and stirred for an hour. The corresponding methyl carboxylate solution was added dropwise and stirred for two hours to yield the desired analogue.
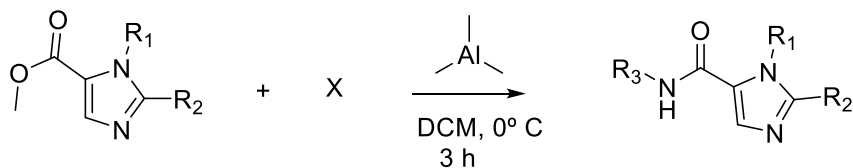
Scheme 12 General Scheme for the aminolysis reaction

Table 3 summarises the eight reactions used for the synthesis of the different analogues following this procedure.
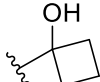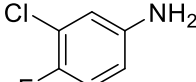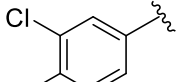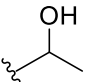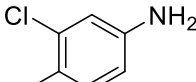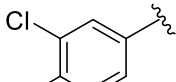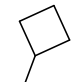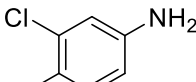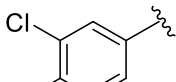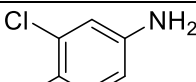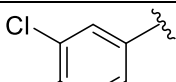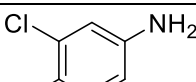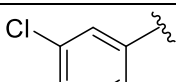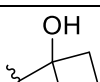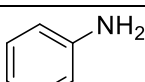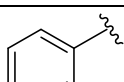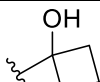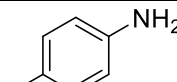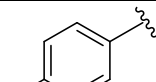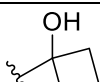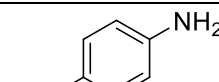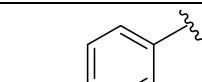
Compound #	R₁	R₂	X	R₃	Iso. Yield
4	Me	1-hydroxycyclobutyl (OH)	3-chloro-4-fluoroaniline (Cl, F, NH₂)	3-chloro-4-fluorophenyl (Cl, F)	47.84 %
5	Me	1-hydroxyethyl (OH, CH₃)	3-chloro-4-fluoroaniline (Cl, F, NH₂)	3-chloro-4-fluorophenyl (Cl, F)	16.72 %
6	cyclobutyl	H	3-chloro-4-fluoroaniline (Cl, F, NH₂)	3-chloro-4-fluorophenyl (Cl, F)	60.12 %
7	Me	H	3-chloro-4-fluoroaniline (Cl, F, NH₂)	3-chloro-4-fluorophenyl (Cl, F)	17.50 %
8	H	H	3-chloro-4-fluoroaniline (Cl, F, NH₂)	3-chloro-4-fluorophenyl (Cl, F)	5.89%
9	Me	1-hydroxycyclobutyl (OH)	aniline (NH₂)	phenyl	9.90 %
10	Me	1-hydroxycyclobutyl (OH)	4-fluoroaniline (F, NH₂)	4-fluorophenyl (F)	9.26 %
11	Me	1-hydroxycyclobutyl (OH)	4-methoxyaniline (MeO, NH₂)	4-methoxyphenyl (MeO)	86.24%

Table 3 Overview of the synthesis of compounds 4 to 11

The compounds **4-11** were analyzed by means of ^{1}H NMR spectrometry and LC-MS. The ^{1}H NMR spectrum of the compound **4** [Figure 10] shows the proton attached to the amide nitrogen in the most downfield part of the spectrum at 10.16 ppm, the only aromatic proton at the 4th position of the imidazole core appears at 7.66 ppm and the proton of the hydroxy group appears at 5.64 ppm.
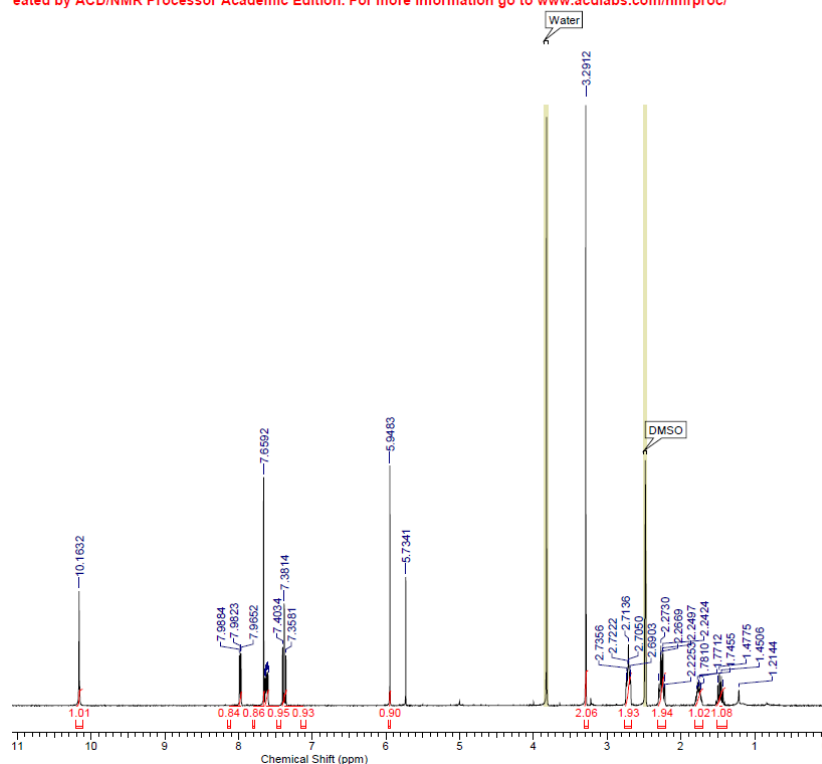
*Figure 10 ^{1}H NMR spectrum of compound **4***

The ^{1}H NMR spectrum of the compound **5** [Figure 11] shows the aromatic proton at the 4th position of the imidazole core appears at 7.66 ppm. The proton attached to the carbon on the 2nd position appears slightly deshielded at 5.01 ppm due being linked to the hydroxy group.
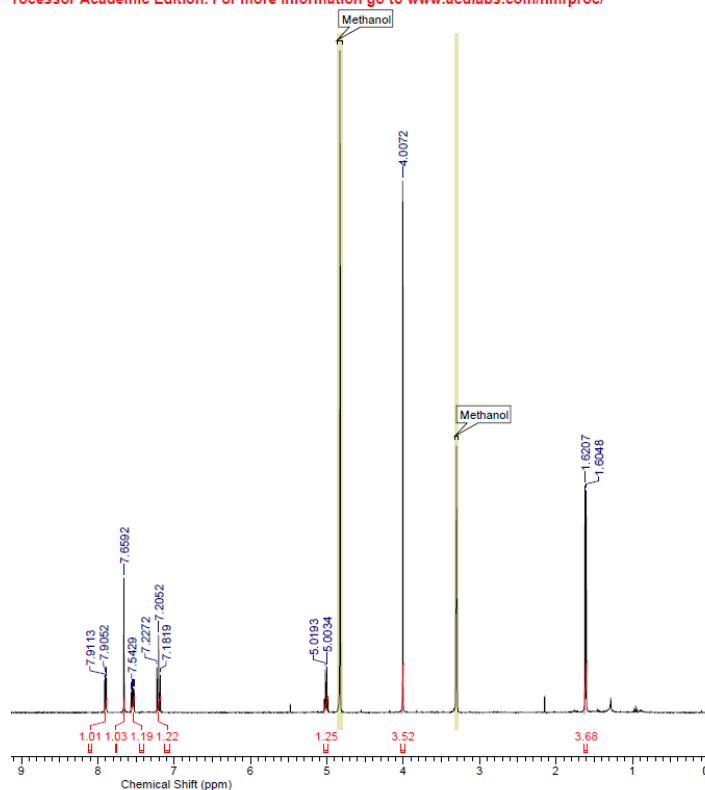
Figure 11 ¹H NMR spectrum of compound 5

The proton attached to the nitrogen atom on the amide group in the ¹H NMR spectrum for the compound **6** appears at the downfield region of the spectrum at 10.10 ppm. Both of the aromatic protons of the imidazole cycle appear at 8.02 and 7.91 ppm. The protons of the cyclobutyl substituent appear in the upfield region of the spectrum in three multiplets, being the proton linked to the nitrogen the most deshielded at 4.81-4.73 ppm [Figure 12].
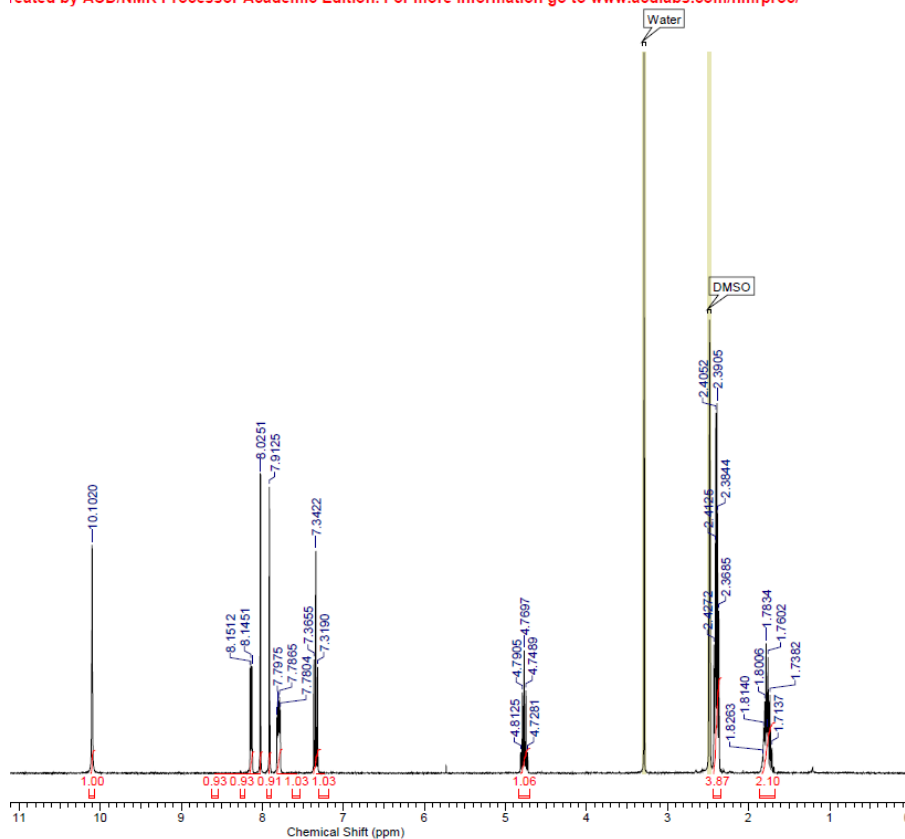
Figure 12 ¹H NMR spectrum of compound 6

The ¹H NMR spectra for the compounds **7** and **8** are significantly simpler than the rest due to the lack of a cyclic substituent in the 2nd position of the imidazole ring. The ¹H NMR spectrum for compound **7** shows all the aromatic protons corresponding for both the phenyl and imidazole rings, 7.79 and 7.75 ppm for the imidazole aromatic protons. The three protons of the methyl substituent on the 1st position of the imidazole appear in a singlet at 3.95 ppm [Figure 13].
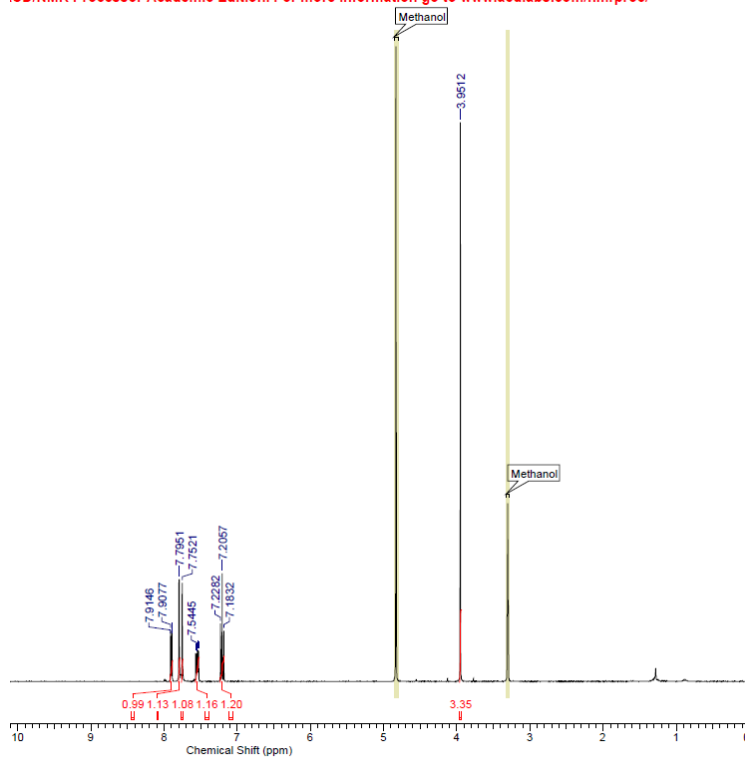
Figure 13 ^{1}H NMR spectrum of compound 7

The ^{1}H NMR spectrum for compound **8** is very similar for that of the compound **7**. All the protons of the compound appear in the aromatic region of the spectrum with the protons of the imidazole ring appearing at 7.79 and 7.75 ppm [Figure 14].
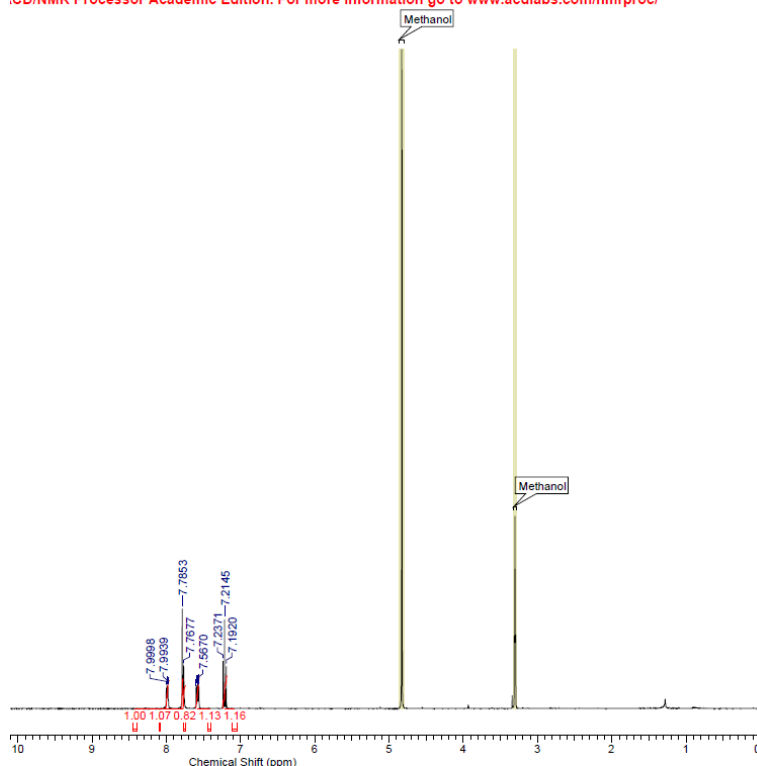
Figure 14 ^{1}H NMR spectrum of compound 8

The ^{1}H NMR spectrum for compound **9** is the first one of the analogues to not have the two halogen substituents in the phenyl ring, due to this the main difference from compound **4** is in the aromatic region. The aromatic proton from the imidazole core appears as a singlet at 7.64 ppm, the six aromatic protons appear combined in three multiplets at 7.63-7.61, 7.35-7.31 and 7.12-7.10 ppm [Figure 15].
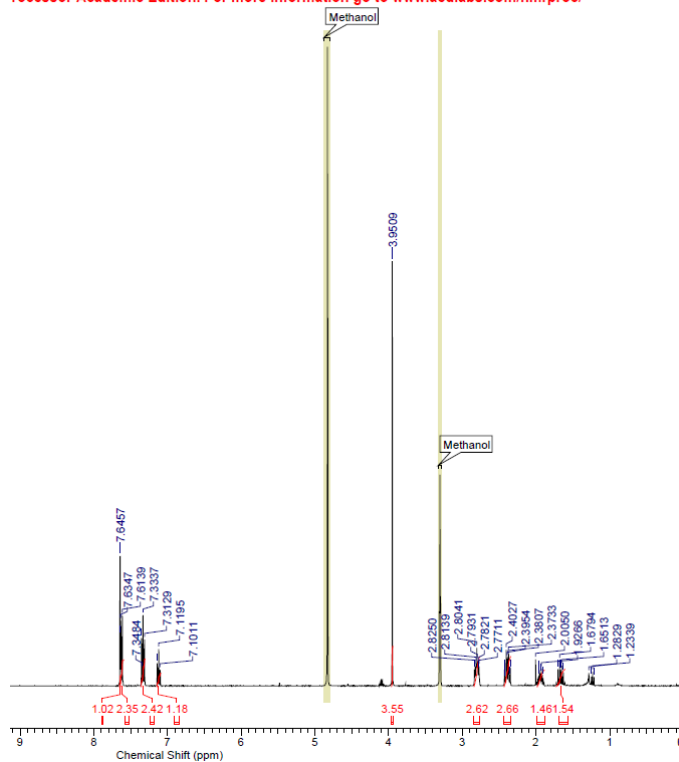
Figure 15 ^{1}H NMR spectrum of compound 9

The main difference between the ^{1}H NMR spectra for compound **4** and **10** is once again the aromatic region. For compound **10** the proton of the imidazole ring appears at 7.63 ppm and the four aromatic protons from the phenyl ring appear combined in two multiplets at 7.65-7.61 and 7.07 ppm [Figure 16].
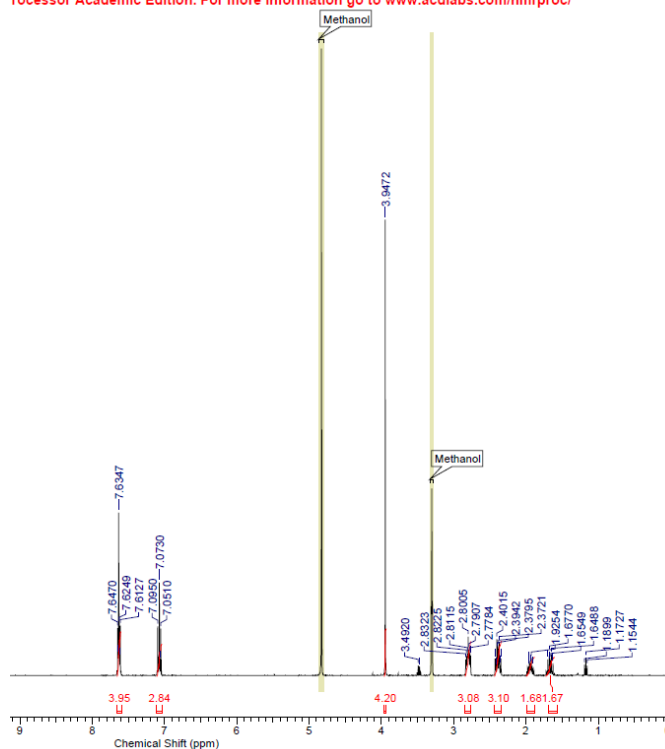
Figure 16 ^{1}H NMR spectrum of compound 10

Compound **11** was used without further purification for a following reaction. The ^{1}H NMR spectrum shows some unidentified impurities in the upfield region of the spectrum. The aromatic proton of the imidazole ring appears as a singlet at 7.61 ppm. The protons for both methyl substituents appear as two singlets at 3.94 and 3.79 ppm [Figure 17].
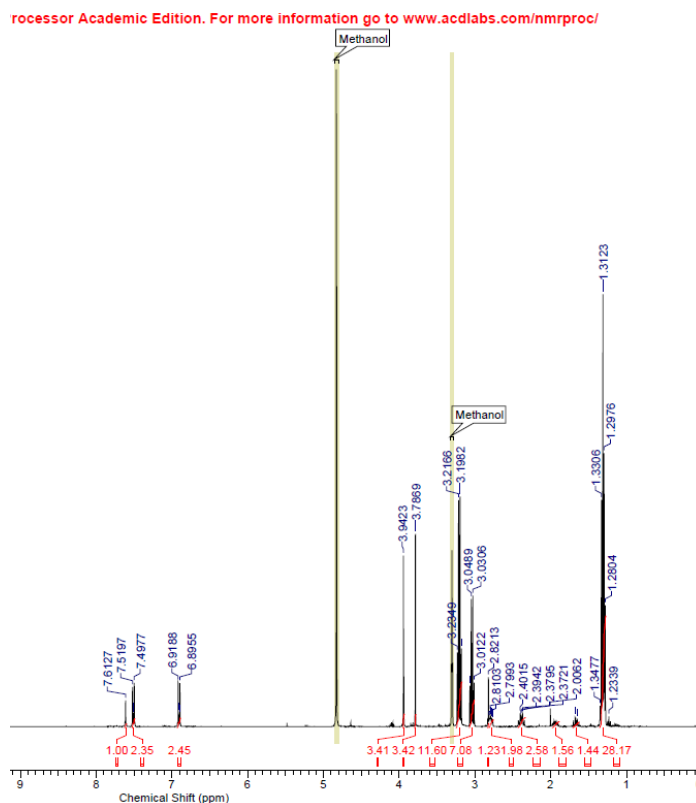
*Figure 17 ¹H NMR spectrum of compound **11***

Compounds **4** to **10** were tested for stabilization of the SMN protein in mice on the SMN-luciferase reporter assay previously mentioned, this reporter assay was used as well for the previous hit compounds obtained by the SAR study. The objective of this project was to increase the activity and potency of the previous analogues by introducing a core which was not tested before. Study of a series of very similar analogues and the effect of those small differences for the activity.

Curves for each tested compound were generated to determine EC_{50} values and percentage increase with a maximal concentration of 30 µM. Each compound was tested on two separate occasions and the values reported are the average of those experiments.

A compound is considered inactive when the SMN-luciferase percentage induction is less than 150% and EC_{50} is less than 1 µM. % needs to be as high as possible, EC_{50} has to be as low as possible.

For compounds **4** to **8** most of the scaffold was kept constant and the substituents on the 1st and 2nd positions of the imidazole ring were modified.

Compound **4** is the most similar structure to the original hit compounds, having the orientation of the amide linker as **LDN-75654** and the same heterocycle substituent as **LDN-27**. In this case the average E_{max} is 227.05% is higher than activation percentage for the previous hit compounds. The average value of $EC_{50} = 3.35$ µM is as well higher than the values for the hit

36

compounds, both of values indicate that the compound is active for the stabilization of SMN on the reporter assay however is not as active as the hit compounds [Figure 18].
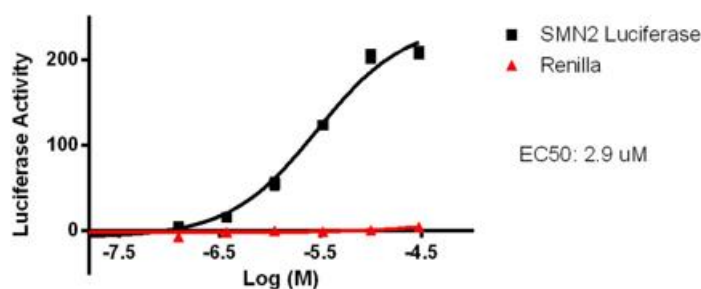

Figure 18 Activation of the SMN-Luciferase reporter assay of 4

The difference between **4** and **5** resides in the substituent of 2nd position of the imidazole ring. The value of E_{max} **5** is 22.95%, since it is lower than 100% the compound it is not active [Figure 19]. The disparity between results indicate that the presence of a cyclic substituent might be significant for the stabilization.
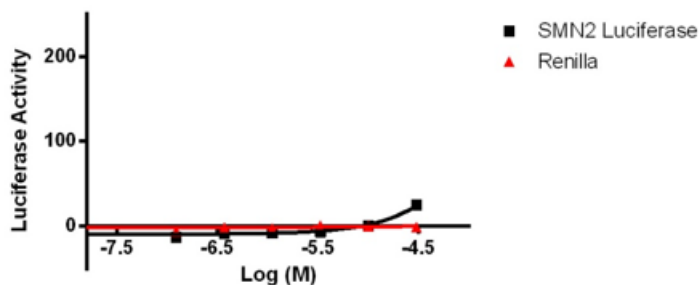
Figure 19 Activation of the SMN-Luciferase reporter assay of 5

In the case of **6** the value of $E_{max} = 126.9$ % indicates some activity, however the value of EC_{50} and the graph indicate that the compound is not active [Figure 20]. This result might indicate that the bigger size of substituent on the 1st position reduces the activity.
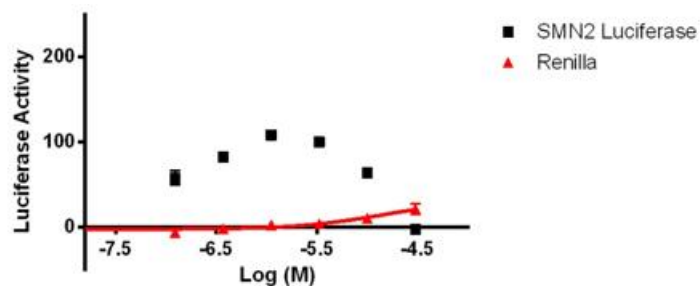
*Figure 20 Activation of the SMN-Luciferase reporter assay of **6***

For the case of **7** the lack of a substituent on the 2nd position reduces the activity almost completely. $E_{max} = 16.65\%$ [Figure 21].
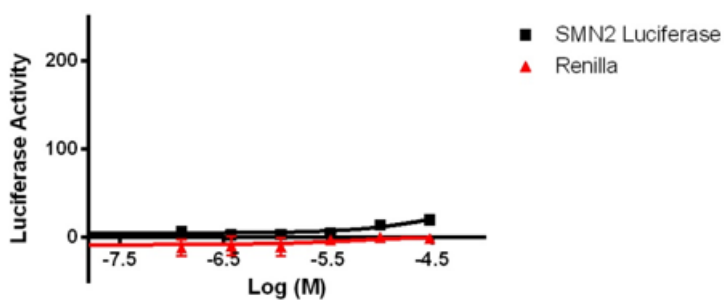
*Figure 21 Activation of the SMN-Luciferase reporter assay of **7***

Surprisingly, the value $E_{max} = 123\%$ is higher than expected for **8**, the lack of substituents made the compound somewhat active but not enough active to become a new lead [Figure 22].
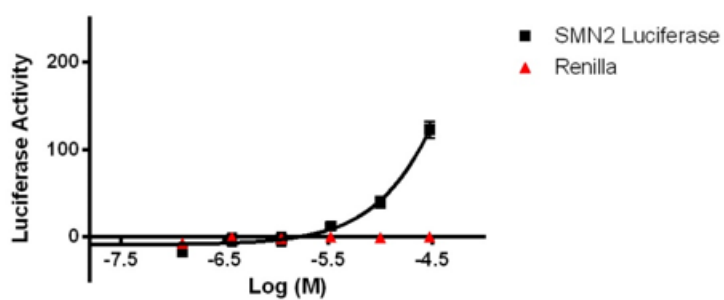
*Figure 22 Activation of the SMN-Luciferase reporter assay of **8***

9 and **10** have different substituents on the phenyl ring while keeping the rest of the structure as **4**. For **9** the value $E_{max}= 83.3$ % [Figure 23] is too low to be considered active for the stabilization of the SMN protein.
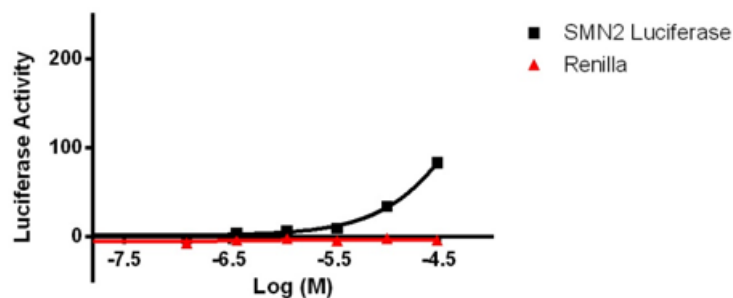
*Figure 23 Activation of the SMN-Luciferase reporter assay of **9***

In the case of **10** the presence of the fluoro substituent gives a slightly higher value $E_{max}= 100.25\%$ than the previous analogue while still being much more inactive than **4** [Figure 24]. This align with the result from the previous SAR in which the halogen atoms seem to be necessary for the activity of this series of small molecules.
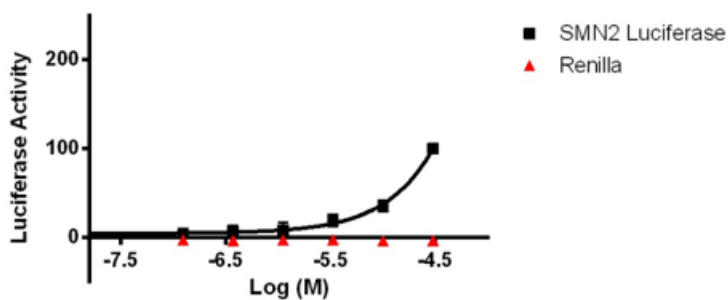
*Figure 24 Activation of the SMN-Luciferase reporter assay of **10***

3.2 N-(3-chloro-4-fluorophenyl)-2-(1-hydroxycyclobutyl)-1-methyl-1H-imidazole-4-carboxamide (13)

These same reaction conditions that were optimized for the synthesis of **1** were used for the synthesis of **12** [Scheme 13].

Methyl 1-methyl-1H-imidazole-4-carboxylate was dried overnight, dissolved in dry THF and cooled down to -78° C. Cyclobutanone was added to the reaction mixture. *N*-BuLi was added dropwise over a period of 15 min. The reaction mixture was stirred at -78° C for 45 min yielding methyl 2-(1-hydroxycyclobutyl)-1-methyl-1H-imidazole-4-carboxylate (**12**).
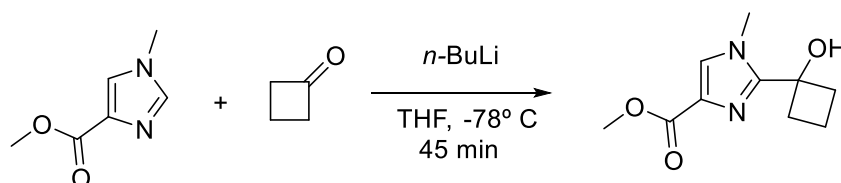
Scheme 13 Synthesis of 12

Compound **12** was used without further purification for the synthesis of compound **13**. The same procedure as for the synthesis of compounds **4-11** was used. 3-Chloro-4-fluoroaniline was dissolved in dry DCM and trimethylaluminum was added dropwise and stirred for an hour at 0° C. **12** was added dropwise to the reaction mixture and stirred for 2 hours at RT to yield compound **13** [Scheme 14].
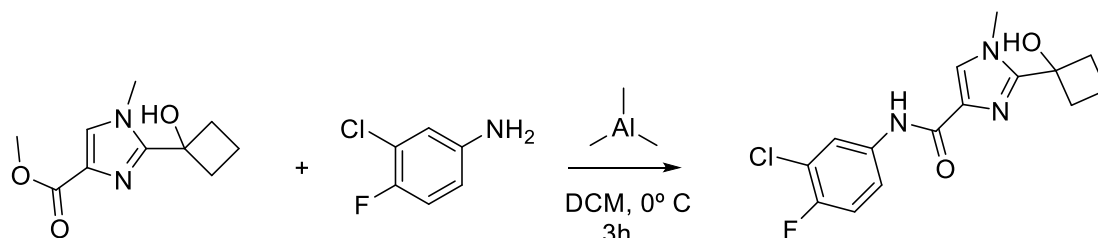
Scheme 14 Reaction scheme for the synthesis of 13

The ^{1}H NMR spectrum of compound **13** shows the aromatic proton of the imidazole ring in the downfield region of the spectrum at 7.72 ppm. The methyl on the 1st position of the imidazole ring appears slightly deshielded at 3.78 ppm due to being linked to a nitrogen. The protons corresponding to the cyclobutyl substituent appear in the upfield region of the spectrum [Figure 25].
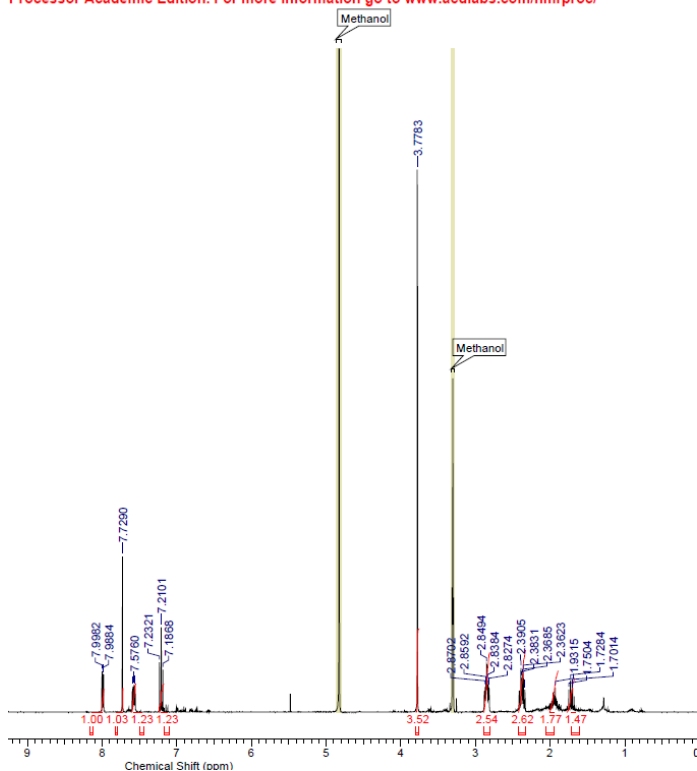
Figure 25 ^{1}H NMR spectrum of compound 13

The result of E_{max}= 59.15% and EC_{50} value indicate that **13** is not active for the stabilization of the SMN protein. This result compared to the values of **4** indicates the effect of the position of the amide linker has on the activity and potency [Figure 26].
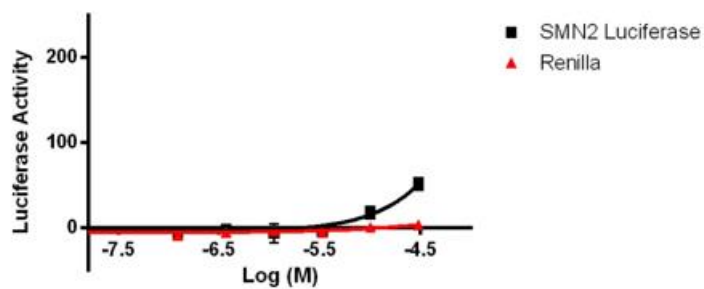

*Figure 26 Activation of the SMN-Luciferase reporter assay of **13***

3.3 2-(1-Hydroxycyclobutyl)-*N*-(4-hydroxyphenyl)-1-methyl-1*H*-imidazole-5-carboxamide (**14**)

After purification of **11** it was further treated with boron tribromide (BBr$_3$) overnight at 0º C for the demethylation of the methyl ether in the para position of the aryl group to yield 2-(1-hydroxycyclobutyl)-*N*-(4-hydroxyphenyl)-1-methyl-1*H*-imidazole-5-carboxamide **14** [Scheme 15].
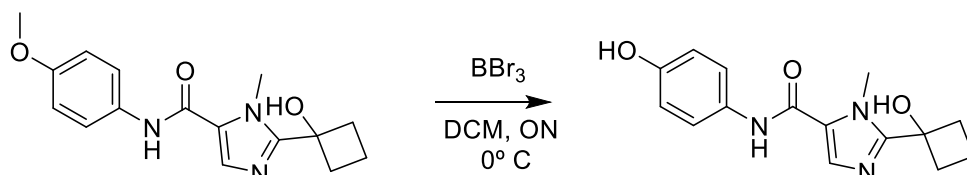
*Scheme 15 Reaction scheme for the synthesis of **14***

The formation of **14** by this procedure was confirmed by ^{1}H NMR spectroscopy [Figure 27], some unknown impurities appear in the aromatic region of the spectrum. The hydroxyl group attached to the phenyl ring appears in the downfield part of the spectrum at 9.28 ppm, the amide proton appears in that same region at 9.86 ppm. The only free proton of the imidazole ring appears in the aromatic region at 7.66 ppm. The second hydroxy group of the molecule attached to the cyclobutyl substituent appears in the spectrum as a singlet at 5.99 ppm.
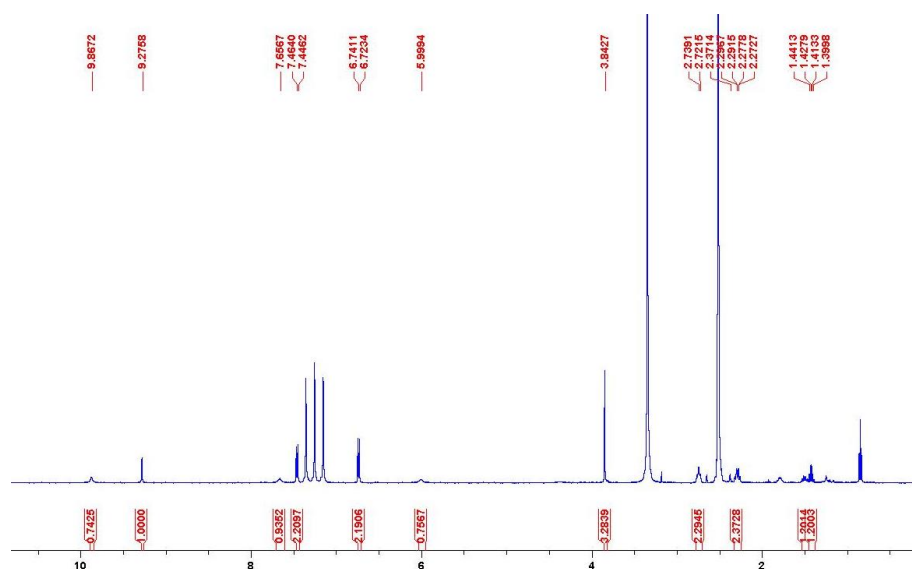
*Figure 27 ^{1}H NMR spectrum of **14***

3.4 N-(3-Chloro-4-fluorophenyl)-2-(1-hydroxycyclobutyl)-N,1-dimethyl-1H-imidazole-5-carboxamide (15)

Compound **4** was treated with sodium hydride and methyl iodide in order to methylate the nitrogen of the amide linker and to test the conditions for a possible cold lab reaction for the radiolabelling reaction. The reaction was tested first at 0º C during 1 hour [Scheme 16].
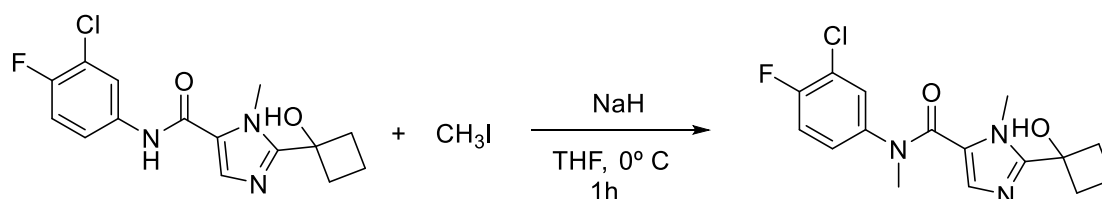
*Scheme 16 Reaction scheme for the cold lab synthesis of **15***

The ^{1}H NMR spectrum of compound **15** shows the proton of the hydroxy group at 6.32 ppm. For the ^{1}H NMR spectrum of the compound **4** the proton linked to the nitrogen of the amide linker appears in the downfield region of the spectrum, in the spectrum for **15** that peak is missing and additional singlet for the protons of a methyl substituent appear at 3.85 ppm [Figure 28]. The non-radioactive sample of **15** was used as the cold standard for the hot lab reaction.
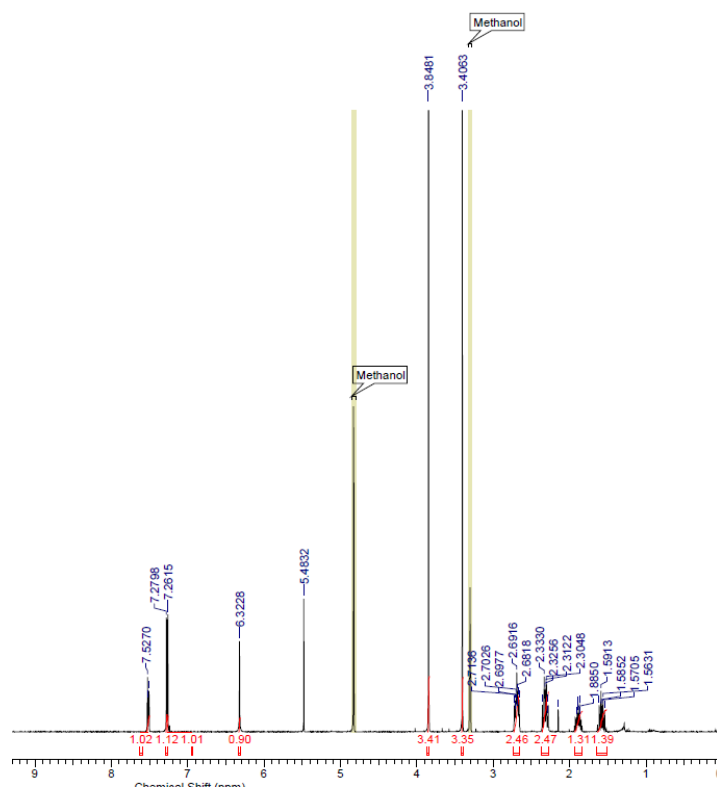
Figure 28 ¹H NMR spectrum of compound 15

The result of the SMN-luciferase reporter assay for **15** follows the tendency observed in the previous SAR work in which *N*-methylation of the amide nitrogen makes the molecule inactive, E_{max}= 0% [Figure 29].
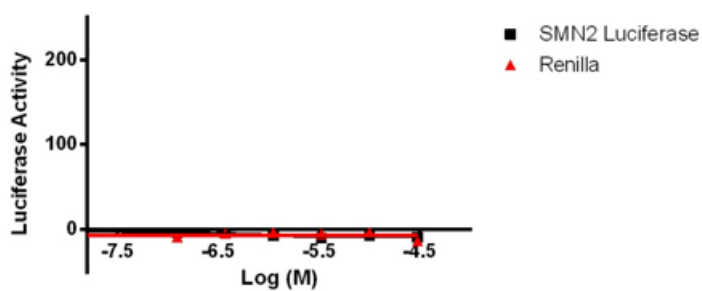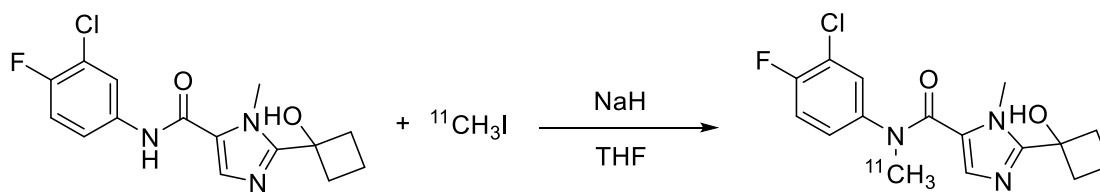

Figure 29 Activation of the SMN-Luciferase reporter assay of 15

In a hot lab a similar reaction was tested for the potential radiolabelling of **4** following the reaction previously mentioned in theory and methods [Scheme 17].

Scheme 17 Radiolabelling reaction of **4**

4 was analysed by HPLC UV with a radioactivity detector in order to figure out the retention time of the reaction precursor before the radiolabelling reaction [Figure 30]. The retention time for **4** is 13:47.
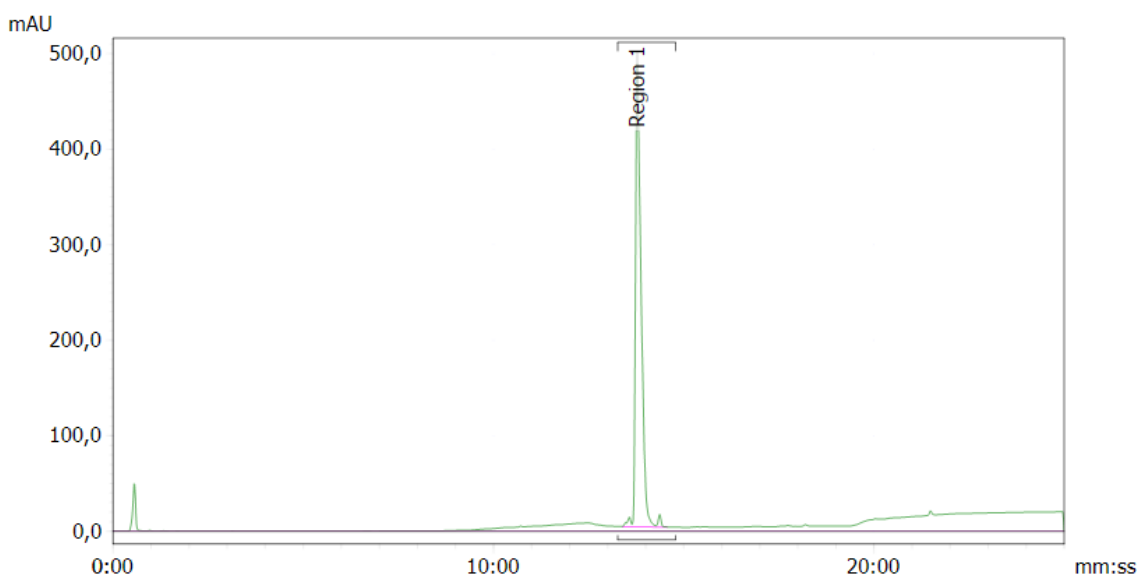
Figure 30 UV chromatogram of **4** as the radiolabelling precursor

15 was also tested to get the retention time as the cold standard in order to analyse its retention time and be able to compare it to the retention time of the hot sample after the radiolabelling methylation reaction [Figure 31]. The retention time for **15** is 12:08.
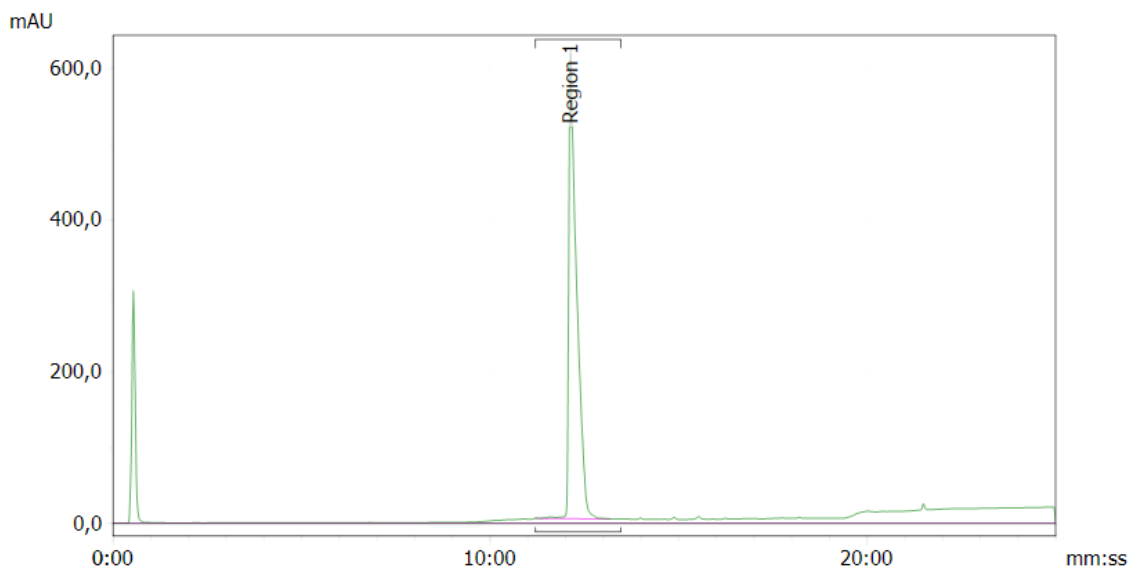
*Figure 31 UV chromatogram of **15** (cold standard)*

Both cold samples of **4** and **15** were run together to evaluate the good separation between both compounds [Figure 32]. The peak of **15** appears labelled as Region 1 in the chromatogram and the peak of **4** appears as Region 2.
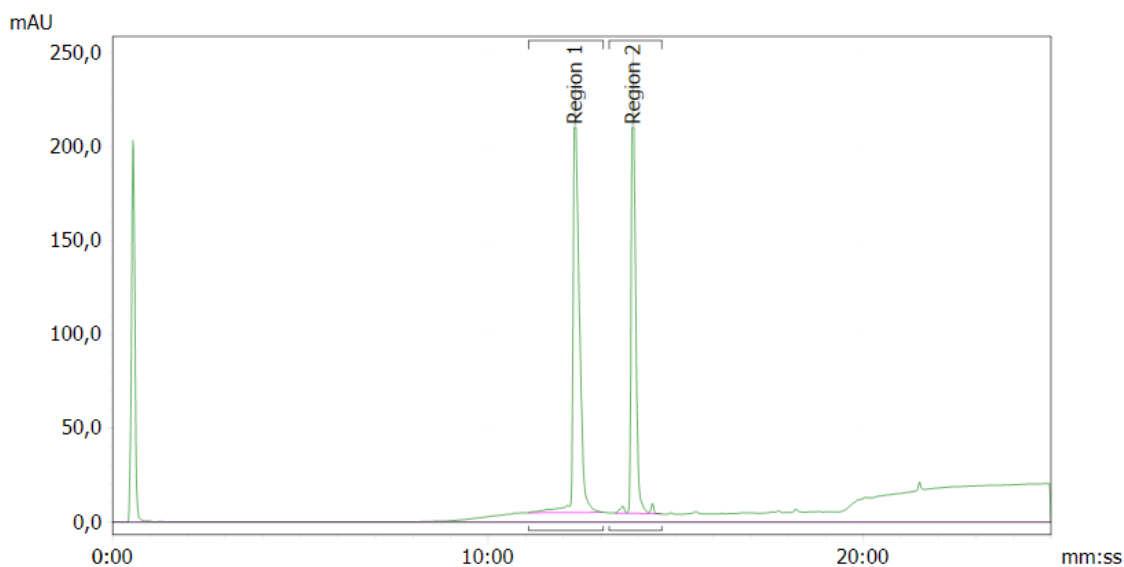

*Figure 32 UV chromatogram of the mixture of **4** and **15***

The UV chromatogram of the product of the radiolabelling reaction [Figure 33] shows only a peak with the retention time 13:48 of the precursor.

Chromatogram: UV
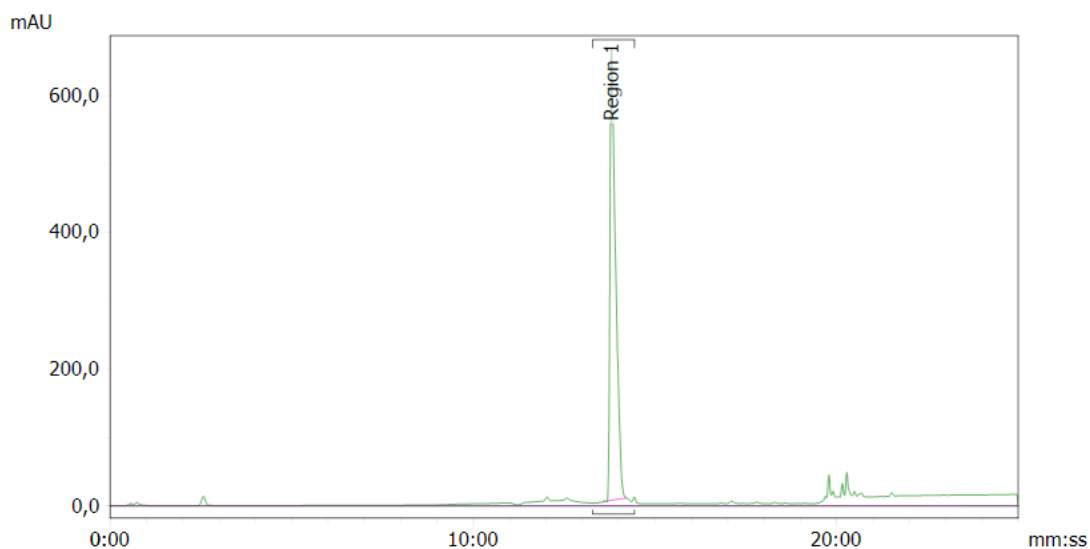
Figure 33 UV chromatogram of the hot radiolabelling reaction

However, the chromatogram of the hot run for the same sample does show a small peak of radioactivity with the retention time 12:50 [Figure 34]. Comparing this peak with the chromatogram and time of retention of the cold standard [Figure 31] the radiolabelling methylation reaction was successful with the conditions used. The disparity on the UV chromatogram [Figure 33] is due to the difference in concentration between the precursor **4** and the radiolabelled compound.

Chromatogram: ^{18}F
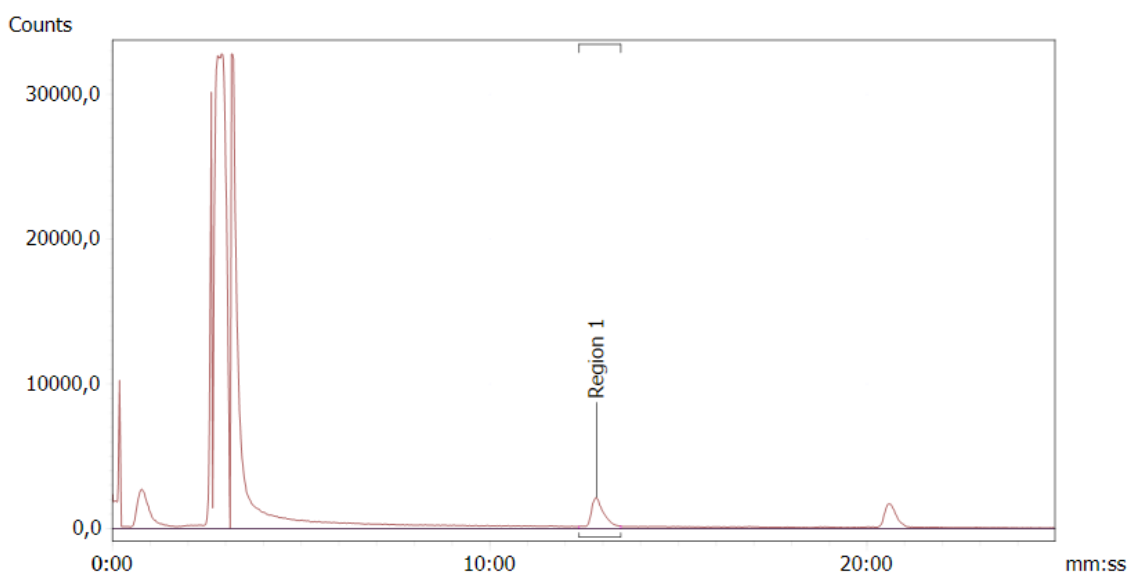
Figure 34 Radioactivity chromatogram of the hot run

## 3.5 Other aminolysis procedures

The most utilized procedures for the synthesis of amides consist of a nucleophilic acyl substitution reaction in which a nucleophile, an amine in this case, displaces the leaving group of the carboxylic acid derivative in a reaction known as aminolysis.

The first procedure used for the synthesis of **4** was based on the reaction described by Drageset et al[30] for the one pot amidation reaction in which the corresponding amide reacts with thionyl chloride to form iminosulfanone to further react with a carboxylic acid to yield the desired amide. The first attempt of this reaction was done using methyl 2-(1-hydroxycyclobutyl)-1-methyl-1*H*-imidazole-5-carboxylate instead of the corresponding acid [Scheme 18]. The carboxylate was dissolved along with 3-chloro-4-flouroaniline and triethylamine in DCM at 0° C. Thionyl chloride was added to the reaction mixture and it was stirred for 20 min. The crude of the reaction was analysed by GC-MS in which the target product was not present.
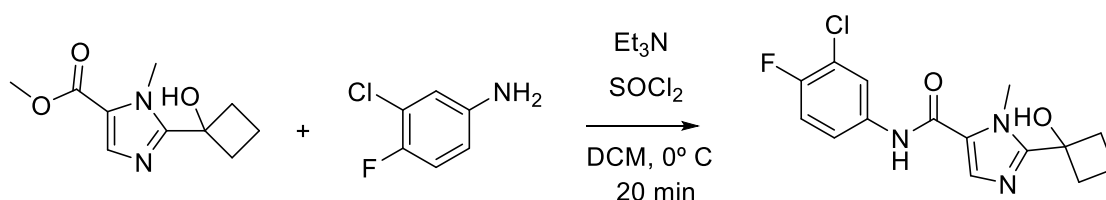
Scheme 18 Reaction scheme for the first unsuccessful aminolysis

To follow the literature of the amidation procedure **1** was hydrolysed to 2-(1-hydroxycyclobutyl)-1-methyl-1*H*-imidazole-5-carboxylic acid (**16**) by stirring **1** overnight in a solution of sodium hydroxide in THF and methanol [Scheme 19]. The formation of the carboxylic acid was confirmed by means of LC-MS but it could not be isolated, and it was utilized in the following reaction without purification.
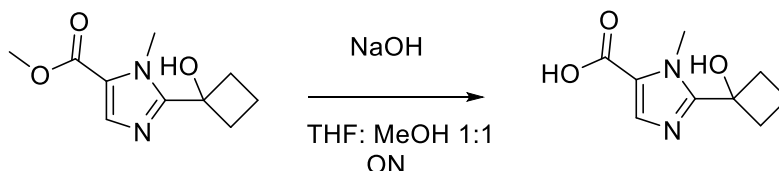

Scheme 19 Reaction scheme of the hydrolysis of 1

A trial for the aminolysis was carried on using pyridine as the base instead of triethylamine and thionyl chloride[31-32] for the *in-situ* formation of the corresponding acid chloride. With a longer reaction time of 1 hour instead of the 20 minutes described in the literature [Scheme 20]. The product was analysed by means of LC-MS in which the m/z 324 u for the product was present

as a trace along with several by-products. The reaction was scaled up but the results could not be reproduced.
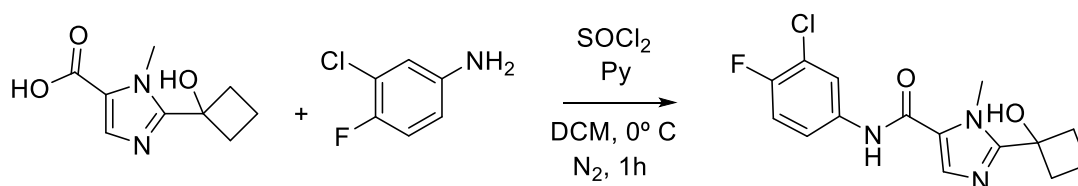
Scheme 20 Reaction scheme for the aminolysis

Other aminolysis procedures have been described in the literature using HATU derivatives such as HOAt, tend to increase the electrophility of the carbonyl centre, efficiency increased due to the neighbouring effect provided by the pyridine nitrogen[33-34].

For this procedure 2-(1-hydroxycyclobutyl)-1-methyl-1*H*-imidazole-5-carboxylic acid and 3-chloro-4-fluoroaniline were dissolved in DMF. HOAt and EDC were added to the reaction mixture and it was stirred overnight at RT [Scheme 21]. As it occurred with the former reaction, **4** was observed when analysed with LC-MS m/z 324 u but when the reaction was scaled up the target compound was not observed and only the starting materials were present.
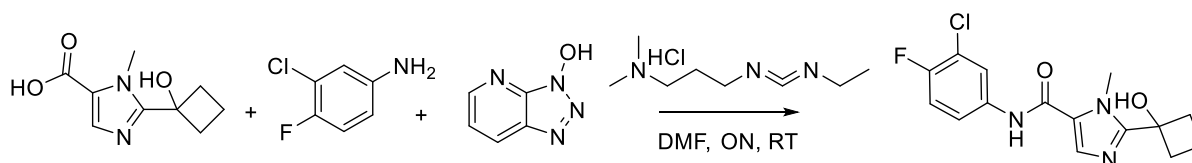
*Scheme 21 Second procedured attempted for the aminolysis*

The reason for the aminolysis reactions not being successful might be the formation of a salt during the hydrolysis of **1**. The salt might be interfering with the reagents in the following reaction avoiding the formation of the desired product.

3.6   Synthesis of methyl 1-methyl-1H-imidazole-5-carboxylate (**17**)

The starting material for the synthesis of **1** was attempted to be synthesised following several different *O*-methylation and *N*-methylation procedures. The first series of attempt was using as starting material 1*H*-imidazole-5-carboxylic acid with the purpose of methylating both the carboxylic acid to form an ester (**17**), as well as the free amino group from the imidazole ring.

For the first attempt powder potassium hydroxide and 1*H*-imidazole-5-carboxylic acid were dissolved in acetone by means of an ultrasonic bath and cooled down to 0º C with and ice/water bath. MeI was added drop wise and the reaction mixture was stirred for 2h [Scheme 22]. The

reaction mixture was analysed by LC-MS. The spectra did not show the desired product, only unknown by-products.
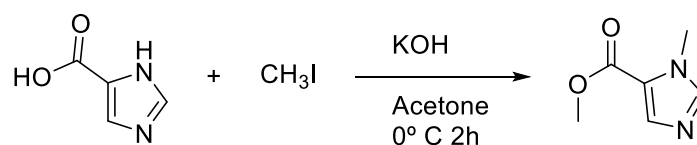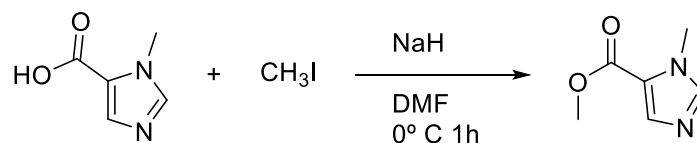

Scheme 22 First attempt for the double methylation

Following the previous reaction, sodium hydride was used as a base and DMF was used instead of acetone as the solvent. 1*H*-Imidazole-5-carboxylic acid and the base were dissolved in anhydrous DMF, cooled down to 0° C and stirred for 1h [Scheme 23]. The LC-MS analysis showed the presence of the product as well as a number of by-products.
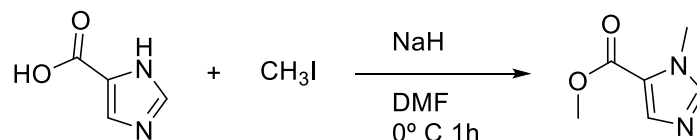
Scheme 23 Second attempt for the double methylation

1-Methyl-1*H*-imidazole-5-carboxylic acid and sodium hydride were dissolved in DMF by means of an ultrasonic bath and cooled down to 0° C before adding MeI dropwise and left to react for an hour [Scheme 24]. The GC-MS showed the presence of the product along with the starting material [Figure 35]. However, in the NMR of the reaction product the solvent peaks of the DMF are present, 8.03, 2.95 and 2.88 ppm [Figure 36] even after drying overnight under high vacuum.

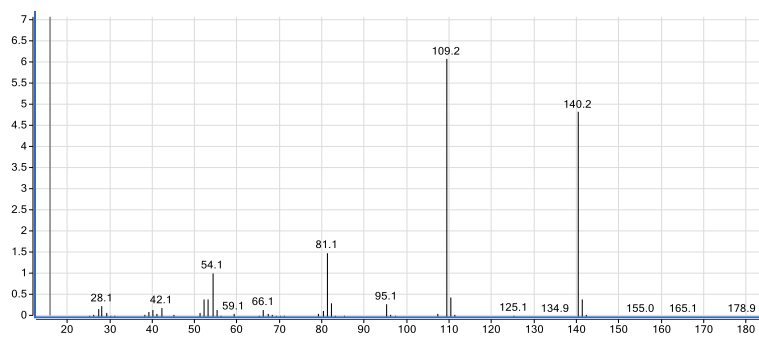*Scheme 24 First attempt for the mono methylation*

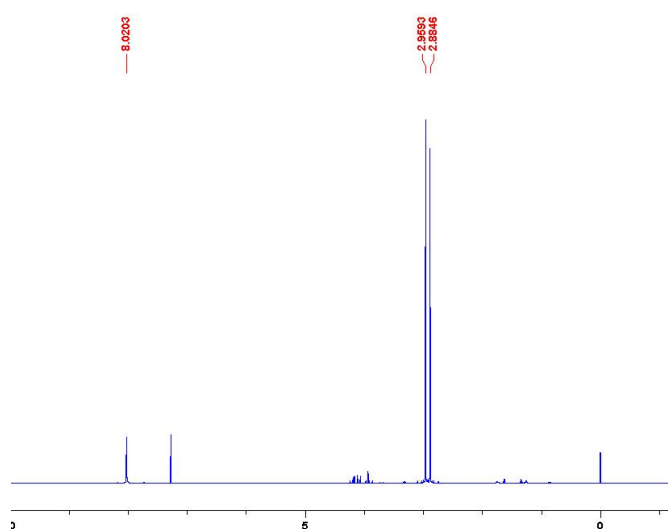*Figure 35 GC-MS spectrum of the first attempt to methylate*

Figure 36 ¹H NMR spectrum of 17, DMF solvent peaks

The last attempt was made by switching the base to potassium carbonate [Scheme 25], that was dissolved along with 1-methyl-1*H*-imidazole-5-carboxylic acid in acetone by means of an ultrasonic bath. MeI was added dropwise and the reaction was stirred at 0° C for 2h to yield **17**. The GC-MS analysis confirmed that the reaction worked for the synthesis of **17** but not to full conversion [Figure 37].
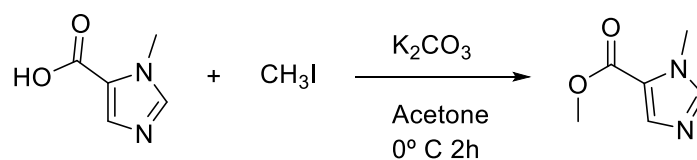
Scheme 25 Reaction scheme of the second attempt for the methylation
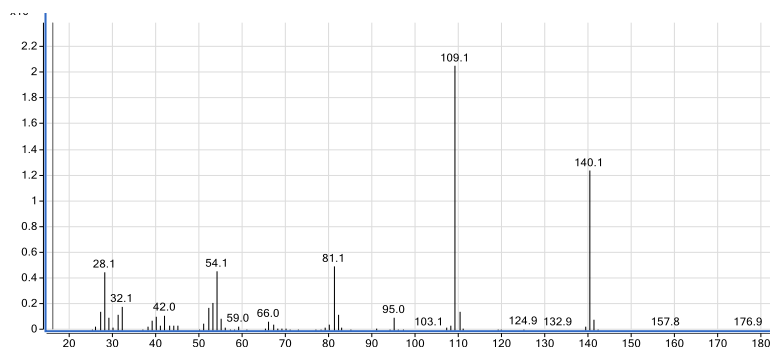
Figure 37 GC-MS spectrum of 17

3.7 Functionalisation of the imidazole ring

The functionalisation of the back bone of the imidazole ring in order to introduce different functional groups is one of the vital steps for the use of imidazole rings in the pharmaceutical industry.

Sandtorv et al[35] developed a method of functionalisation of the imidazole ring by introducing halogen atoms by means of *N,N'*-dihalogenated analogues of 5,5-dimethylhydantoin. These reagents can be used to synthesize mono-halogenated, di-halogenated or tri-halogenated imidazole after being activated with a catalytic amount of a strong mineral acid.

For the mono-bromination the imidazole ring was dissolved in water and *N,N'*-dibromo-5,5-dimethylhydantoin (DBH) was added as a solid in small portions followed by a few drops of sulphuric acid [Scheme 26] to yield **18**. The reaction mixture was quenched with a NaOH solution and neutralized with acetic acid until pH 6. As it was described in the literature the product m/z 147 was contaminated with other impurities as shown by the LC-MS analysis [Figure 38].
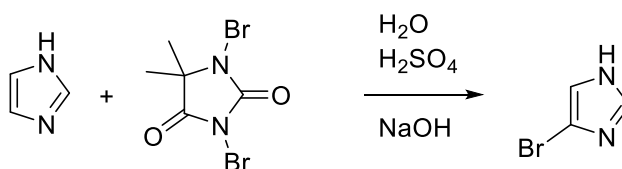
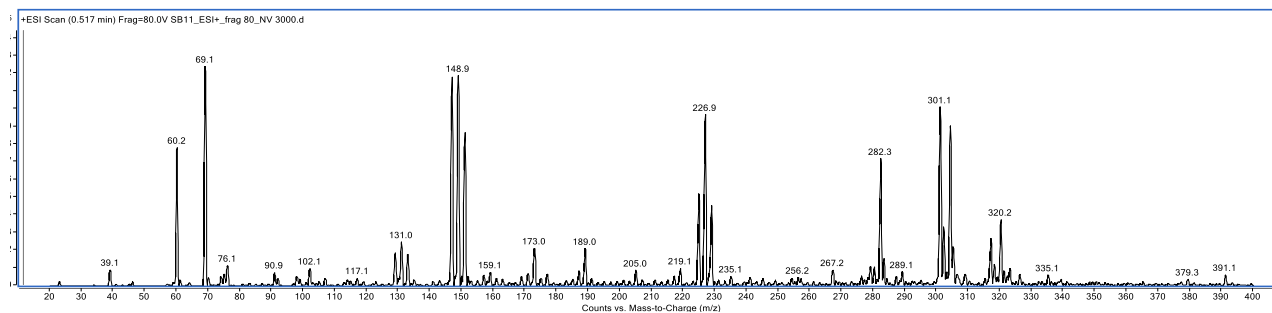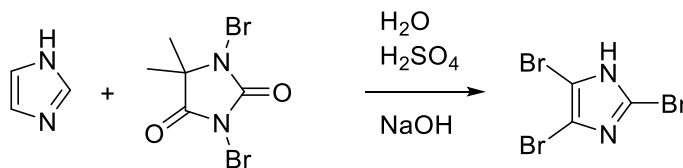*Scheme 26 Reaction scheme for the synthesis of 18*

*Figure 38 LC-MS spectrum of **18***

2,4,5-Tribromo-1*H*-imidazole (**19**) was synthesized by dissolving the imidazole ring in water, the DBH was added in one portion followed by the drop-wise addition of sulphuric acid [Scheme 27]. The reaction mixture was quenched with a NaOH solution and neutralized with acetic acid. The reaction mixture was cooled in the fridge until the product had precipitated. The LC-MS analysis confirmed the formation of the product, m/z 302 [Figure 39].

*Scheme 27 Reaction scheme for the synthesis of **19***
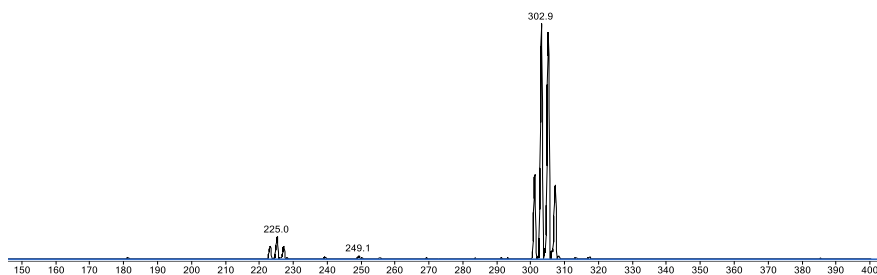
*Figure 39 LC-MS spectrum of **19***

For the synthesis of 4(5)-Iodo-1*H*-imidazole (**21**) a conventional procedure was utilized, 4,5-diiodo-1*H*-imidazole (**20**) was synthesised by dissolving imidazole in NaOH solution. A solution of KI and I_2 in water was added drop-wise. The reaction mixture was stirred overnight at RT [Scheme 28].
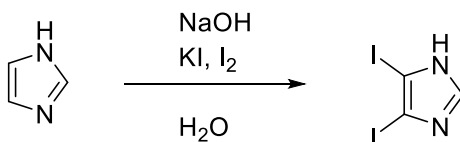
Scheme 28 Reaction scheme for the synthesis of 20

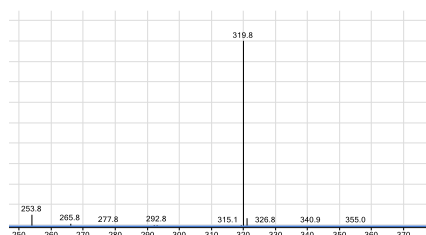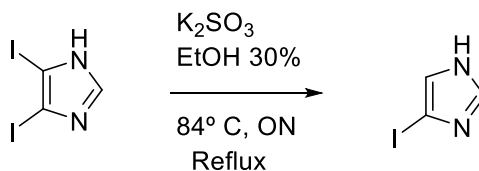The formation of **20** was confirmed by means of GC-MS analysis m/z 319 [Figure 40].

Figure 40 GC-MS spectrum of 20

Selective dehalogenation of **20** to yield 4(5)-Iodo-1*H*-imidazole (**21**) was done by dissolving 4,5-diiodo-1*H*-imidazole in a potassium sulphite solution with 30% ethanol, heating up to 84° C with reflux and it was stirred for 22h [Scheme 29].

Scheme 29 Reaction scheme for the selective dehalogenation of 20 to yield 21

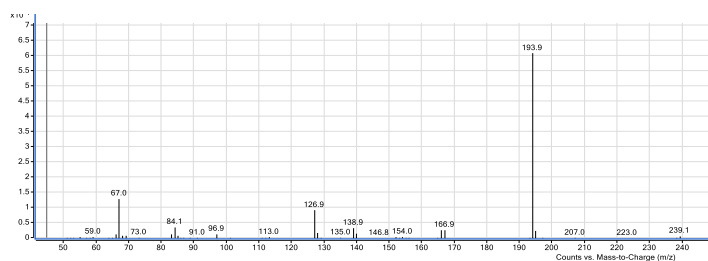The product **21** was confirmed by GC-MS analysis m/z 194 [Figure 41]

Figure 41 GC-MS spectrum of 21

A similar procedure as was previously described for **18** and **19** was also used for the synthesis of **21**. Imidazole and potassium iodide were dissolved in water while the reaction flask was

cooled to 0° C with an ice-bath and a NaOH solution was added. Sulphuric acid was added to DIH and the mixture was added drop-wise to the reaction mixture and it was neutralized with acetic acid to yield 4(5)-Iodo-1*H*-imidazole [Scheme 30]. GC-MS analysis revealed the formation of the desired product m/z 194 [Figure 42]. It was not further used.
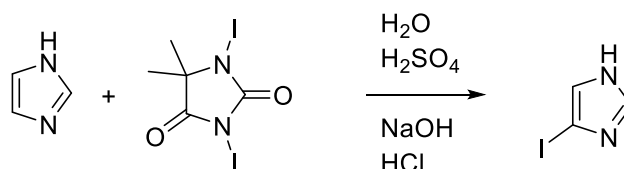
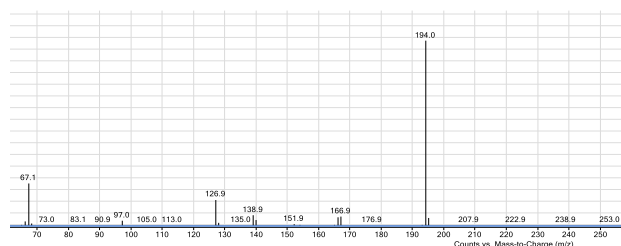

Scheme 30 Second method used for the synthesis of 21

Figure 42 GC-MS spectrum of 21 synthesized by means of DIH

N-Methylation of **18** was formed by dissolving the imidazole with potassium hydroxide in acetone by means of an ultrasonic bath. MeI was added dropwise and the reaction mixture was stirred at 0° C for two hours [Scheme 31] to yield **22**. Confirmed by LC-MS analysis m/z 161 [Figure 43].
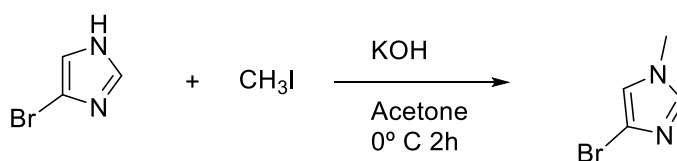
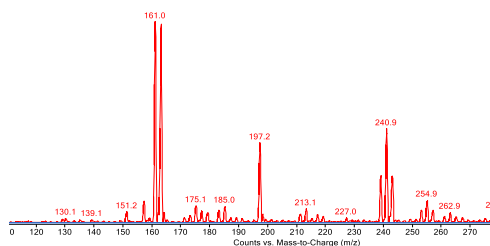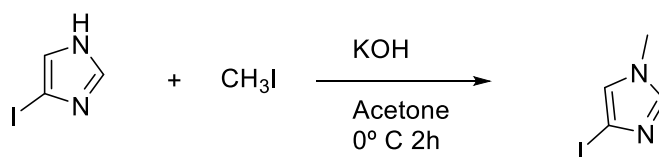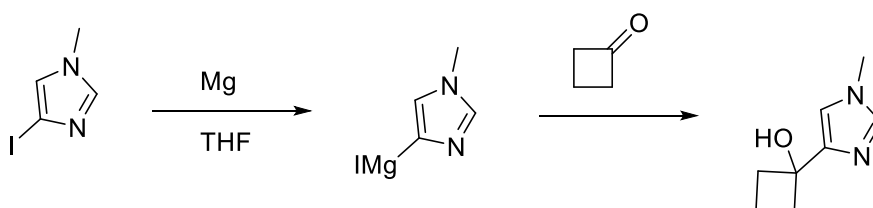*Scheme 31 Reaction scheme for the synthesis of 22*

Figure 43 LC-MS spectrum of 22

55

The same procedure was used for the *N*-methylation of 4(5)-iodo-1*H*-imidazole to yield 4-iodo-1-methyl-1*H*-imidazole (**23**) [Scheme 32]. The analysis of GC-MS confirmed the formation of the product, and unknown impurity was also in the GC-chromatogram.
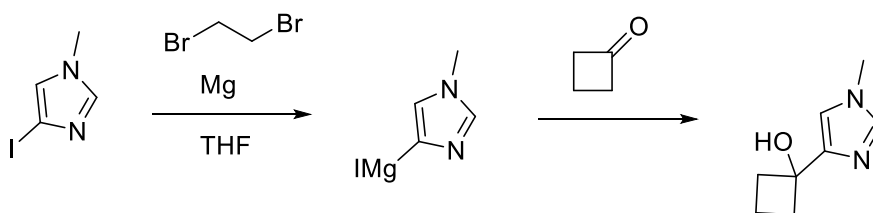

Scheme 32 Reaction scheme for the synthesis of 23

Cyclobutanone was attempted to be attached to the back bone of the imidazole by means of a Grignard reaction to yield **24**. **23** was previously dried and dissolved in anhydrous THF and it was added dropwise to a round bottom flask containing magnesium, the reaction mixture was stirred for 30 min and cyclobutanone was added dropwise [Scheme 33]. The reaction mixture was stirred for 10 min at RT. The reaction crude was analysed by means of GC-MS, the spectrum revealed that the reaction was unsuccessful. The magnesium might have not been activated and consequently not react with **23**.

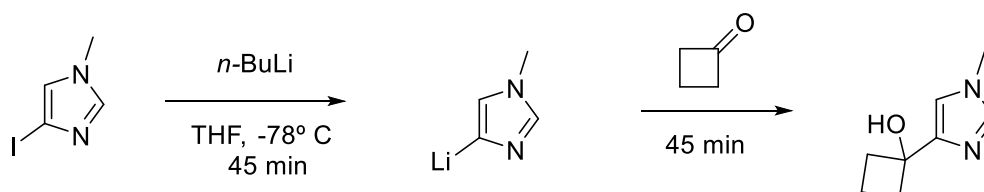*Scheme 33 Reaction scheme for the first attempt to synthesize 24*

To help with the activation of the magnesium, dibromoethane was added to the first step of the Grignard reaction while keeping the same conditions for the reaction [Scheme 34]. The crude was analysed by means of a GC-MS and the spectrum revealed that the reaction did not form the desired product.

Scheme 34 Reaction scheme for the second attempt of the Grignard reaction

Since the previous reaction did not yield the desired product, butyl lithium was used for a lithium-halogen exchange instead. **23** was dissolved in anhydrous THF and *n*-BuLi was added drop-wise over a period of 15 min. The reaction mixture was stirred at -78° C during 45 min before adding cyclobutanone and stirred for 45 min [Scheme 35]. GC-MS was used to analyse the reaction mixture and unfortunately the desired product was not formed.

*Scheme 35 Reaction scheme for the lithium-halogen exchange to yield **24***

A different series of analogues of **LDN-75654** was attempted to be synthesized starting by using 4-nitroimidazole as starting material in order to have the different substituents in other positions and study the effect on the activity by testing the analogues on the SMN-Luciferase reporter assay.

To *N*-methylate 4-nitroimidazole it was dissolved along with powdered potassium hydroxide in acetone with the aid of an ultrasonic bath before adding MeI drop-wise while keeping the reaction mixture to 0° C with an ice bath for 90 min to yield **25** [Scheme 36]. The reaction mixture was analysed by LC-MS, the spectrum showed that the reaction was not complete since both the starting material m/z 112 and the target product m/z 128 appear [Figures 44 and 45].
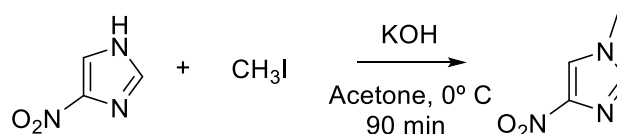
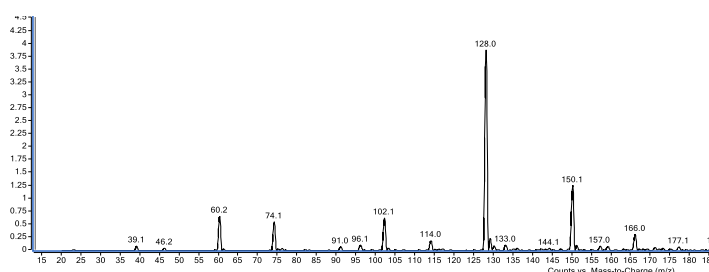*Scheme 36 Reaction scheme for the synthesis of **25***
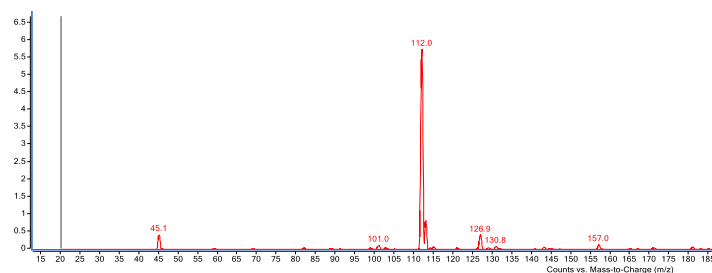

*Figure 44 LC-MS spectrum positive of **25***

Figure 45 LC-MS spectrum negative for 25

The 1-methyl-4-nitro-1*H*-imidazole **25** synthesized in the previous reaction was attempted to be reduced by a mixture of cobalt sulphate and sodium borohydride as described in the literature[36] [Scheme 37] to yield **26**. The analysis of the reaction mixture by LC-MS showed the formation of a coupling product m/z 177 and unknown impurity m/z 199 [Figure 46].
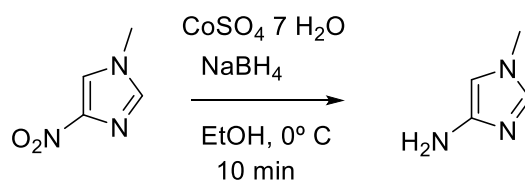
Scheme 37 Reaction scheme for the synthesis of 26

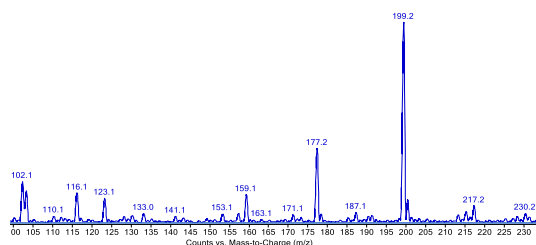*Figure 46 LC-MS spectrum of 26*

A different procedure was attempted for the reduction of **25** with palladium hydroxide (Pd(OH)$_2$) over carbon with hydrogen gas to yield **26**. The imidazole and the palladium hydroxide were dissolved in anhydrous methanol. A balloon of hydrogen was bobbled on the reaction mixture and the reaction was heated up to 52º C overnight [Scheme 38].

The LC-MS analysis did not show the formation of the desired product.
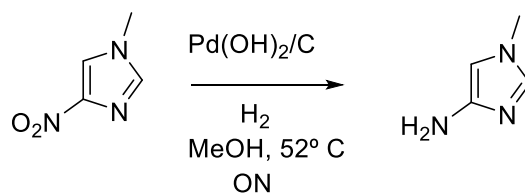
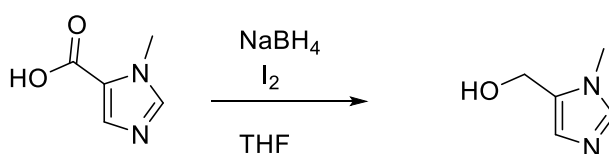*Scheme 38 Second attempt for the synthesis of 26*

In the search of the right procedure for the amidation reaction other paths were studied. Previous work done in the group described the possibility of the synthesis of an amide bond from an alcohol through a domino oxidative amidation followed by transamidation[37] in which the hydroxy group forms an intermediate amide by reacting with the dichlorohidantoin DCH. The intermediate then further reacts with the corresponding secondary amide to yield the desired amide by transamidation.

In order to follow this procedure, the carboxylic acid of 1-methyl-1*H*-imidazole-5-carboxylic acid must be reduced to the corresponding alcohol **27**. One of the most common procedures used to reduce carboxylic acids to primary alcohols is by using lithium aluminium hydride as reducing agent. To a 1-methyl-1*H*-imidazole-5-carboxylic acid solution in anhydrous THF LiAlH$_4$ was added drop-wise during a period of 10 min [Scheme 39]. After 1 h the reaction mixture was quenched with acid water. A GC-MS was used to analyse the reaction mixture, the target molecule was present along with the coupling product and the corresponding aldehyde as an intermediate of the reduction.
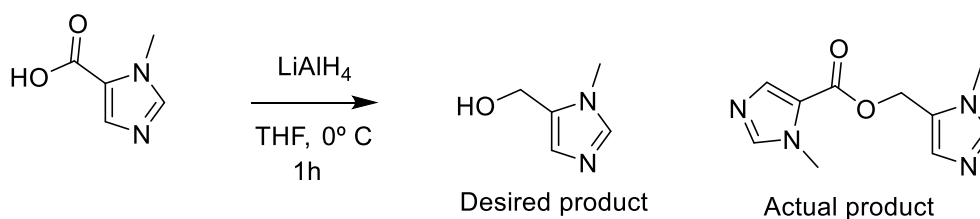
Scheme 39 First attempt for the synthesis of 27

A procedure for reducing carboxylic acids into alcohols by means of sodium borohydride NaBH$_4$ and iodine I$_2$[38-39] [Scheme 40]. The carboxylic acid solution in THF was added slowly to a suspension of NaBH$_4$ in THF and stirred until gas is no longer be formed. A solution of I$_2$ in THF is then added slowly at RT, the reaction mixture was stirred for 1 h. The target compound was not accomplished by following this method.

Scheme 40 Second attempt for the synthesis of 27

4 SUMMARY AND FURTHER WORK

4.1 Summary

The primary aim of this project was to synthesize new analogues of the previously developed lead compounds, **LDN-75654** and **LDN-27**, with the intent of improving the pharmacokinetic properties and activities reported for the post-translationally stabilization of the SMN protein for the treatment of SMA. The main target molecule originally designed for this project, **4**, contained similarities to both lead compounds being the most substantial difference the imidazole ring as the heterocycle core of the molecule. A series of seven different analogues were developed by altering the substituents of the structure but maintaining the imidazole core and direction of the amide linker. One structural isomer, **13**, was also developed in order to study the effect on the position of the substituents in the activity.

The synthesis of the analogues was a two-step synthesis starting from a commercially available starting material, methyl 1-methyl-1*H*-imidazole-5-carboxylate for the majority of the analogues, treated with *n*-BuLi and the corresponding ketone or aldehyde at low temperature, following the trimethylaluminum mediated aminolysis.

From the eleven analogues successfully developed, nine of them were tested by the SMN-luciferase reporter assay to study the activity on the stabilization of the SMN protein. Although the only analogue presenting significant activity was **4**, it did not improve the activities reported for the previous lead compounds, implying that the substituents optimized for **LDN-27** by means of a SAR study are not ideal for the imidazole core-based analogues.

4 was also used to test a radiolabelling reaction to obtain a radiolabelled version of **15**. A good separation method and good reaction conditions were achieved and the desired hot sample was synthesized and analyzed.

During this project a number of attempted reactions were not accomplished as desired.

The synthesis of methyl 1-methyl-1*H*-imidazole-5-carboxylate, starting material for most of the analogues synthesised in this project, was attempted by four slightly different procedures without achieving a procedure that is reproducible and has good enough conversion to be used for the synthesis of the analogues.

The synthesis of **24** was attempted following two different procedures, a Grignard reaction and a Lithium-halogen exchange, both reactions were unsuccessful and the desired target molecule was not accomplished. The starting materials, **22** and **23**, were also synthesized following different procedures during this project.

A different series of analogues based on 4-nitroimidazole was attempted. The first reaction using it as starting material to yield **25** after being methylated. Unfortunately, the two methods attempted to reduce the nitro group of **25** to yield **26** were not successful. The attempted reduction reaction used to synthesize **27** was also unsuccessful.

4.2   Further work

Based on the testing data obtained by the SMN-luciferase reported assay on the activity of the different analogues synthesized during this project it has been determined that the substituents previously optimized for the hit compound with the thiazole core are not as optimal for the imidazole core analogues. A new SAR study would be interesting for the imidazole core small molecules. Considering the activation of **4** on the reporter assay, the imidazole ring is still an interesting approach.

The success on the radiolabelling attempted during this project presents an interest in developing and attempting similar radiolabelling reactions for the rest of the analogues as the starting point of a new project focused on developing a series of possible PET 3D scan tracers.

A number of synthetic routes attempted during this project hold potential for improvement, such as the synthesis of **17** as the starting material for most of the analogues synthesized. A different set of reactions and conditions could be attempted to attempt the synthesis of the compounds not accomplished during this project.

5 EXPERIMENTAL

General methods

Chemicals

Most of the chemicals used to synthesize the imidazole core analogues were purchased commercially and used as received. The exception is 1,3-diiodo-5,5-dimethylhydantoin (DIH) that was previously produced in the group by means of continuous flow.

Experimental description

TLC analyses were performed on coated aluminium foils embedded with fluorescent indicator 254 nm or on glass. The mobile phase used consisted of various mixtures of hexane and ethyl acetate or dichloromethane and methanol.

Manual flash chromatography was performed using silica gel as stationary phase. Automatic flash column chromatography was carried on a Teledyne isco combiflash rf column with Agela Flash Column Silica-CS 60 Å.

Spectroscopic descriptions

NMR spectra were obtained on a Bruker Biospin AV500 (500 MHz for ^{1}H, 125 MHz for ^{13}C). Chemical shifts are reported in ppm relative to the signal of the remaining protons of the deuterated solvent used. Coupling constants are given in Hz and the multiplicity is reported as singlet (s), doublet (d), triplet (t), quartet (qt) and multiplet (m).

GC-MS analyses were performed on a capillary gas chromatograph with a fused silica column and helium as the carrier gas. The gas chromatograph was connected to a mass spectrometer using electron ionisation (EI) as ionisation source.

LC-MS and MS-MS analysis were performed on an Aglient 6420A triple quadrupole (QqQ configuration) mass analyser using electrospray ionisation (ESI). It is connected to an Agilent 1200 series LC module (binary pump, column compartment/oven and autosampler). The column used was an Agilent ZORBAX SB-C18, RRHT; 2.1 x 50 mm x 1.8 ⌈m.
Agilent 1260 Infinity Quaternary LC system interfaced to an Agilent 6120 Single Quadrupole mass spectrometer were also used for LC-MS analysis.

HPLC purification was done with an Agilent 1260 Infinity II attached to a 6120 Quadrupole LC/MS.

The radiolabelled sample of **15** was analyzed with an Agilent 1260 Infinity instrument attached to a Radio-HPLC detector Posi-RAM model 4 Lablogic with a Luna Omega 3 µm Polar C18 50 x 2.1 mm column.

Experimental procedures

Methyl 2-(1-hydroxycyclobutyl)-1-methyl-1*H*-imidazole-5-carboxylate **1**: Methyl 1-methyl-1H-imidazole-4-carboxylate (270.40 mg, 1.93mmol) was dried overnight on a desiccator and dissolved in dry THF (10 ml) and cooled to -78º C with a dry ice/acetone bath under nitrogen inert atmosphere. Cyclobutanone (270.48 mg, 0.290 mL, 3.86 mmol) was added to the reaction mixture. *N*-Buthyl lithium (*n*-BuLi) (247.19mg, 1.54mL, 2.5 M) was added dropwise during a period of 15 min. After 45 min the reaction mixture was quenched with a saturated ammonium chloride solution (NH$_4$Cl) (20 ml), extracted with EtOAc (3x25 ml) and dried over magnesium sulphate. The purification was made by means of an autoflash column DCM: MeOH 95:5 to yield methyl 2-(1-hydroxycyclobutyl)-1-methyl-1*H*-imidazole-5-carboxylate (190.50mg, 0.906 mmol, 46.96 % yield). ^{1}H NMR (400 MHz, 25 ºC, DMSO) δ 7.54 (s, 1H), 5.98 (s, 1H), 3.81 (s, 3H), 3.79 (s, 3H), 3.29 (s, 1H), 2.70 (m, 2H), 2.26 (m, 2H), 1.75 (m, 1H), 1.44 (m, 1H) ppm.

The same procedure was used for the synthesis of methyl 2-(1-hydroxyethyl)-1-methyl-1*H*-imidazole-5-carboxylate **2** (11.50 mg, 0.062 mmol, 22.08% yield). ^{1}H NMR (400 MHz, 25 ºC, DMSO) δ 7.53 (s, 1H), 5.43 (d, 1H, J = 6.36 Hz), 4.85 (t, 1H, J = 6.36 Hz), 3.86 (s, 3H), 3.75 (s, 3H), 1.46 (d, 3H, J = 6.36 Hz) ppm.

Methyl 1-cyclobutyl-1*H*-imidazole-5-carboxylate **3**: Methyl 1H-imidazole-5-carboxylate (248.20 mg, 1.97 mmol) and caesium carbonate (Cs$_2$CO$_3$) (1.28 g, 3.94 mmol) were dissolved in *N,N*-Dimethylformamide (DMF) (15 ml) and bromocyclobutane (292.26 mg, 0.203 ml, 2.16 mmol) was added to the reaction mixture and it was stirred at RT overnight. H$_2$O (20 ml) was added and the reaction mixture was extracted with EtOAc (3x30 ml) and dried over sodium sulphate. Purified by means of an autoflash column DCM: MeOH 95:5 to yield 4 (146.22 mg, 1.97 mmol, 41.23% yield). ^{1}H NMR (400 MHz, 25 ºC, DMSO) δ 8.17 (s, 1H), 7.63 (s, 1H), 5.10 (q, 1H, J = 8.8 Hz), 3.29 (s, 1H), 2.48 (d, 2H, J = 1.96 Hz), 2.34 (m, 2H), 2.29 (m, 2H), 1.76 (m, 2H) ppm.

General procedure for the synthesis of **4-11**. 3-Chloro-4-fluoroaniline was dissolved in dry DCM (2 ml) under inert atmosphere and cooled to 0º C with an ice/water bath. Trimethylaluminum (102.35 mg, 0.709 ml, 1.42 mmol) was added dropwise over a period of 10 min and the reaction mixture was stirred for 1h. Methyl 2-(1-hydroxycyclobutyl)-1-methyl-1H-imidazole-5-carboxylate (99.50 mg, 0.473 mmol) was dissolved in dry DCM (2 ml) and added dropwise over a period of 15 min to the previous reaction mixture and was stirred at RT for 2 h. Change colour to yellow. After the reaction time the reaction mixture was quenched with a phosphate buffer and stirred for 15 min, diluted in DCM and the aluminium salts filtered off. The filtrate was washed with H$_2$O (3x25 ml) and dried over sodium sulphate. The purification of the title compound was done by autoflash column DCM:MeOH 95:5 to yield *N*-(3-chloro-4-fluorophenyl)-2-(1-hydroxycyclobutyl)-1-methyl-1*H*-imidazole-5-carboxamide **4** (22.10 mg, 0.068 mmol, 14.42% yield). ^{1}H NMR (400 MHz, 25 ºC, DMSO) δ 10.16 (s, 1H), 7.98 (dd, 1H, J = 6.8, 2.4 Hz), 7.66 (s, 1H), 7.62 (m, 1H), 7.38 (t, 1H, J = 9 Hz),

5.95 (s, 1H), 3.29 (s, 3H), 2.73-2.69 (m, 2H), 2.27-2.22 (m, 2H), 1.78-1.74 (m, 1H), 1.48-1.45 (m, 1H) ppm.

N-(3-chloro-4-fluorophenyl)-2-(1-hydroxyethyl)-1-methyl-1*H*-imidazole-5-carboxamide **5**: (4 mg, 0.013 mmol, 16.72% yield) ^{1}H NMR (400 MHz, 25 ºC, MeOH) δ 7.90 (dd, 1H, J = 6.0, 2.7 Hz), 7.66 (s, 1H), 7.54 (m, 1H), 7.20 (t, 1H, J = 9 Hz), 5.01 (d, 1H, J = 6.36 Hz), 4.00 (s, 3H), 1.61 (d, 3H, J = 6.36 Hz) ppm.

N-(3-chloro-4-fluorophenyl)-1-cyclobutyl-1*H*-imidazole-5-carboxamide **6**: (39.20 mg, 0.133 mmol, 60.12% yield) ^{1}H NMR (400 MHz, 25 ºC, DMSO) δ 10.10 (s, 1H), 8.14 (dd, 1H, J = 6.8, 2.4 Hz), 8.02 (s, 1H), 7.91 (s, 1H), 7.78 (m, 1H), 7.34 (t, 1H, J = 9 Hz), 4.77 (q, 1H, J = 8.8 Hz), 2.42-2.36 (m, 4H), 1.83-1.71 (m, 2H) ppm.

N-(3-chloro-4-fluorophenyl)-1-methyl-1*H*-imidazole-5-carboxamide **7**: (15.20 mg, 0.060 mmol, 17.50% yield) ^{1}H NMR (400 MHz, 25 ºC, MeOH) δ 7.90 (dd, 1H, J = 6.8, 2.5 Hz), 7.79 (s, 1H), 7.75 (s, 1H), 7.54 (m, 1H), 7.20 (t, 1H, J = 9 Hz), 3.95 (s, 3H) ppm.

N-(3-chloro-4-fluorophenyl)-1*H*-imidazole-5-carboxamide **8**: (11.20 mg, 0.046 mmol, 5.89% yield) ^{1}H NMR (400 MHz, 25 ºC, MeOH) δ 8.00-7.99 (m, 1H), 7.78 (m, 1H), 7.76 (s, 1H), 7.56 (m, 1H), 7.23-7.19 (m, 1H) ppm.

2-(1-hydroxycyclobutyl)-1-methyl-*N*-phenyl-1*H*-imidazole-5-carboxamide **9**: (5.20 mg, 0.019 mmol, 9.90% yield) ^{1}H NMR (400 MHz, 25 ºC, MeOH) δ 7.64 (s, 1H), 7.63-7.61 (m, 2H), 7.35-7.31 (m, 2H), 7.12-7.10 (m, 1H), 3.95 (s, 3H), 2.82-2-77 (m, 2H), 2.40-2.37 (m, 2H), 2.00-1.93 (m, 1H), 1.68-1.65 (m, 1H) ppm.

N-(4-fluorophenyl)-2-(1-hydroxycyclobutyl)-1-methyl-1*H*-imidazole-5-carboxamide **10**: (4.60 mg, 0.016 mmol, 8.68% yield) ^{1}H NMR (400 MHz, 25 ºC, MeOH) δ 7.65-7.61 (m, 2H), 7.63 (s, 1H), 7.07 (t, 2H, J = 8.8 Hz), 3.95 (s, 3H), 2.83-2.77 (m, 2H), 2.40-2.37 (m, 2H), 1.92-1.90 (m, 1H), 1.68-1.65 (m, 1H) ppm.

2-(1-hydroxycyclobutyl)-*N*-(4-methoxyphenyl)-1-methyl-1*H*-imidazole-5-carboxamide **11**: (64.90 mg, 0.215 mmol, 86.24% yield) ^{1}H NMR (400 MHz, 25 ºC, MeOH) δ 7.61(s, 1H), 7.50 (d, 2H, J = 8.8 Hz), 6.90 (d, 2H, J = 9.32 Hz), 3.94 (s, 3H), 3.79 (s, 3H), 2.82-2.80 (m, 2H), 2.40-2.37 (m, 2H), 2.00-1.98 (m, 1H), 1.66-1.64 (m, 2H) ppm.

Methyl 2-(1-hydroxycyclobutyl)-1-methyl-1*H*-imidazole-4-carboxylate **12**: Similar procedure used as for the synthesis of **1**. (153.20 mg, 0.728 mmol, 38.99% yield). It was further used without purification.

N-(3-chloro-4-fluorophenyl)-2-(1-hydroxycyclobutyl)-1-methyl-1*H*-imidazole-4-carboxamide **13**: same procedure as for the synthesis of **4**. (30.20 mg, 0.093 mmol, 12.80% yield) ^{1}H NMR (400 MHz, 25 ºC, MeOH) δ 7.99-7.98 (m, 1H), 7.73 (s, 1H), 7.57 (m, 1H), 7.21 (t, 1H, J = 9 Hz), 3.78 (s, 3H), 2.87-2-82 (m, 2H), 2.39-2.36 (m, 2H), 2.00-1.98 (m, 1H), 1.93-1.70 (m, 1H) ppm.

2-(1-hydroxycyclobutyl)-*N*-(4-hydroxyphenyl)-1-methyl-1*H*-imidazole-5-carboxamide **14**: 12 (59.70 mg, 0.198 mmol) was dissolved in DCM and cooled down to 0º C with and ice bath. Tribromo boron (BBr₃) (54.59 mg, 0.218 ml, 0.218 mmol) was added dropwise over a period of 5 min. The reaction mixture was stirred overnight at 0º C. Water (20 ml) was added and extracted with a DCM:Isopropanol 90:10 (3x40 ml). The compound was purified by prep

HPLC. ^{1}H NMR (400 MHz, 25 ℃, DMSO) δ 9.87 (s, 1H), 9.28 (s, 1H), 7.66 (s, 1H), 7.45 (d, 2H, J = 8.94 Hz), 6.73 (d, 2H, J = 8.78 Hz), 5.99 (s, 1H), 3.84 (s, 3H), 2.74-2.72 (m, 2H), 2.37-2.27 (m, 2H), 1.44-1.43 (m, 1H), 1.41-1.40 (m, 1H).

N-(3-chloro-4-fluorophenyl)-2-(1-hydroxycyclobutyl)-N,1-dimethyl-1H-imidazole-5-carboxamide **15**: **3** (27.80 mg, 0.086 mmol) and sodium hydride (NaH) (3.43 mg, 0.086 mmol) were dissolved in dry THF (3 ml) and cooled down to 0º C. Methyl iodide (12.19 mg, 0.005 ml, 0.086 mmol) was added dropwise over a 5 min period and the reaction mixture was stirred for 1.5 h at 0º C. The reaction mixture was quenched with water (15 ml) and extracted with EtOAc (3x25 ml) and dried over sodium sulphate. Purified by autoflash column chromatography DCM: MeOH 90:5 to yield the compound (16.90 mg, 0.050 mmol, 58.27% yield) ^{1}H NMR (400 MHz, 25 ℃, MeOH) δ 7.52 (m, 1H), 7.28-7.26 (m, 1H), 6.32 (s, 1H), 3.85 (s, 3H), 3.41 (s, 3H), 2.71-2.68 (m, 2H), 2.33-2.30 (m, 2H), 1.88-1.80 (m, 1H), 1.59-1.56 (m,1H) ppm.

This same procedure was used for the radiolabelling with ^{11}C but at room temperature in a hot lab.

For the synthesis of 2-(1-hydroxycyclobutyl)-1-methyl-1H-imidazole-5-carboxylic acid **16**: **1** (78.50 mg, 0.373 mmol) was hydrolysed by dissolving it in a 1:1 THF:MeOH (1 ml). A 1M NaOH solution (1.49 ml, 1.49 mmol) was added to the reaction mixture and it was stirred ON. The solvent was removed under reduced pressure, **16** was used without further purification or isolation.

Several procedures were used for the synthesis of methyl 1-methyl-1H-imidazole-5-carboxylate **17**: The first one used for the methylation of 1H-imidazole-5-carboxylic acid (566 mg, 5.05 mmol) was to dissolve it along KOH (374 mg, 6.65 mmol) in acetone (5 ml) by means of an ultrasonic bath, cooled down to 0º C with an ice/water bath. MeI (0.62 ml, 1.42 g, 10 mmol) was added drop-wise and the reaction was stirred for 90 min. The reaction mixture was diluted with water (10 ml) and extracted with EtOAc (3 x 10 ml), dried over Na_2SO_4 and the solvent removed under reduced pressure.

The second procedure used consisted in dissolving 1H-imidazole-5-carboxylic acid (0.53 g, 4.77 mmol) and NaH (0.72 g, 30 mmol) on anhydrous DMF under inert atmosphere. Excess MeI (1.4 ml) was added drop-wise at 0º C. After 1h the reaction mixture was solid, water (10 ml) was added to dissolve the reaction mixture, EtOAc (3 x 25 ml) was used to extract the reaction mixture, dried over Na_2SO_4 and the solvent reduced under pressure to yield an orange oil **17** (0.53 g, 3.80 mmol, 79.53% yield, contaminated with DMF). This same procedure was used to attempt the methylation of 1-methyl-1H-imidazole-5-carboxylic acid (0.92 g, 8.12 mmol) with NaH (1.18 g, 49.03 mmol) and MeI (4.58 ml, 10.44 g, 73.55 mmol) to yield **17** (0.87 g, 6.24 mmol, 85.96% yield contaminated with DMF).

The last procedure used consisted in dissolving 1-methyl-1H-imidazole-5-carboxylic acid (0.25 g, 1.95 mmol) and K_2CO_3 (1.11 g, 8 mmol) in acetone (10 ml) with the aid of an ultrasonic bath. MeI (0.4 ml, 0.83 g, 5.85 mmol) was added drop-wise and the reaction mixture was stirred

at 0º C for 90 min. The reaction mixture was diluted with water (15 ml) and extracted with EtOAc (3 x 30 ml), dried over Na_2SO_4 and the solvent removed under reduced pressure.

For the synthesis of 4-bromo-1H-imidazole **18**: imidazole (0.08 g, 1.16 mmol) was dissolved in water (10 ml), DBH (0.10 g, 3.60 mmol) was added followed by H_2SO_4 (2 ml) in few portions. The reaction was quenched with NaOH (3.8 M, 20 ml) and neutralized with acetic acid until pH ~6. 1/3 of the solvent was evaporated under reduced pressure and the insoluble salts were filtered off. Enough NaCl was added in order to make a saturated solution and diethyl ether (3 x 30 ml) was used to extract the reaction mixture, dried over Na_2SO_4 and the solvent removed under reduced pressure to yield a white precipitate (0.058 g, 0.38 mmol, 33.5% yield) contaminated with DBH).

2,4,5-tribromo-1H-imidazole **19**: was synthesized by dissolving imidazole (0.086 g, 1.26 mmol) in water (10 ml), DBH (0.58 g, 2.04 mmol) was added in one portion to yield a yellow solution. H_2SO_4 (1 ml) was added drop-wise. A NaOH solution (3.8 M, 20 ml) was added to quench the reaction and the pH was adjusted until pH ~6 with acetic acid. The reaction mixture was kept in the fridge until complete precipitation of **19** (0.089mg, 0.3 mmol, 23.27% yield).

To synthesize 4,5-diiodo-1H-imidazole **20**: imidazole (11.09 g, 162.9 mmol) was dissolved in a NaOH solution (4 M, 600 ml). A separate solution was made of KI (147.2 g, 886.7 mmol) and I_2 (88.18 g, 347.4 mmol) in water and it was added drop-wise to the imidazole solution. The reaction mixture was stirred for 20 h at RT. The reaction mixture was neutralized until the product precipitated with acetic acid. The crystals were washed with several portions of $NaSO_3$ and ice water. The product was not dried or purified further for the next reaction.

4-iodo-1H-imidazole **21**: was synthesized by two different procedures. The first one being the selective dehalogenation of **20** (21.75 g,68.01 mmol) for which it was dissolved in a 30% ethanol solution (400 ml) along with K_2SO_3 (187.4 g, 1183 mmol) and refluxed at 84º C for 22h. The reaction mixture was cooled down to RT and the inorganic salts were filtered off. The ethanol was removed under reduced pressure and NaCl was added to make a saturated solution of the aqueous phase before being extracted with ether:THF (1:1) (3 x 300 ml), dried over Na_2SO_4 and the solvent was removed under reduced pressure.

The second method used DIH for the synthesis of **21**: Imidazole (411 mg, 6.04 mmol) was dissolved in water (50 ml) and cooled down to 0º C with an ice bath. A DIH solution (0.54 g, 1.42 mmol) was made in sulfuric acid (5 ml) and the solution was added drop-wise to the imidazole solution. A NaOH solution (3.8 M, 50 ml) was added to the reaction mixture and the pH was adjusted to 6 with acetic acid. The reaction mixture was first extracted with ether (3 x 40 ml) and then with a 10% HCl solution (3 x10 ml). The water was removed under reduced pressure and the product precipitated. The pH was adjusted to 6 with a sodium bicarbonate solution and extracted with ether (3 x 30 ml), the solvent was removed under reduced pressure to yield **21** (0.17 g, 0.91 mmol, 15.11% yield).

Both 4-bromo-1-methyl-1*H*-imidazole **22** and 4-iodo-1-methyl-1*H*-imidazole **23** were synthesized by following one of the procedures attempted for the synthesis of **17**. The corresponding imidazole and KOH were dissolved in acetone by means of an ultrasonic bath and cooled down to 0º C. Excess MeI was added drop-wise and the reaction mixture was stirred for 90 min. Water was added and the reaction mixture was extracted with EtOAc, dried over Na_2SO_4 and the solvent removed under reduced pressure to yield the corresponding product. **22** (0.036g, 0.17 mmol, 36.87% yield), **23** (0.13 g, 0.62 mmol, 67.97% yield).

23 was used to attempt the synthesis of 1-(1-methyl-1*H*-imidazol-4-yl)cyclobutan-1-ol **24** using two different procedures, unfortunately neither of them yielded the desired product.

For the first attempt a Grignard reaction was used. For this Mg (0.075 g, 3.10 mmol) was dried beforehand in a round bottle flask. Anhydrous THF (5 ml) was added to the flask. A solution of **23** (0.13 g, 0.62 mmol) in THF was added to the reaction flask and it was stirred for 30 min. Cyclobutanone (0.23 ml, 0.22 mg, 3.11 mmol) was added drop-wise. After 10 min a saturated solution of ammonium chloride (10 ml) was added and the reaction mixture was extracted with DCM (3 x 15 ml). No reaction occurred.

For the second attempt of the Grignard reaction. Dibromoethane (0.14 ml, 0.30 g, 1.60 mmol) was added to the Mg solution in order to activate the Mg. After 10 min, the solution of **23** was added to the reaction flask. The rest of the procedure was the same.

The second procedure used to attempt the synthesis of **24** was by lithium-halogen exchange. **23** (0.15 g, 0.71 mmol) was dissolved in dry THF (10 ml), *n*-BuLi (0.56 ml, 1.41 mmol) was added drop-wise over a period of 10 min, the reaction mixture was stirred at -78º C for 45 min. Cyclobutanone (0.08 ml, 0.08 g, 1.14 mmol) was added and the reaction mixture was stirred for 45 min more. The reaction mixture was quenched with water (15 ml) and extracted with EtOAt (3 x 25 ml), dried over Na_2SO_4 and the solvent removed under reduced pressure. The desired product was not formed.

1-methyl-4-nitro-1*H*-imidazole **25**: 4-nitroimidazole (0.56 g, 5 mmol) and KOH (0.37 g, 6.65 mmol) were dissolved in acetone (10 ml) by means of an ultrasonic bath and cooled down to 0º C with an ice bath. MeI (0.33 ml, 0.76 g, 5.35 mmol) was added drop-wise. After 90 min water (10 ml) was added and was extracted with EtOAc (3 x 10 ml), dried over Na_2SO_4 and the solvent was removed under reduced pressure to yield **25** (0.13 g, 1.03 mmol, 20.61% yield).

1-methyl-1*H*-imidazol-4-amine **26**: Two different attempts to reduce the nitro group of **25** were tested.

For the first one **25** (0.066 mg, 0.51 mmol) was dissolved in EtOH (5 ml). A solution of $CoSO_4$ (0.144 g, 0.51 mmol) was made in water (0.7 ml) and added drop-wise while cooling down to 0º C with an ice bath. $NaBH_4$ (0.077 mg, 2.04 mmol) was added in portions to the reaction mixture. The reaction mixture was stirred at RT for 10 min. The catalyst was filtered off and the reaction mixture was diluted with water (50 ml) and extracted with EtOAc (2 x 40 ml), dried over Na_2SO_4 and the solvent was removed under pressure. The desired product **26** was not obtained.

The second reduction procedure to synthesize **26** consisted in dissolving **25** (0.11 g, 1.00 mmol) and Pd(OH)$_2$/C (15% w/w) in dry DCM (25 ml), H$_2$ was introduced to the reaction with a balloon, the reaction was heated at 52º C overnight. The palladium catalyst was filtered off with a celite filter and it was washed with methanol and water. The product was not obtained either by this method.

(1-methyl-1*H*-imidazol-5-yl)methanol **27**: To reduce the carboxylic group of 1-methyl-1*H*-imidazole-5-carboxylic acid (0.11 g, 0.79 mmol) it was dissolved in dry THF (10 ml) under inert atmosphere. LiAlH$_4$ (1.59 ml, 0.06 g, 1.59 mmol) was added and the reaction was stirred at 0º C during 1 h. Water (10 ml) was added while keeping the temperature at 0º C. The reaction mixture was extracted with EtOAc (3 x 25 ml), dried over Na$_2$SO$_4$ and the solvent was removed under reduced pressure. **27** was not obtained by following this procedure, only the coupling product was observed.
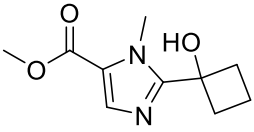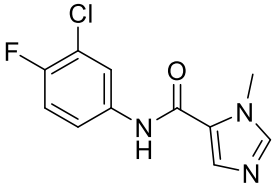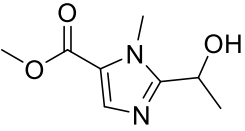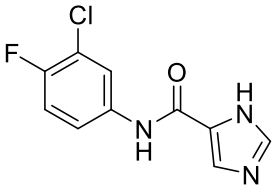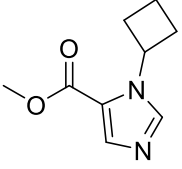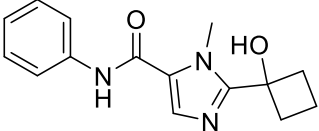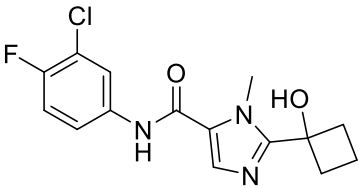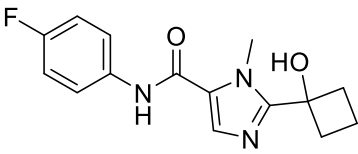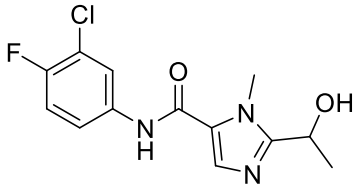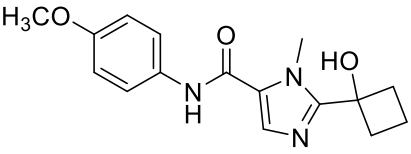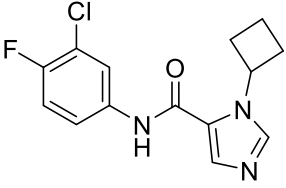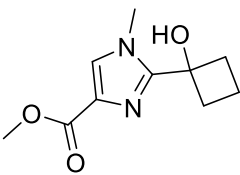
6 REFERENCES
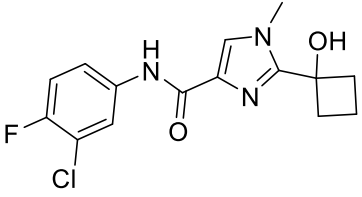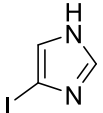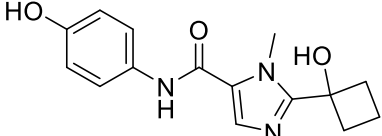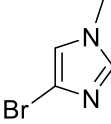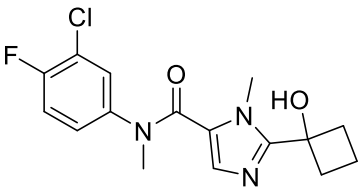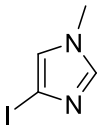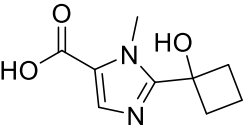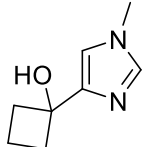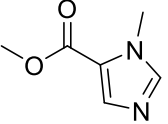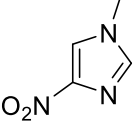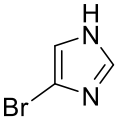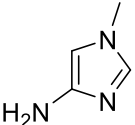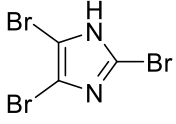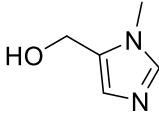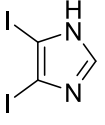
1. J. Pearn, *J. Med. Genet.* **1978**, 15, 409-413.
2. S. Tisdale, L. Pellizzoni, *J. Neureosci*, **2015**, 35, 8691-8700
3. A. Carré, C. Empey, *J Genet Counsel,* **2016**, 25, 32–43.
4. R.N. Singh, M.D. Howell, E.W. Ottesen, N.N. Singh, *Biochim Biophys Acta,* **1860**, 2017, 299-315.
5. H. Chaytow, Y-T. Huang, T. H. Gillingwater, K. M. E. Faller, *Cell Mol Life Sci*, **2018**, 75, 3877-3894.
6. M. E. R. Butchbach, *Front Mol Biosci*, **2016**, 3.
7. J. J. Cherry, E. J. Androphy, *Future Med Chem*, **2012**, 4, 1733-1750.
8. M. A. Farrar, M. C. Kiernan, *Neurotherapeutics*, **2015**, 12, 290-302.
9. M. J. MacLeod, J. E. Taylor, P. W. Lunt, C. G. Mathew. S. A. Robb, *Eur J Paediatr Neurol*, **1999**, 3, 65-72.
10. H. K. Shorrock, T. H. Gillingwater, E. J. N. Groen, *Drugs*, **2018**, 78, 293-305.
11. A. N. Calder, E J. Androphy, K. J. Hodgetts, *J Med Chem*, **2016**, 59, 10067-10083.
12. J. J. Cherry, M. C. Evans, J. Ni, G. D. Cuny, M. A. Glicksman, E. J. Androphy, *J Biomol Screen*, **2012**, 17, 481-495.
13. J. J Cherry et al. *EMBO Mol Med*, **2013**, 5, 1035-1050.
14. Rietz, et al. *J. Med. Chem.* **2017**, 60, 4594-4610.
15. K. Shalini, P. K. Sharma. N. Kumar, *Der Chemica Sinica*, **2010**, 1, 36-47.
16. A. Verma, S. Joshi, D. Singh, *J Chem*, **2013**, 329412.
17. C. Vidal, J. Garcia-Alvarez, A. Hernan-Gomez, A. R. Kennedy, E. Hevia, *Angew Chem Int Ed*, **2014**, 53, 5969-5973.
18. M. Hatano. K. Ishihara, *Synthesis*, **2008**, 11, 1647-1675.
19. A. Basha, M. Lipton, S. M. Weinreb, *Tetrahedron lett*, **1977**, 48, 4171-4174.
20. T. Gustafsson, F. Ponten, P. H. Seeberger, *Chem Commun*, **2008**, 1100-1102.
21. S.W. Chung, D. P. Ucello, H. Choi, J.I Montgomery, *J. Chen Synlett*, **2011**, 14, 2072-2074.
22. H. Friebolin, 'Basic One- and Two-Dimensional NMR Spectroscopy', *Wiley-VCH,* 5th edition, **2011.**
23. J. E. McMurry, 'Organic Chemistry', *International Edition*, 8th edition, **2012**.
24. J. Clayden, N. Greeves, S. Warren, 'Organic Chemistry', *Oxford*, 2nd edition, **2012**.
25. J. H. Gross, 'Mass Spectrometry: A Textbook', **2004**, ISBN 3-540-40739-1.
26. R. Martin Smith, 'Understanding Mass Spectra', *Wiley, Hoboken NJ*, 2nd edition, **2004.**
27. J. J. Pitt, *Clin Biochem Rev*, **2009**, 30, 19-34.
28. Encyclopedia of Food Sciences and Nutrition, **2003**, 1274-1280, 2nd edition.
29. X. Deng, J. Rong, L. Wang, N. Vasdez, L. Zhang, L. Josephson, S. H. Liang, *Angew Chem Int Ed*, **2019**, 58, 2580-2605.
30. A. Drageset, V. Elumalai, H-R. Bjørsvik, *React Che Eng,* **2018**, 3, 550-558.
31. S. Zuffanti, *J Chem Educ,* **1948**, 25, 481.
32. A. Leggio, E. L. Belsito, G De Luca, M. L. Di Gioia, V. Leotta, E. Romio, C. Siciliano, A. Liguori, *RSC Adv*, **2016**, 6, 34468-34475.
33. C. A. G. N. Montalbetti, V. Falque, *Tetrahedron lett*, **2005**, 10827-10852.
34. M. M. Joullie, K. M. Lassen, *Arkivoc*, **2010**, 7, 189-250.
35. A. H. Sandtorv, H-R Bjørsvik, *Adv Synth Catal*, **2013**, 355, 499-507.

36. F. J. Lundevall, V. Elumalai, A. Drageset. C. Totland, H-R. Bjørsvik, *Eur J Org Chem*, **2018**, 3416-3425.
37. A. Drageset, H-R Bjørsvik, *Eur J Org Chem,* **2018**, 4436-4445.
38. J. V. Bhaskar Kanth, M. Periasamy, *J Org Chem*, **1991**, 56, 5964-5965.
39. J. W. Simek, T. Tuck, K. C. Bush, *J Chem Educ,* **1997**, 74, 107-108.

7 APPENDIX

List of compounds

Compound number	Structure	Compound number	Structure
1		7	
2		8	
3		9	
4		10	
5		11	
6		12	

13		21	
14		22	
15		23	
16		24	
17		25	
18		26	
19		27	
20			

NMR spectrum of **1**

379-30_PROTON_01
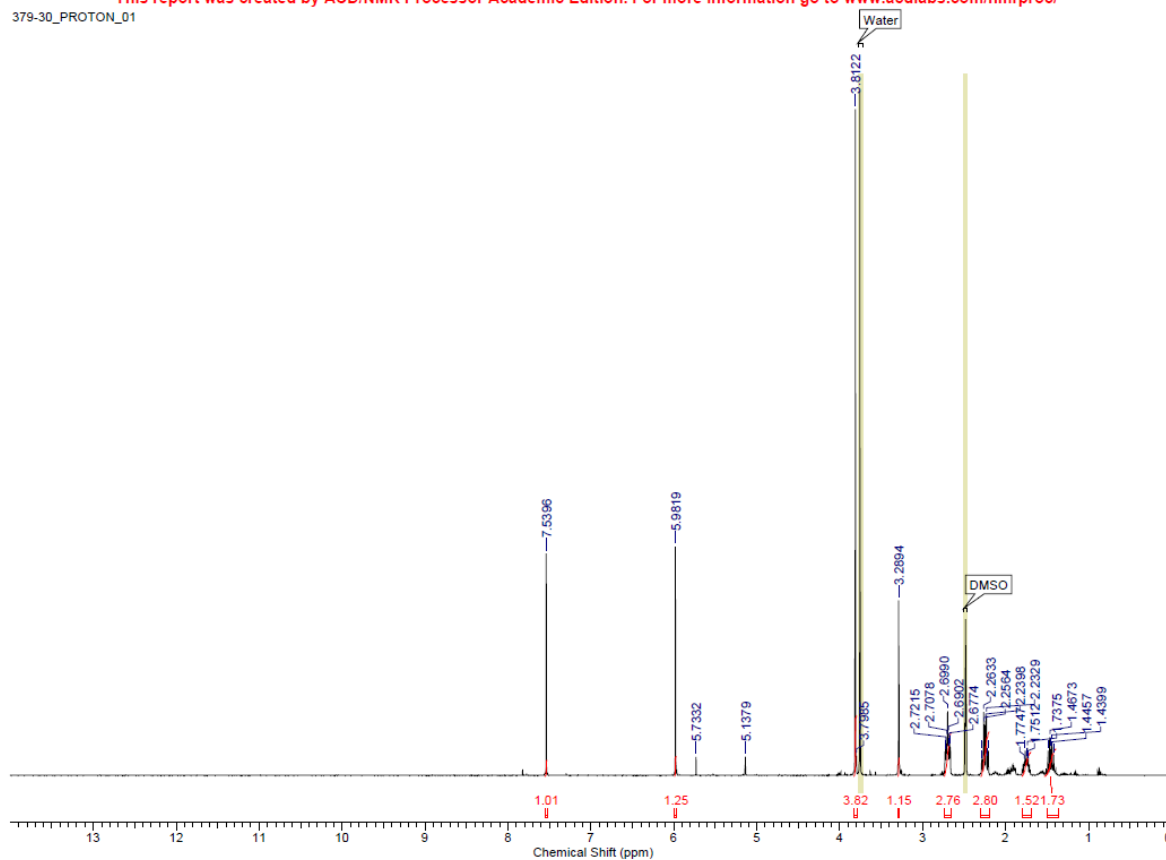
LC-MS of **1**

NMR spectrum of **2**

379-63_PROTON_01

LC-MS spectrum of **2**

*MSD1 SPC, time=1.019:1.977 of C:\CHEM32\1\DATA\379-63-clean.D   ES-API, Pos, Scan, Frag: 70, "pos"

Max: 744629
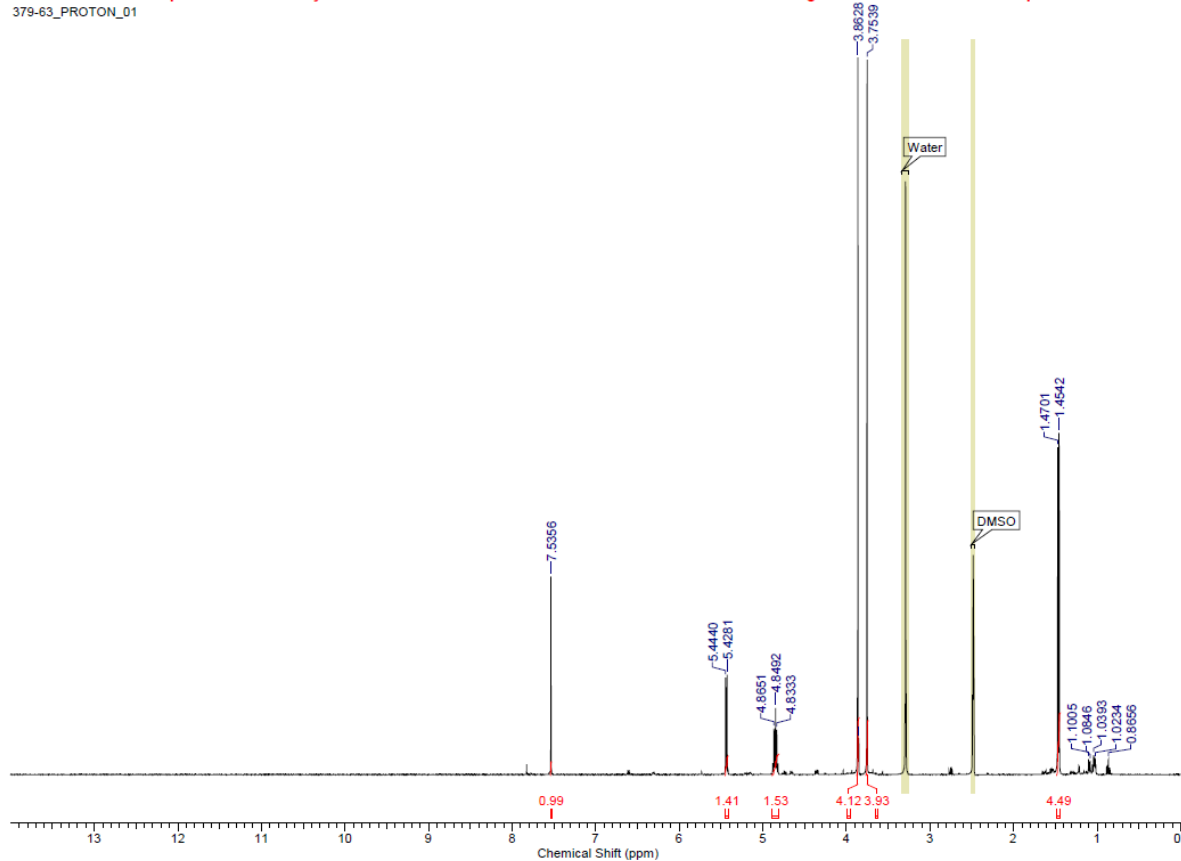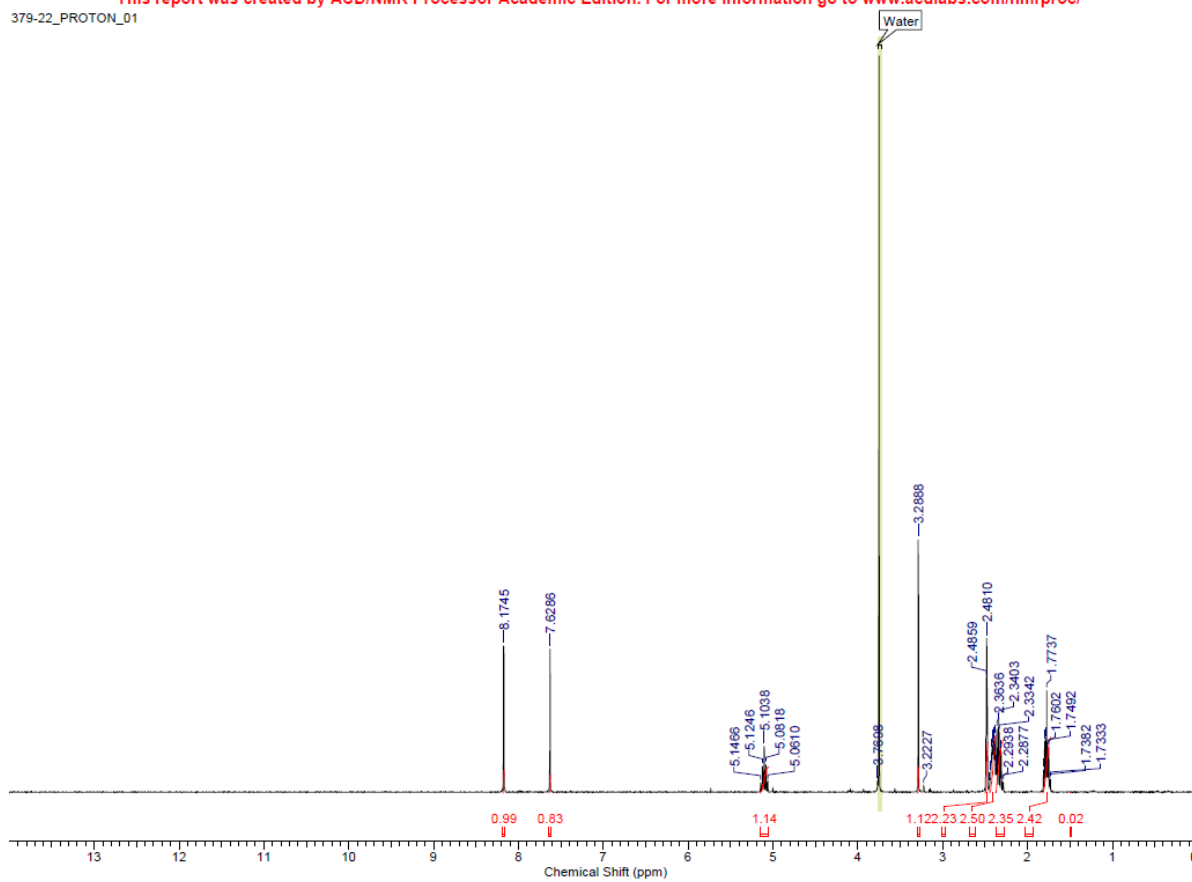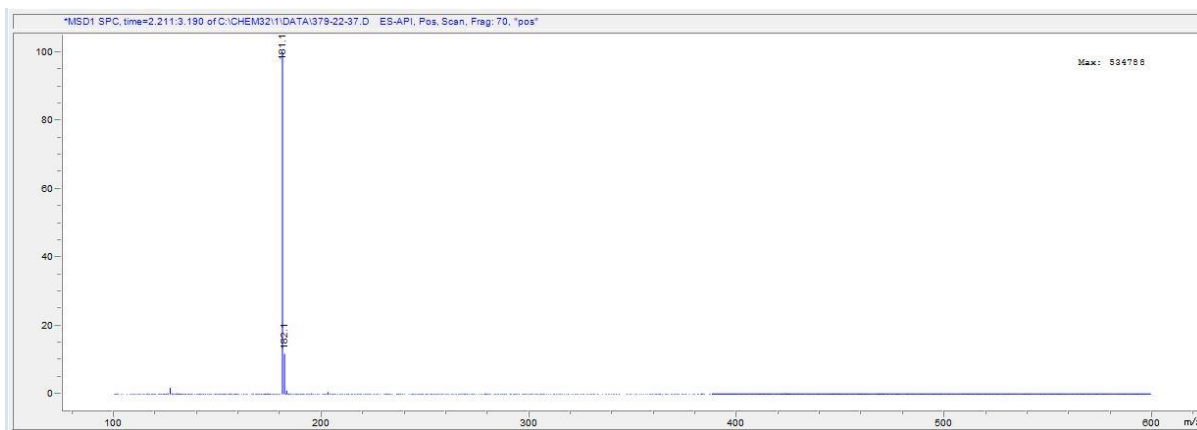
NMR spectrum of **3**

LC-MS spectrum of **3**

NMR spectrum of **4**

379-41_PROTON_01
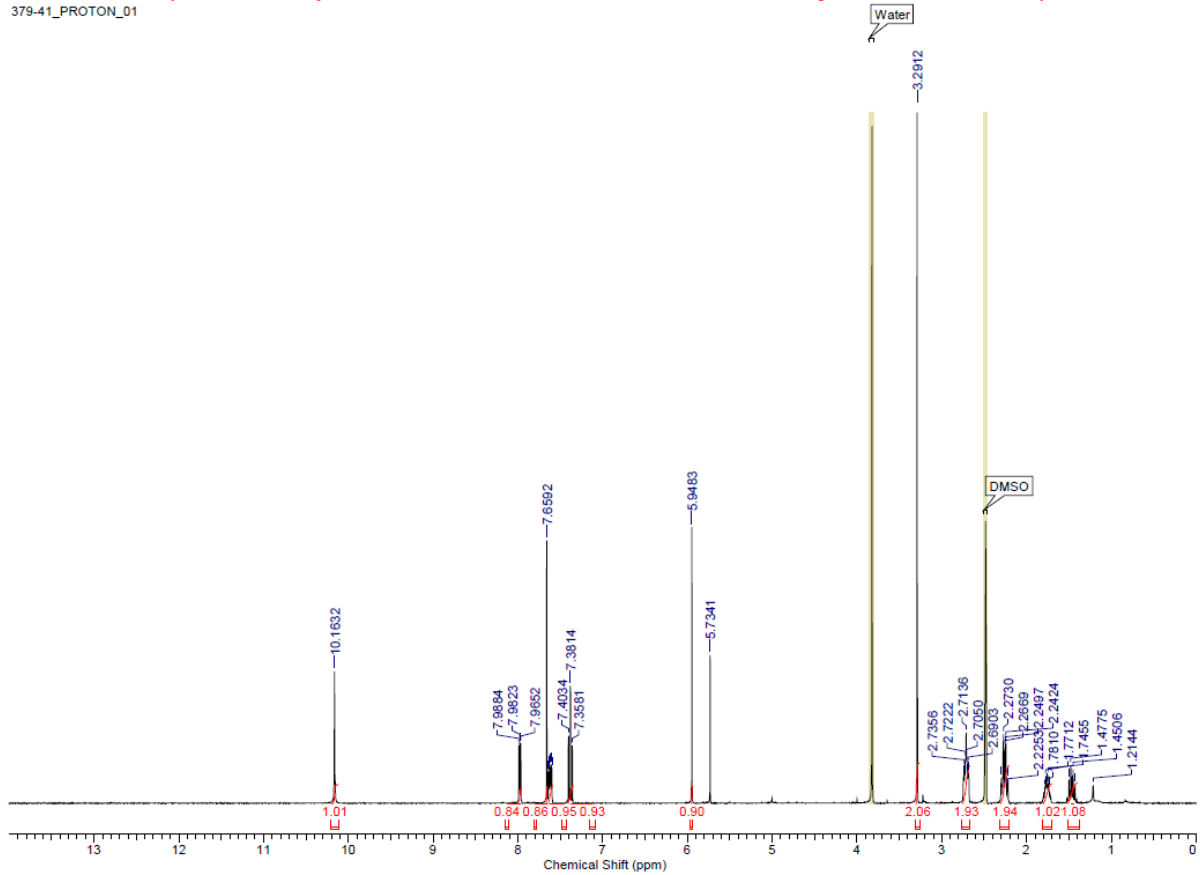
LC-MS spectrum of **4**

NMR spectrum of **5**

379-52_PROTON_01

Methanol

4.0072

Methanol

1.6207
1.6048

7.9113
7.9052

7.6592

7.5429

7.2272
7.1819
7.2052

5.0193
5.0034

1.01 1.03 1.19 1.22   1.25   3.52   3.68

Chemical Shift (ppm)

LC-MS spectrum of **5**

*MSD1 SPC, time=3.101:3.836 of C:\CHEM32\1\DATA\379-52-5.D   ES-API, Pos, Scan, Frag: 70, "pos"

Max: 34020

298.1

300.0

299.0

301.1

124.2

m/z

NMR spectrum of **6**

379-42_PROTON_01

Water

DMSO

10.1020

8.1512
8.1451

8.0251
7.9125

7.9975
7.7865
7.7804 7.3655
7.3190

7.3422

4.8125 4.7905 4.7697
4.7281 4.7489

2.4052 2.3905
2.4125 2.3844
2.4272 2.3685

1.8263 1.8140 1.7834 1.7602
1.8006 1.7137 1.7382

1.00   0.93 0.93 0.91 1.03 1.03   1.06   3.87 2.10

Chemical Shift (ppm)

LC-MS spectrum of **6**

*MSD1 SPC, time=4.359:5.873 of C:\CHEM32\1\DATA\379-42-44.D   ES-API, Pos, Scan, Frag: 70, "pos"

Max: 62783

294.1

296.1

295.1
297.0

316.1

NMR spectrum of **7**

i4_PROTON_01

Methanol

3.9512

Methanol

7.9146
7.9077
7.7951
7.7521
7.5445
7.2282
7.2057
7.1832

0.99 1.13 1.08 1.16 1.20

3.35

Chemical Shift (ppm)

13 12 11 10 9 8 7 6 5 4 3 2 1 0

LC-MS spectrum of **7**

*MSD1 SPC, time=2.979:4.025 of C:\CHEM32\1\DATA\379-54ac.D ES-API, Pos, Scan, Frag: 70, "pos"

Max: 182223

254.1

255.1

100 80 60 40 20 0

100 200 300 400 500 600 m/z
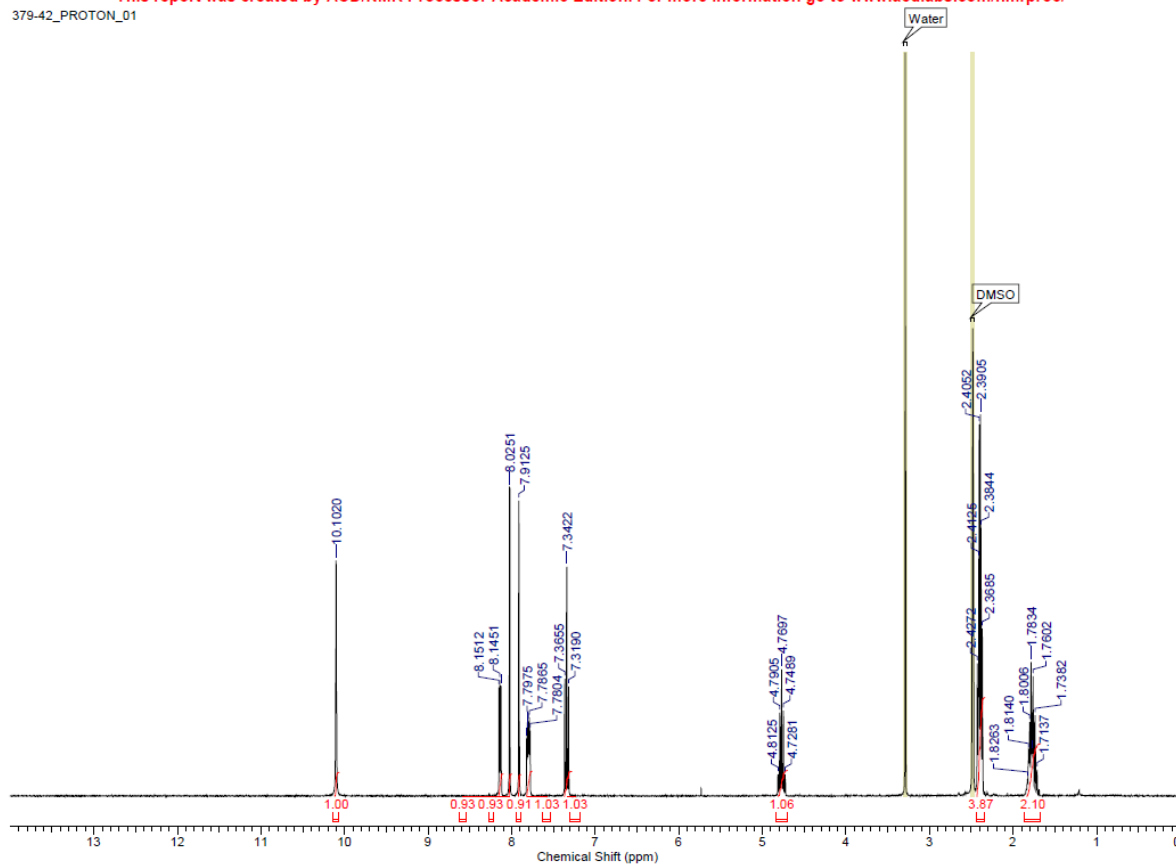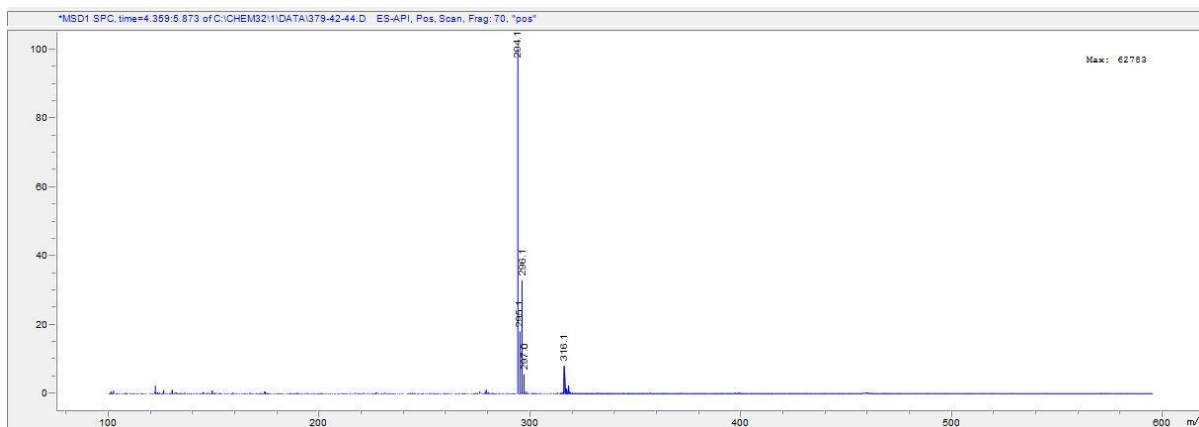
NMR spectrum of **8**

79-53_PROTON_01

LC-MS spectra of **8**

Positive
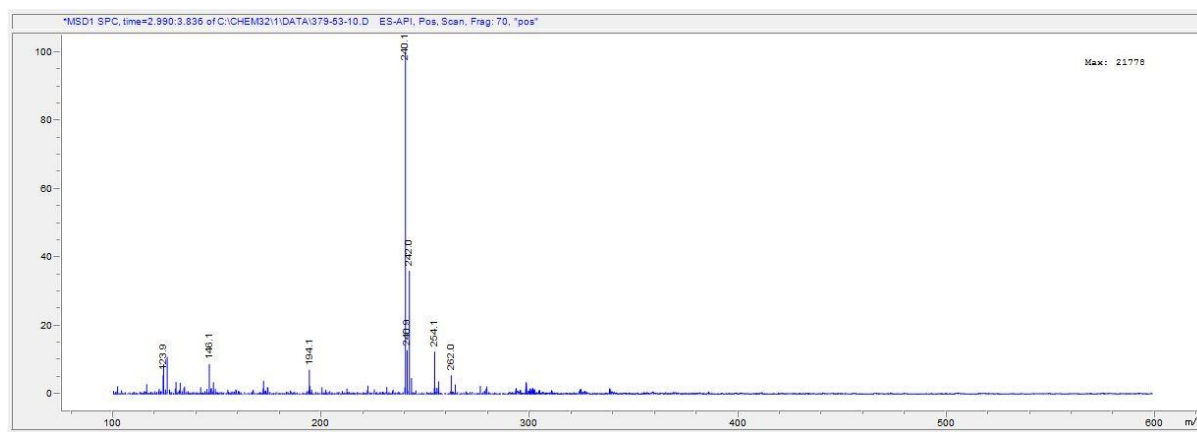
Negative

Max: 14804

NMR spectrum of **9**

379-57_PROTON_01

Methanol

—3.9509

Methanol

—7.6457

7.6347
7.6139
7.3337
7.3129
7.1195
7.1011

7.3484

2.8250
2.8139
2.8041
2.7931
2.7821
2.7711
2.4027
2.3954
2.3807
2.3733
2.0050
.9266
1.6794
1.6513
1.2829
1.2339

1.02 2.35 2.42 1.18

3.55

2.62 2.66 1.46 1.54

13   12   11   10   9   8   7   6   5   4   3   2   1   0
Chemical Shift (ppm)
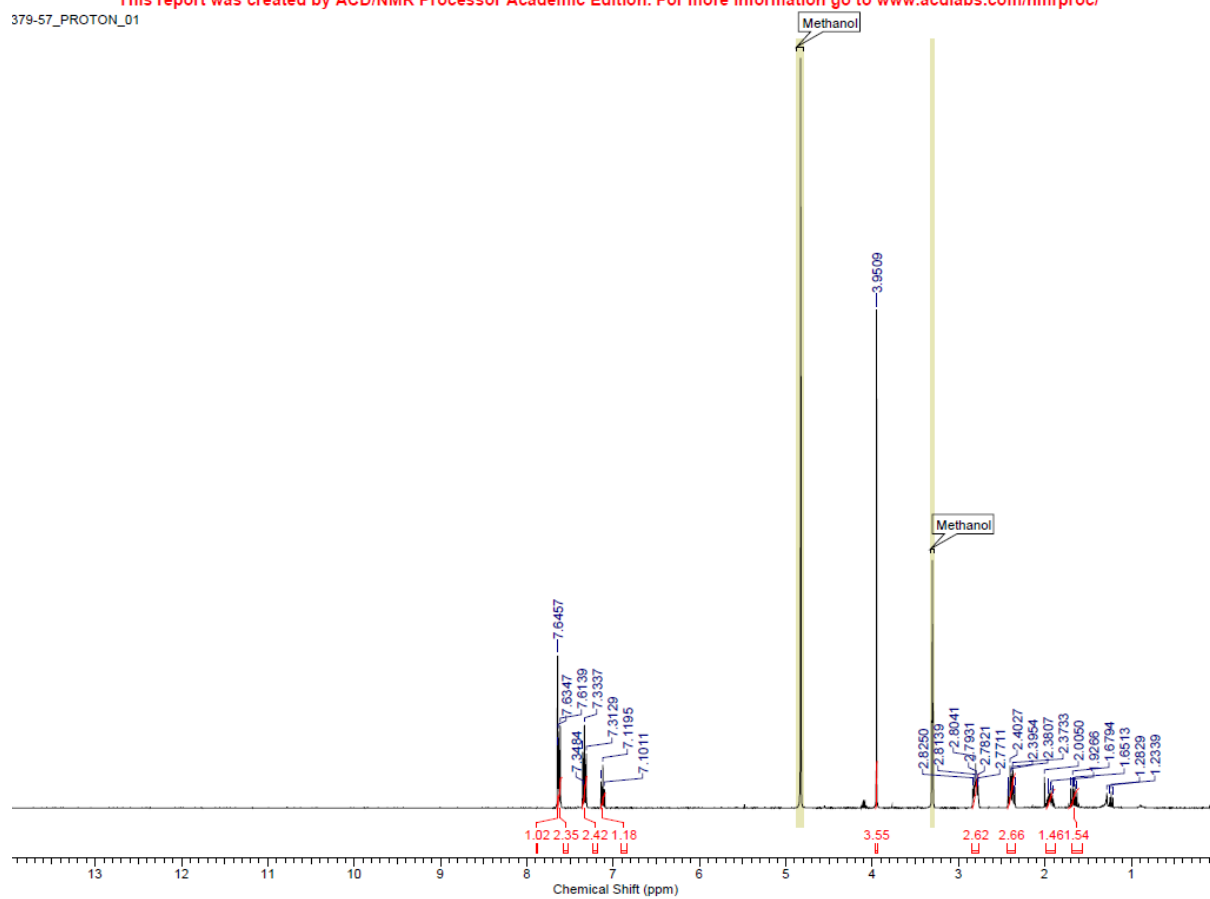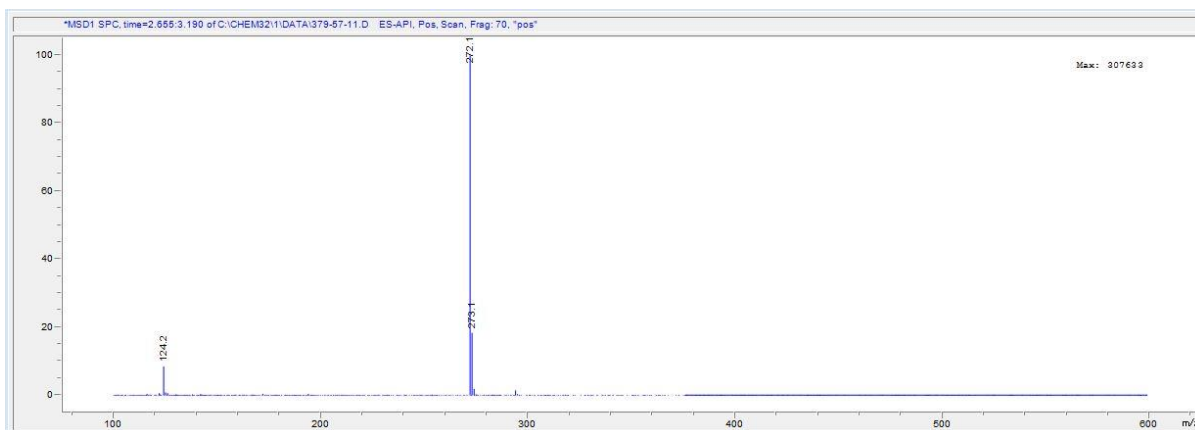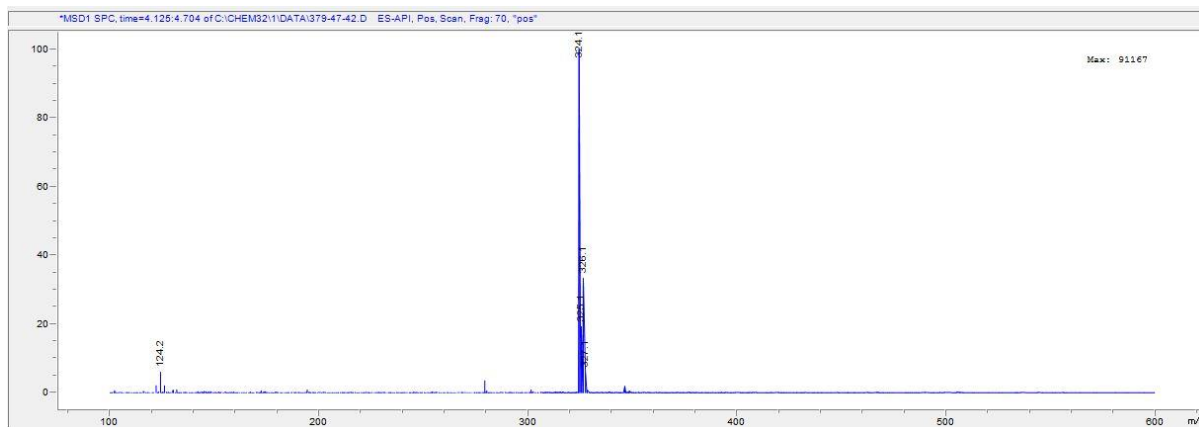
LC-MS spectrum of 9

NMR spectrum of **10**
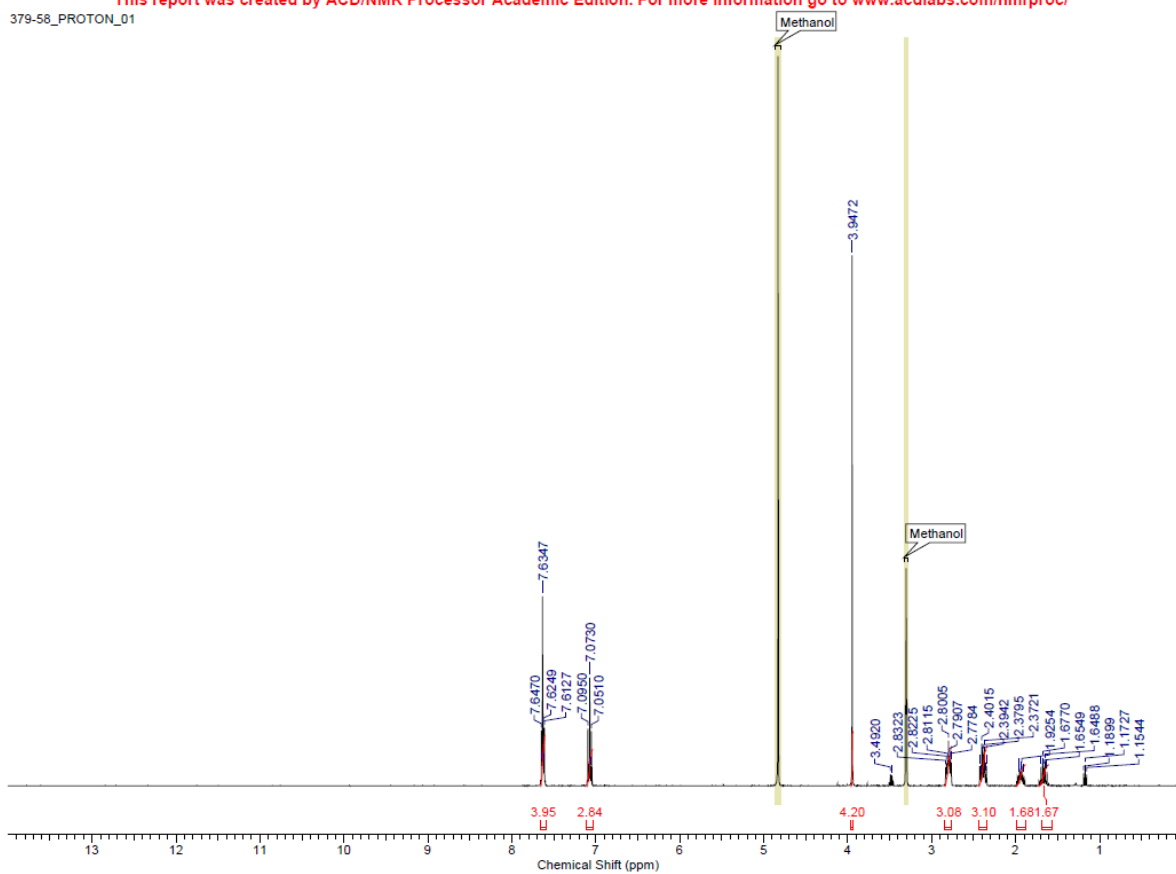
LC-MS spectrum of 10
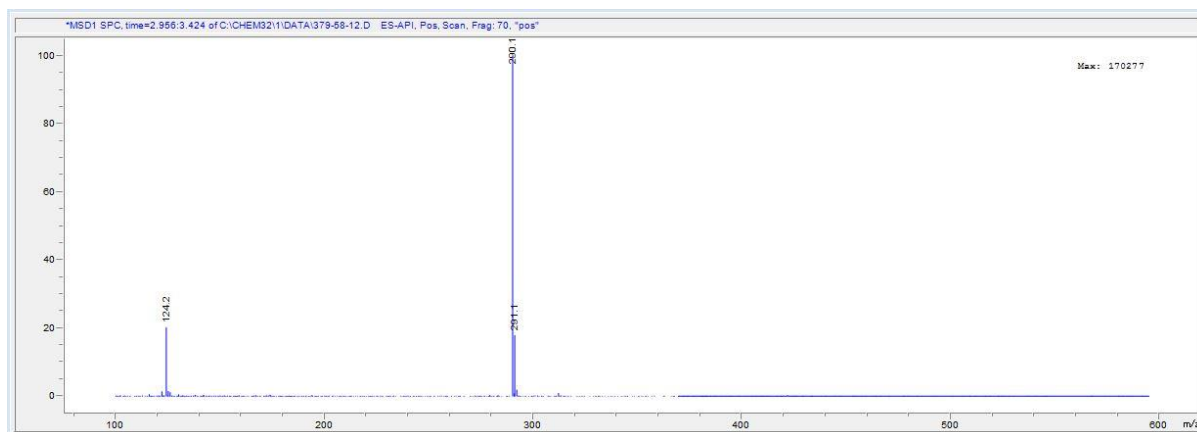
*MSD1 SPC, time=2.956:3.424 of C:\CHEM32\1\DATA\379-58-12.D   ES-API, Pos, Scan, Frag: 70, "pos"

Max: 170277

NMR spectrum of 11

379-61_PROTON_01
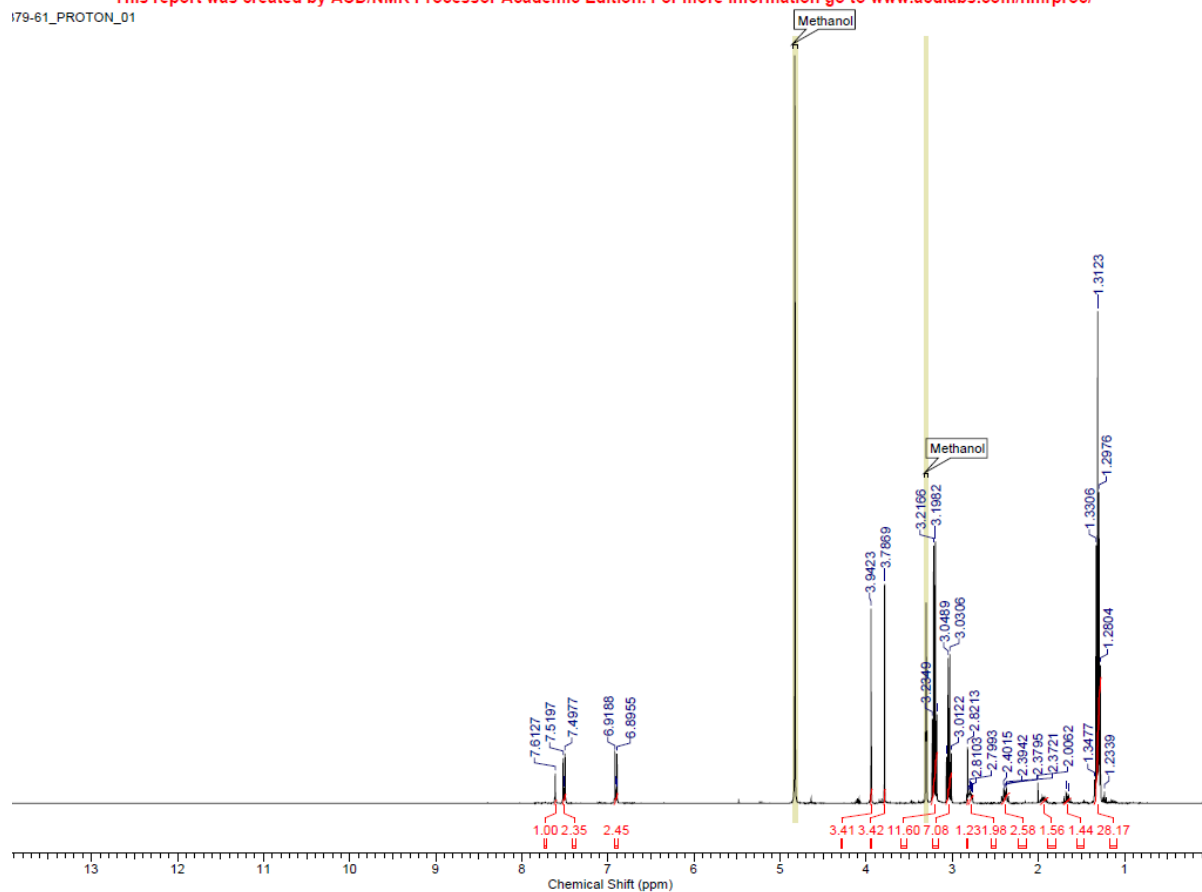
LC-MS spectrum of **11**
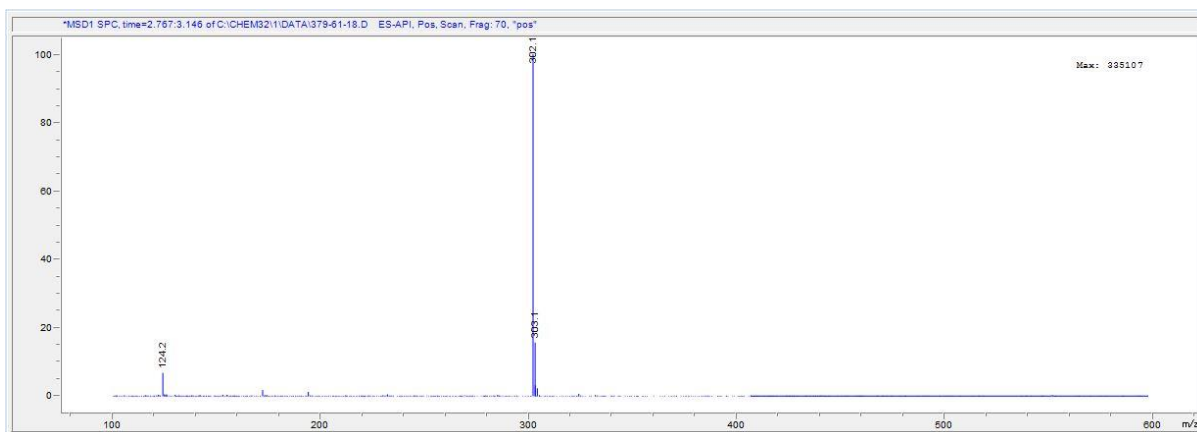
LC-MS spectrum of **12**

NMR spectrum of **13**

379-47_PROTON_01

Methanol

-3.7783

Methanol

-7.7290

-7.9982
-7.9884
-7.5760
-7.2321
-7.2101
-7.1868

-2.8702
-2.8592
-2.8384
-2.8274
-2.3905
-2.3831
-2.3685
-2.3623
-1.9315
-1.7504
-1.7284
-1.7014

1.00 1.03 1.23 1.23   3.52   2.54   2.62 1.77 1.47

Chemical Shift (ppm)

13   12   11   10   9   8   7   6   5   4   3   2   1   0

LC-MS spectrum of **13**

*MSD1 SPC, time=4.125:4.704 of C:\CHEM32\1\DATA\379-47-42.D   ES-API, Pos, Scan, Frag: 70, "pos"

Max: 91167

324.1

326.1

124.2

100   200   300   400   500   600   m/z
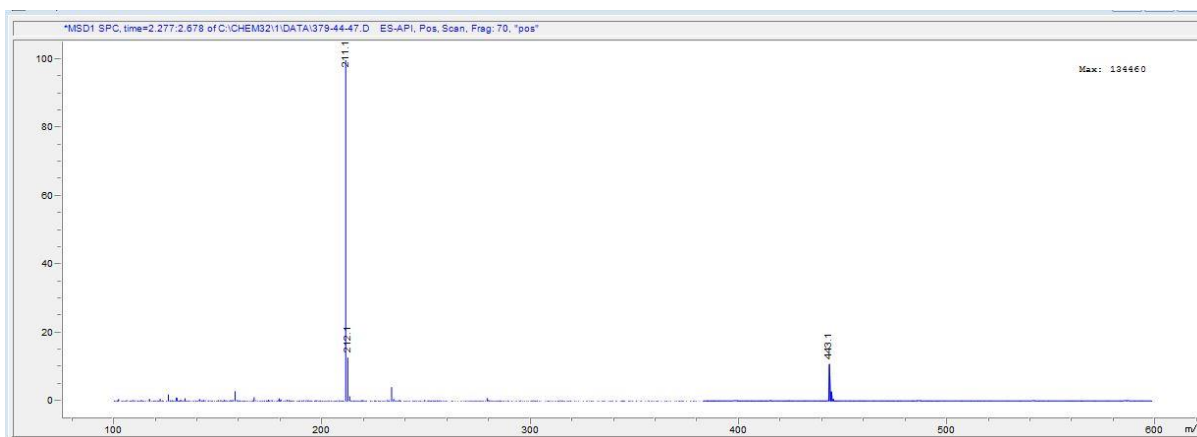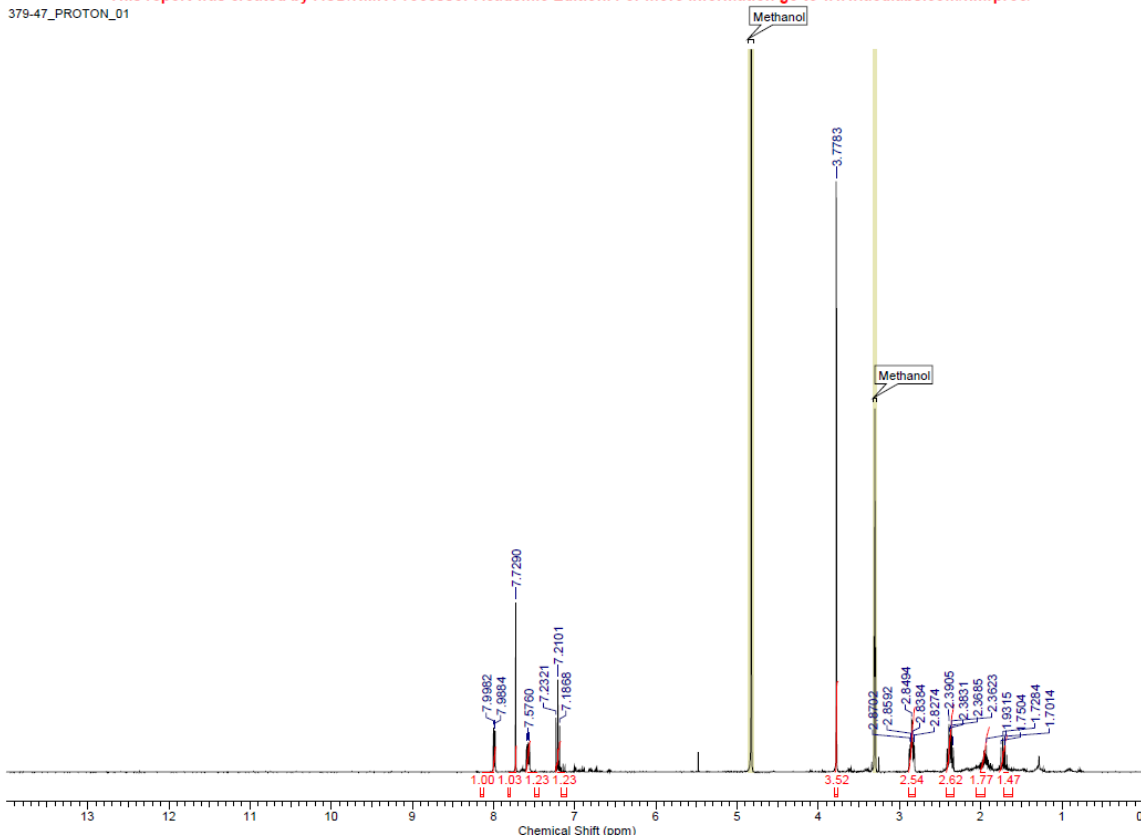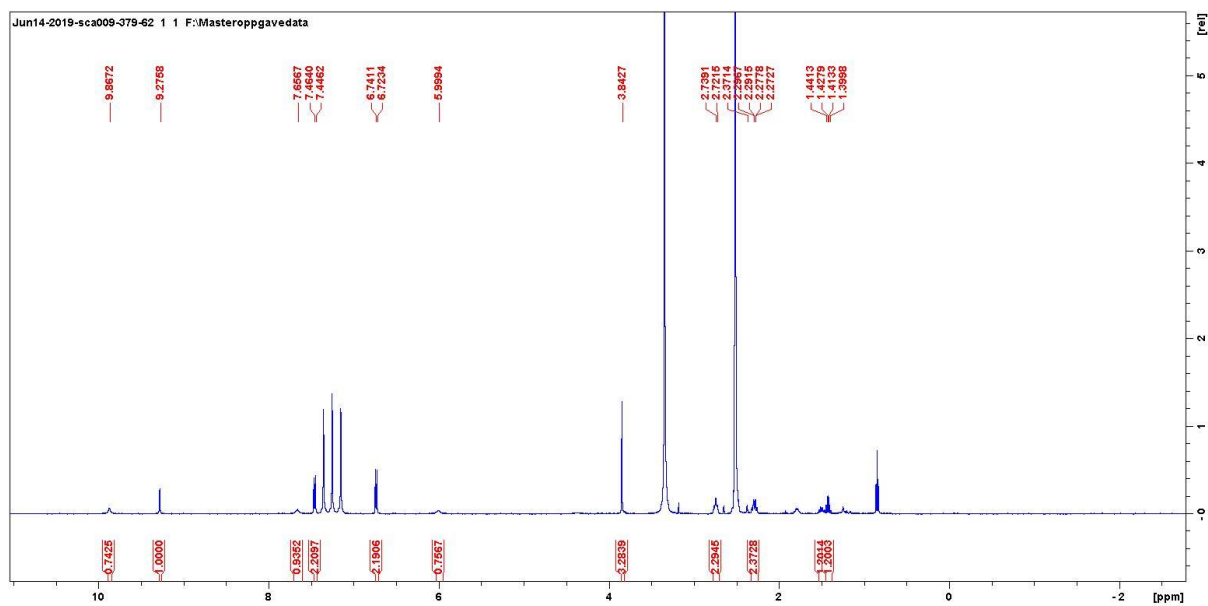
NMR spectrum of **14**

LC-MS spectrum of **14**

NMR spectrum of **15**

379-51_PROTON_01

Methanol

—3.8481
—3.4063

Methanol

7.2798
7.2615
—7.5270
—6.3228
—5.4832

2.7136
2.7026
2.6977
2.6916
2.6818
2.3330
2.3256
2.3122
2.3048
1.8850
1.5913
1.5852
1.5705
1.5631

1.02 1.12 1.01   0.90   3.41 3.35   2.46 2.47 1.31 1.39

13   12   11   10   9   8   7   6   5   4   3   2   1   0

Chemical Shift (ppm)

LC-MS spectrum of **15**

*MSD1 SPC, time=3.079:3.702 of C:\CHEM32\1\DATA\379-51-9.D   ES-API, Pos, Scan, Frag: 70, "pos"

Max: 101716

338.1

100   200   300   400   500   600   m/z
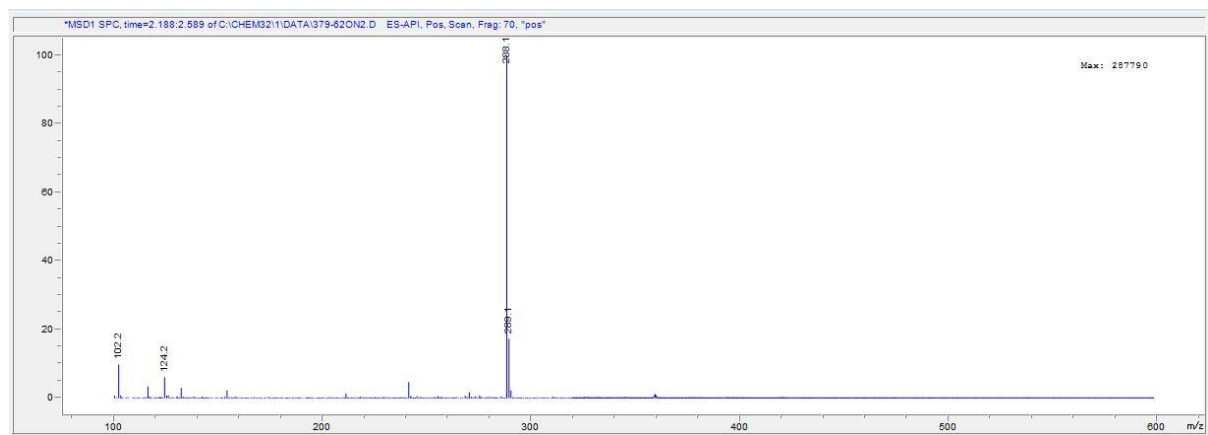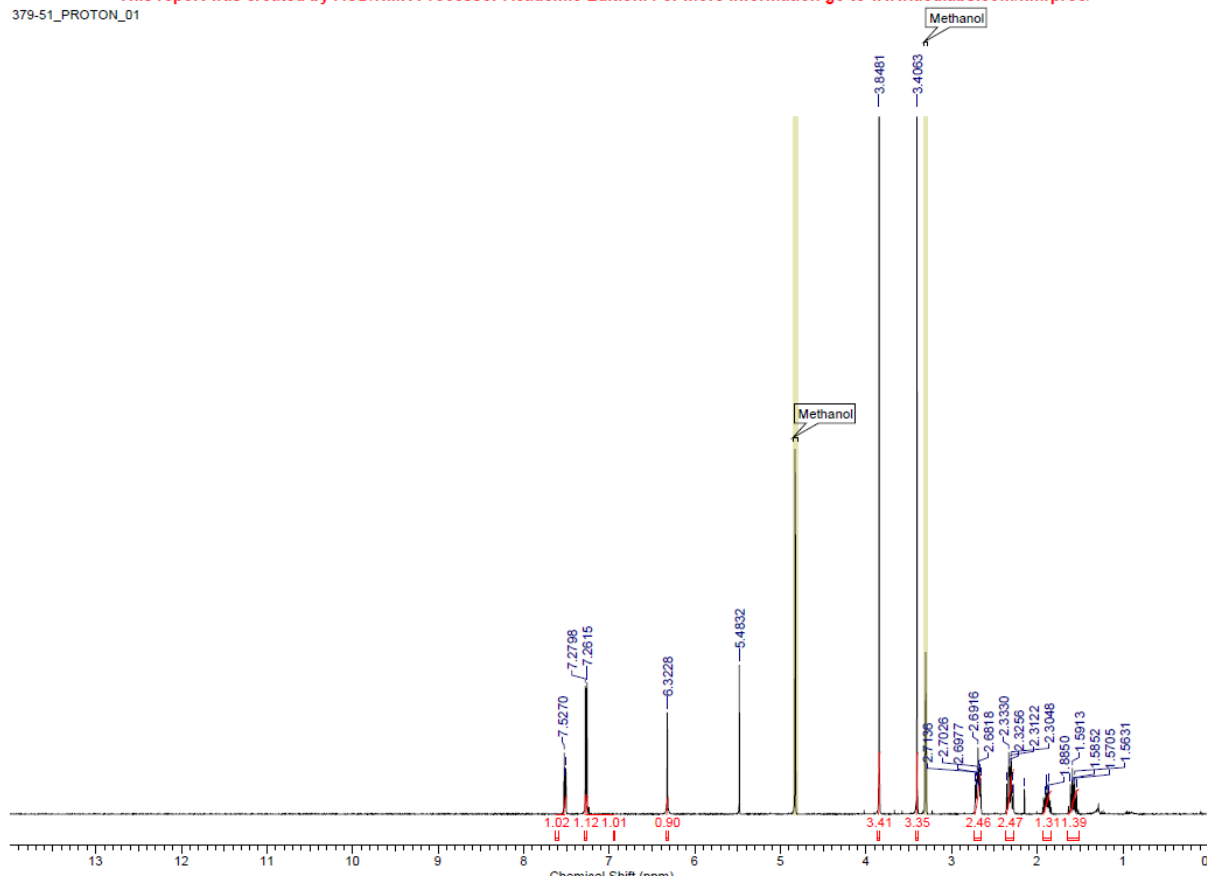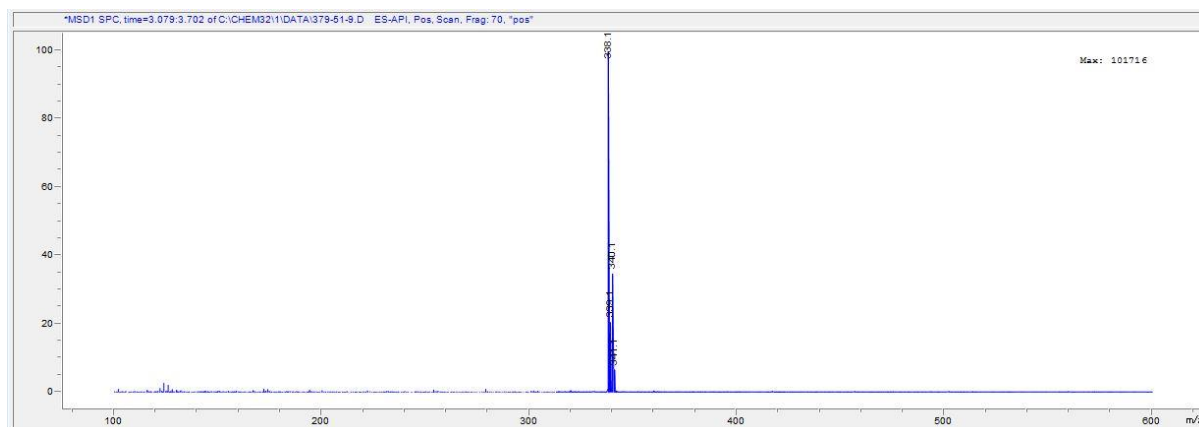
LC-MS spectrum of **16** (third procedure)

87
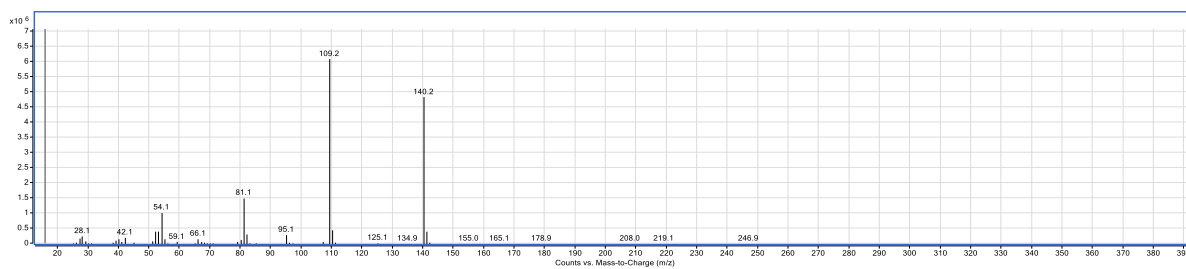
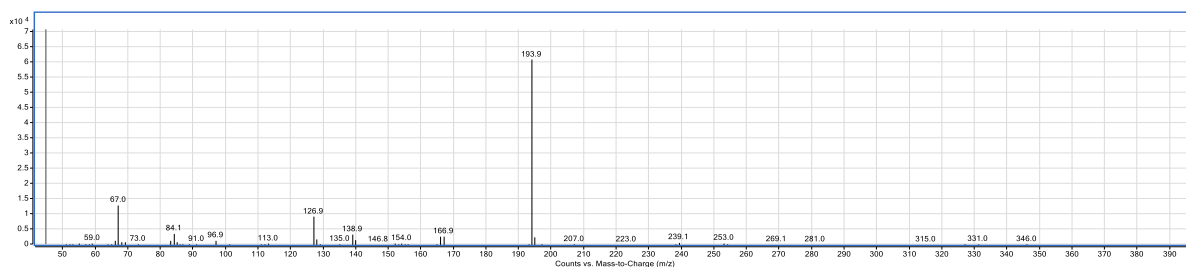LC-MS spectrum of **16** (fourth procedure)
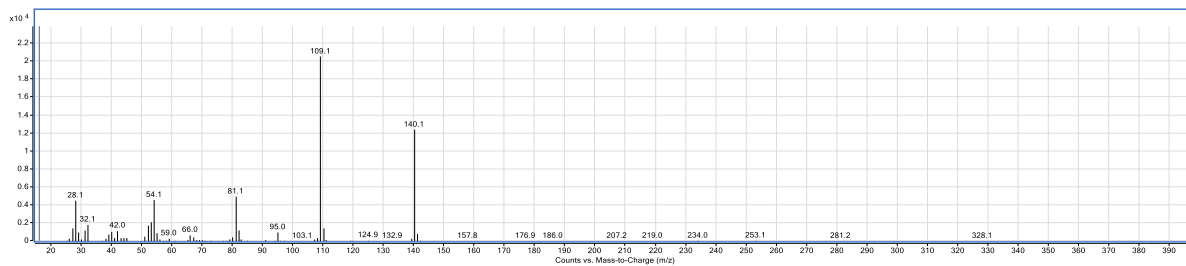
LC-MS spectrum of **19**
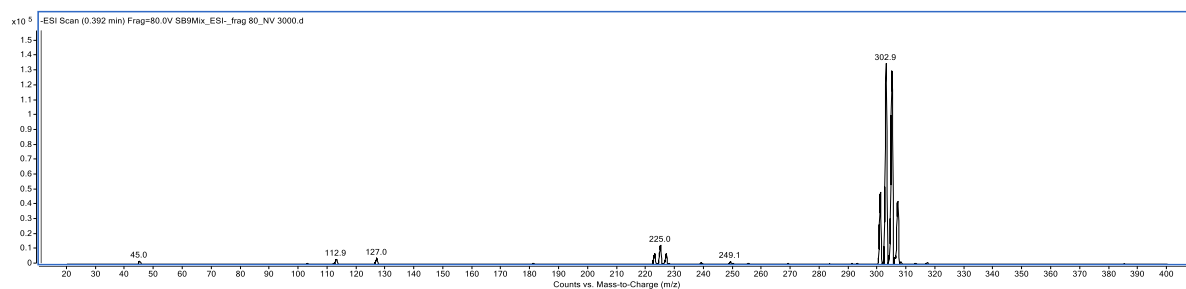
GC-MS spectrum of **20**
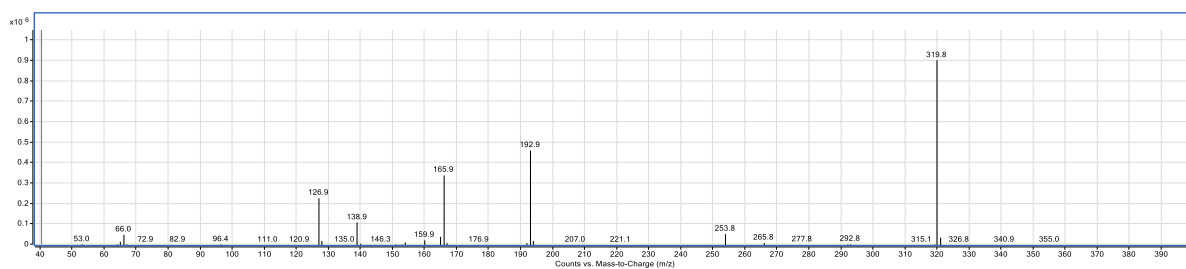
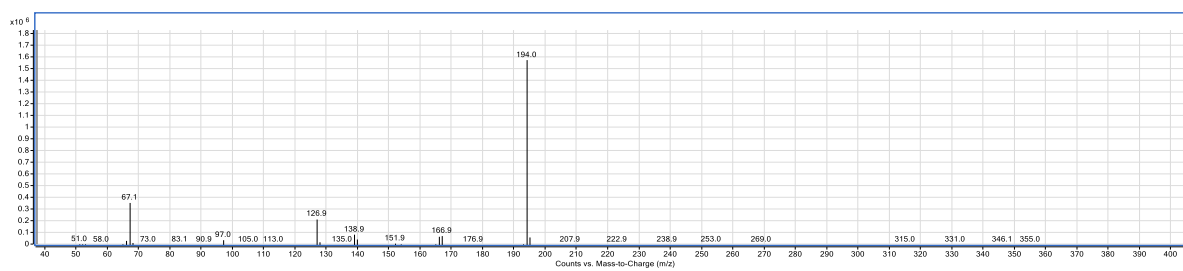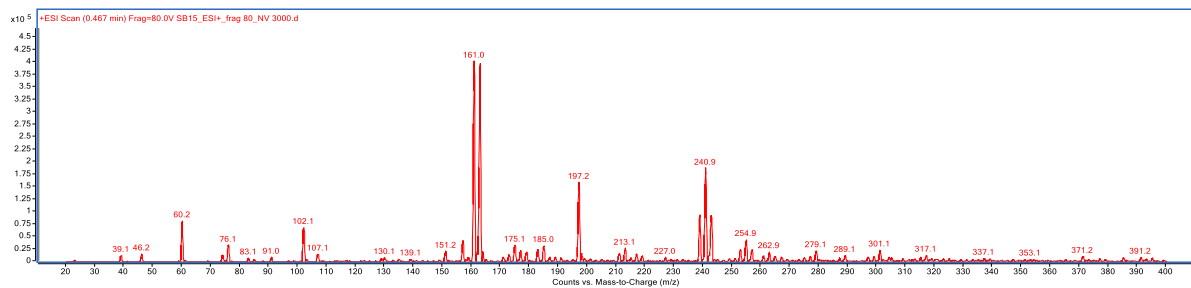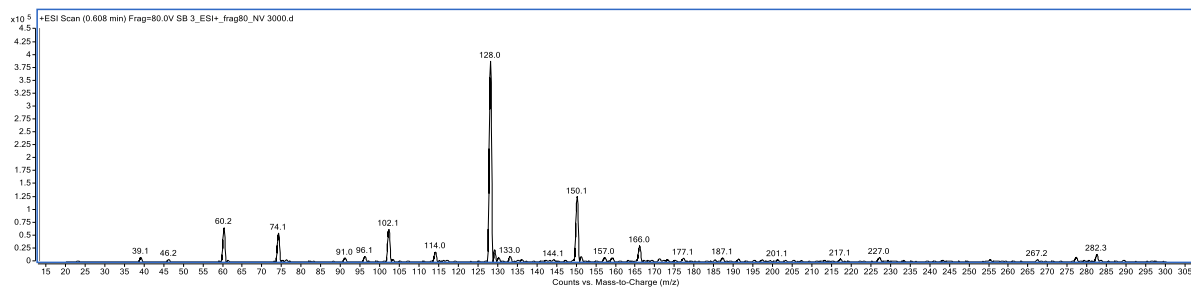
GC-MS spectrum of **21** (First procedure)

GC-MS spectrum for **21** (Second procedure)

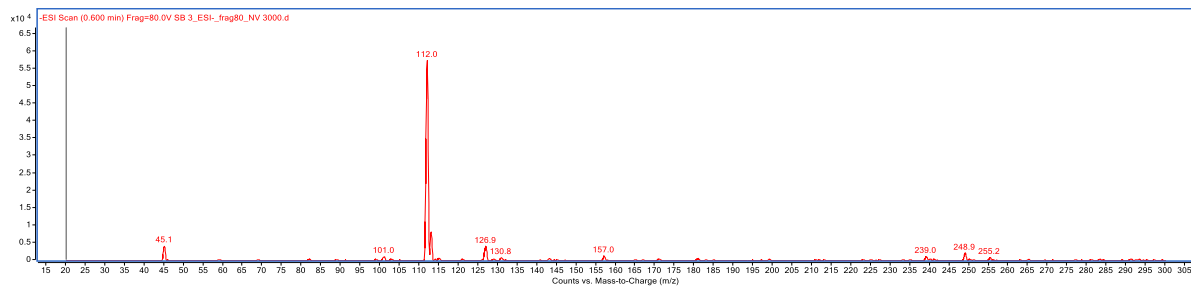## LC-MS spectrum of **22**

LC-MS spectrum positive of **25**

LC-MS spectrum negative of **25**

LC-MS spectrum for **26** (first procedure)

+ESI Scan (0.574 min) Frag=80.0V SB 4.2_ESI+_frag80_NV 3000.d